UNIVERSITY OF TROMSØ UiT

FACULTY OF BIOSCINCES, FISHERIES AND ECONOMICS
DEPARTMENT OF ARCTIC AND MARINE BIOLOGY

The dually targeted transcription factor TF1 and its role in the expression of plastid- and nuclear-encoded photosynthesis genes

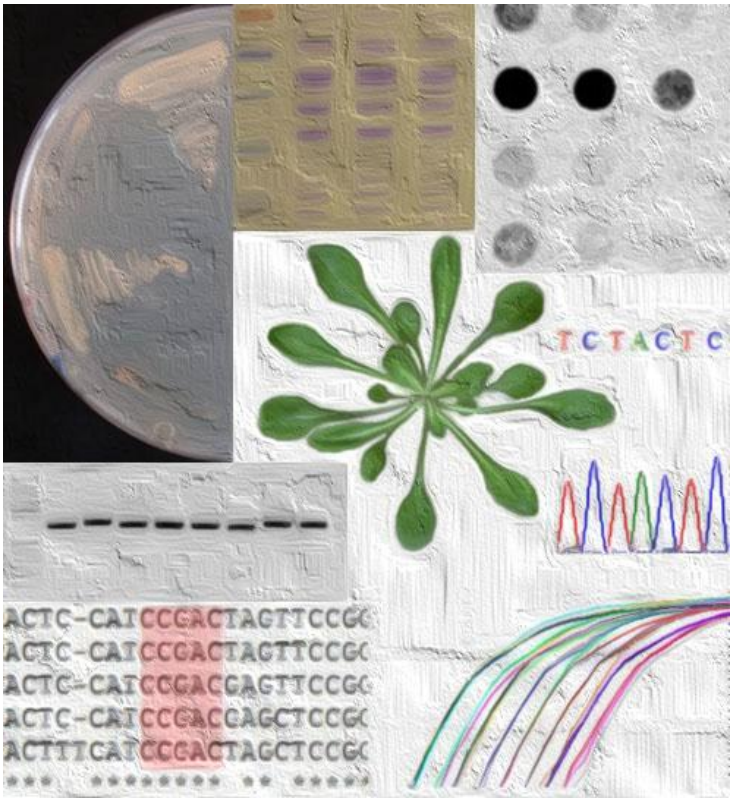

Stian Olsen

BIO-3910 Master`s thesis in Biology

September 2012

Table of Contents

Acknowledgements

I would like to express my gratitude to my supervisor Prof. Kirsten Krause, both for introducing me to this project and for providing me with guidance and knowledge along the way. Her enthusiasm and generous giving of her time have been most appreciated.

The work presented in this thesis was carried out in the lab of the Molecular Environments Research Group at the Department of Arctic and Marine Biology. I would like to use this opportunity to thank all the people in this group for their aid, support and friendship throughout the course of my study.

Special thanks go to Dr. Bernd Ketelsen for his help with the yeast one-hybrid assays and to Dr. Lan Yin for her collaboration in the analysis of plastid and nuclear gene expression.

Finally, I wish to thank my family, and especially Christin, for constant support and encouragement.

Abbreviations

3-AT	3-amino-1,2,4-triazole
^{32}P-UTP	Uridine triphosphate containing phosphorous-32
^{33}P-UTP	Uridine triphosphate containing phosphorous-33
Amp	Ampicillin
AP2	APETALA 2
ATP	Adenosine triphosphate
BLAST	Basic Local Alignment Search Tool
Bp	Base pair(s)
BSA	Bovine serum albumin
Carb	Carbenicillin
ChIP	Chromatin immunoprecipitation
cDNA	Complementary DNA
CTP	Cytidine triphosphate
Cq	Quantification cycle
DBP	DNA-binding protein
ddNTP(s)	Dideoxynucleoside triphosphate(s)
dH_2O	Deionized water
DNA	Deoxyribonucleic acid
dNTP(s)	Deoxyribonucleside triphosphate(s)
DO	Drop out
DRE	Dehydration-Responsive Element
DREB(s)	Dehydration-Responsive Element Binding protein(s)
dsDNA	Double-stranded DNA
DTT	Dithiothreitol
EDTA	Ethylenediaminetetraacetic acid
EREBP	Ethylene response element binding protein
ERF	Ethylene-Responsive Factor
EtBr	Ethidium bromide
EtOH	Ethanol
for	Forward
gDNA	Genomic DNA
GFP	Green fluorescent protein
GTP	Guanosine triphosphate

h	Hour(s)
HA	Hemagglutinin
His	Histidine
HRP	Horseradish peroxidase
Inv	Inverted
Kan	Kanamycin
Kb	Kilobases
LB	Lysogeny broth
Leu	Leucine
MCS	Multiple cloning site
MeOH	Methanol
min	Minute(s)
mut	Mutated
NCBI	The National Center for Biotechnology Information
NEP	Nuclear-encoded RNA Polymerase
NLS	Nuclear Localization Signal
Oligo(s)	Oligonucleotide(s)
PCR	Polymerase chain reaction
PEG	Polyethylene glycol
PEP	Plastid-encoded RNA Polymerase
PS	Photosystem
pTP	Plastid transit peptide
PVDF	Polyvinylidene difluoride
qPCR	Quantitative real-time PCR
RAV	Related to ABI3/VP1
rev	Reverse
RFU	Relative fluorescence unit
RNA	Ribonucleic acid
ROS	Reactive oxygen species
rpm	Revolutions per minute
RT-qPCR	Reverse transcription qPCR
RuBisCO	Ribulose-1,5-bisphosphate carboxylase oxygenase
SD	Selective dropout medium
SDS	Sodium dodecyl sulfate

SDS-PAGE	Sodium dodecyl sulphate polyacrylamide gel electrophoresis
sec	Second(s)
SOB	Super optimal broth
SSC	Saline-sodium citrate
ssDNA	Single-stranded DNA
SSPE	Saline-sodium phosphate EDTA
TAE	Tris-acetate-EDTA
TBS	Tris-buffered saline
TBS-T	Tris-buffered saline-Tween 20
T-DNA	Transfer DNA
TE	Tris-EDTA
Tic-Toc	Translocon of inner chloroplast membrane-Translocon of outer chloroplast membrane
T_m	Melting temperature
Tris	Tris(hydroxymethyl)aminomethane
UV	Ultraviolet
WT	Wild type
Y1H	Yeast one-hybrid
YAPD	Yeast extract adenine peptone dextrose medium

Explanatory Remarks

Gene symbols are written in italics when referring to the gene itself, and without italics when the respective gene products are concerned. The gene product of locus tag At2g44940 is described as the ethylene-responsive transcription factor ERF034 (Nakano et al., 2006) in the NCBI database, but will in this thesis be referred to as TF1.

Abstract

In plant cells, the distribution of genes on three spatially separated subgenomes calls for the necessity of maintaining a coordinated regulation of gene expression between these DNA-containing compartments. Especially, the translocation of nuclear-encoded gene products to plastids and mitochondria, which is crucial for the development and metabolic operation of these semi-autonomous organelles, requires continuous intercompartmental communication. This correspondence is provided by anterograde and retrograde pathways, involving nucleus-to-plastid and plastid-to-nucleus signalling, respectively. Because of their ability to target more than one DNA-containing compartment, dually targeted transcription factors have been suggested as possible participators in coordination of gene expression between subgenomes. In this study, the effect of the plastid- and nucleus-targeted AP2/EREBP transcription factor TF1 on the expression of plastid- and nuclear-encoded photosynthesis genes was investigated using run-on transcription assays and RT-qPCR, respectively. The comparison of transcription rates between a *TF1* knock-down mutant (ΔTF1) and wild type (WT) *Arabidopsis thaliana* at different points in the 24 hours day/night cycle revealed that expression of the *TF1* gene is required for light-promoted transcription of the plastid-encoded photosynthesis genes *psaA*, *psaB*, *psbA* and *rbcL.* In contrast, the light-induced increase in transcription of the nuclear photosynthesis genes *RBCS1A* and *PSBO2* was not dependent on TF1. This observation would suggest a dual role for TF1 in the light-regulated transcription of plastid-encoded photosynthesis genes and in the retrograde pathway maintaining coordinated transcription of these genes with the corresponding nuclear genes. Yeast one-hybrid assays identified two DNA sequence-motifs which were specifically bound by TF1, namely the DRE motif (TACCGACAT) and the inverted and mutated GCC box (GGAGGAT). The discovery of these DNA-motifs in the promoter regions of the TF1-regulated genes *psbA* and *psaA/B* indicated that TF1 might directly target these genes. Ultimately, the data obtained in this study, together with previously obtained information regarding this dually targeted transcription factor, lead to the proposal of a tentative model for the functional role of TF1 in the light-mediated coordination of gene expression in plastids and the nucleus, which will serve as a basis for further experiments.

1. Introduction

1.1 Distribution of the genetic information in plants onto three compartments

The total genome of a plant cell is composed of three subgenomes that are located within different intracellular compartments: the nucleus, the mitochondria and the plastids. The largest part of the genomic information is stored on nuclear localized chromosomes (25 498 genes in *Arabidopsis thaliana* (Arabidopsis Genome Initiative, 2000)), while the two organellar genomes contain rather few genes. In *A. thaliana* there are 128 plastid-encoded (Sato et al., 1999) and 57 mitochondrial-encoded (Unseld et al., 1997) genes.

Both mitochondria and plastids are the results of endosymbiosis, a process in which a free-living bacterium was engulfed by another cell and subsequently transformed into a semi-autonomous organelle. The most important step in conversion from autonomous endosymbiont to organelle was the reduction of the endosymbiont genome, during which most of the genes were transferred to the nucleus (Dyall et al., 2004). This gene transfer rendered the organelles dependent on nuclear-encoded gene products to perform their metabolic and regulatory tasks. A previous study by Richly and Leister (2004) predicted about 2100 nuclear-encoded proteins to be imported into the chloroplasts, meaning that less than 10% of the plastid proteome is actually encoded on the plastid genome.

Naturally, the requirements for the production of many gene products change over time due to alterations in the surroundings of the cell (e.g. light, temperature, nutrient- and water-availability). In order to function properly, a cell must be able to regulate the level of expressed gene products in accordance with external changes. Consequently, at any given time in the life course of a cell, only a fraction of the genes encoded in its genomes is expressed. Considering the spatial separation of the genes required to operate a plant cell, and the semi-autonomous nature of the organelles, mechanisms to ensure finely tuned coordination of gene expression between the three DNA-containing compartments are necessary.

1.2 Regulation of gene expression

In eukaryotes, the process of making a functional protein from nuclear-, plastid- or mitochondrial-encoded genes can be regulated at four main levels (Becker et al., 2006):

1. Transcription
2. RNA processing and translocation
3. Translation
4. Post-translational modifications

In addition to regulating the DNA-mRNA-protein information flow, the expression of nuclear-encoded genes is affected by the accessibility of the genes for the transcription machinery. In the nucleus, DNA and histones are packed together to form nucleosomes, which are further packed into chromatin fibres and chromosomes. Chromatin remodelling by histone modifications can be used to alternate between a highly condensed form called heterochromatin (which is transcriptionally inactive), and the less condensed, transcriptionally active, euchromatin. The small and circular organellar genomes are also packaged by histone-like proteins and other architectural proteins, but it has not been shown conclusively whether this impacts gene regulation (Melonek et al., 2012).

The majority of evidence indicates that the nuclear genome is stable and identical in all cells of a given multicellular organism. However, there are examples of gene deletions, replications and DNA rearrangements (Becker et al., 2006). The organellar genomes of eukaryotic organisms are known to be highly polyploid, both due to there being several mitochondria and plastids within one cell, and because there are more than one genome copy within a single organelle. In barley, the plastome copy number has been shown to be dependent on the developmental stage of the cell (Baumgartner et al., 1989; Olsen et al., manuscript in preparation).

In addition to the abovementioned modifications, methylation of certain nucleotides is thought to be involved in gene silencing in all three subgenomes of plant cells (reviewed in Vanyushin and Ashapkin (2011)).

1.2.1 Transcription of nuclear genes

Transcriptional activation of nuclear genes requires a set of proteins termed general transcription factors which assemble at the core promoter of a gene by binding to specific core promoter elements (e.g. the TATA box). The general transcription factors are needed for recruitment and correct positioning of the RNA polymerase at the transcription start site and are alone only capable of keeping a low transcription rate (Thomas and Chiang, 2006). However, in addition to the binding sites in the core promoter, several other *cis*-regulatory sequences (with gene specific identity and location) exist. Binding of proteins to these sequences can have promoting or repressing effects on the transcription rate of the adjacent gene, either by interacting directly with the transcriptional machinery or indirectly through different cofactors. Proteins that induce such effects on transcription by binding to specific DNA sequences are termed regulatory transcription factors (Becker et al., 2006).

An illustration of nuclear transcriptional regulation by the activity of transcription factors is depicted in Figure 1.

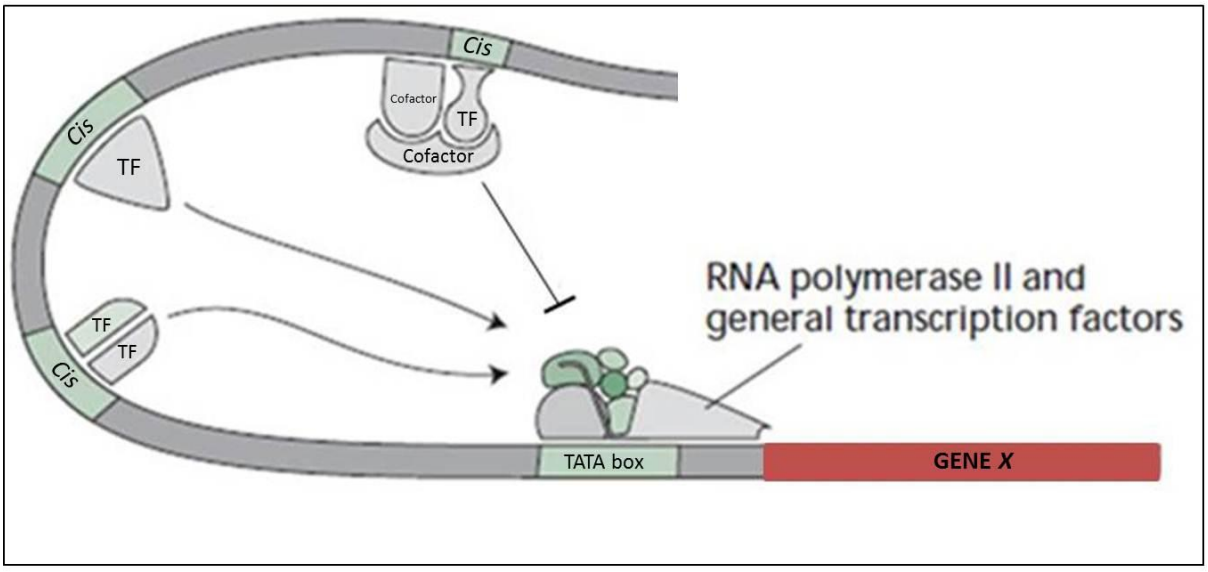

Figure 1: Eukaryotic regulation of transcription, here illustrated with RNA polymerase II which transcribes nuclear mRNA from protein-coding genes. The binding of regulatory transcription factors (TF) to specific *cis*-regulatory motifs (*Cis*) can increase or decrease the transcription rate (in this case of gene X) by interacting directly with the transcriptional machinery or indirectly through cofactors. Modified after Taiz and Zeiger (2006).

1.2.2 Transcription of plastid genes

In the genomes of plastids, most genes are organized in collectively transcribed operons, reflecting their prokaryotic origin. However, even though the size of the plastid genome is small compared to the genome of its bacterial ancestor, the complexity of the machinery regulating transcription is considerably higher in chloroplasts than in free-living prokaryotes. This increase in complexity is mainly achieved by the involvement of nuclear-encoded genes. In chloroplasts of higher plants, the transcription of genes is executed by two different RNA polymerases: the phage-like, nuclear-encoded RNA polymerase (NEP) and the bacteria-like, plastid-encoded RNA polymerase (PEP) (reviewed in Liere et al. (2011)). Most of the genes on the chloroplast genome have both NEP and PEP promoters, while a few housekeeping genes are only transcribed by NEP and some photosynthesis genes only by PEP (Hajdukiewicz et al., 1997; Krause et al., 2000). As a way of nuclear control over PEP, the activity of this polymerase is controlled by its need of nuclear-encoded sigma-factors (Kanamaru and Tanaka, 2004). In addition, genes encoding core subunits of PEP are themselves transcribed by NEP.

Although plastid gene expression is mostly controlled by nuclear-encoded proteins through post-transcriptional mechanisms, the transcriptional activity of chloroplasts has been shown to be affected by factors such as plant hormones, temperature and light (reviewed in Liere et al. (2011)). This regulation is, like nuclear transcription, mediated by factors that interact with the transcription machinery (NEP or PEP) and promote or repress its activity. In addition to the nuclear-encoded sigma factors, other nuclear-encoded transcription factors with plastid localization signals might be involved in regulation of plastid gene expression (Schwacke et al., 2007).

1.2.3 Post-transcriptional regulation of nuclear and plastid genes

After transcription, RNA processing events like 5’capping, addition of poly-A tails and RNA splicing are involved in regulation of nuclear gene expression by controlling which transcripts are transported out of the nucleus for translation on ribosomes in the cytosol, and which are degraded. Once present in the cytosol, there are mechanisms for controlling which mRNAs are translated into polypeptides and at what rate, either by inducing changes to ribosomes

or on the mRNA itself (e.g. alterations in the secondary structure of a transcript can positively or negatively affect the accessibility of the start codon). The expression of a gene (as defined by the final activity of the product) can also be regulated after translation of an mRNA by controlling protein folding, modification, subunit assembly, degradation and intracellular localization (Becker et al., 2006).

In plastids, post-transcriptional mechanisms are thought to be even more important for the regulation of gene expression (reviewed in Woodson and Chory (2008)). They encompass transcript maturation (e.g. splicing**,** editing and the processing of 5'- and 3'-ends) and regulation of translation rates, and are governed by post-transcriptional regulators of organelle gene expression (ROGEs) encoded on the nuclear genome. The proposed mechanism for regulation of gene expression by ROGEs is that they act as adaptors, connecting mRNA with the translation machinery and/or RNA metabolism enzymes. ROGEs are very sequence specific and often regulate the expression of only one target gene. An exception to this high specificity is the plastid gene *matK* encoding an intron maturase that has been found to interact with seven different intron-containing transcripts (Zoschke et al., 2010).

The activity of plastid-encoded peptides is also regulated by post-translational modifications (e.g. phosphorylation/dephosphorylation of amino acids and reduction/oxidation of sulfhydryl groups) that affect folding and subunit assembly of plastid-encoded polypeptides, which again can affect the proteins degradation rate. These processes are again mainly controlled by nuclear-encoded proteins (e.g. the plastid-localized FtsH and Clp proteases (Adam et al., 2006)).

1.3 Coordination of nuclear and plastid gene expression

All complexes involved in the main metabolic reactions executed by plastids (e.g. photosynthesis, biosynthesis of amino acids, starch and fatty acids (Neuhaus and Emes, 2000) are a mosaic of organelle-encoded and nuclear-encoded proteins. This necessitates a highly coordinated regulation of gene expression between the nucleus and the plastids to ensure the matching expression of proteins imported from the cytosol and organelle-encoded proteins.

Such a regulation is obtained by nucleus-to-plastid (anterograde) signalling on one hand, and plastid-to-nucleus (retrograde) signalling on the other hand. Ultimately, both types of signals are governed by external cues from the environment (see Figure 2).

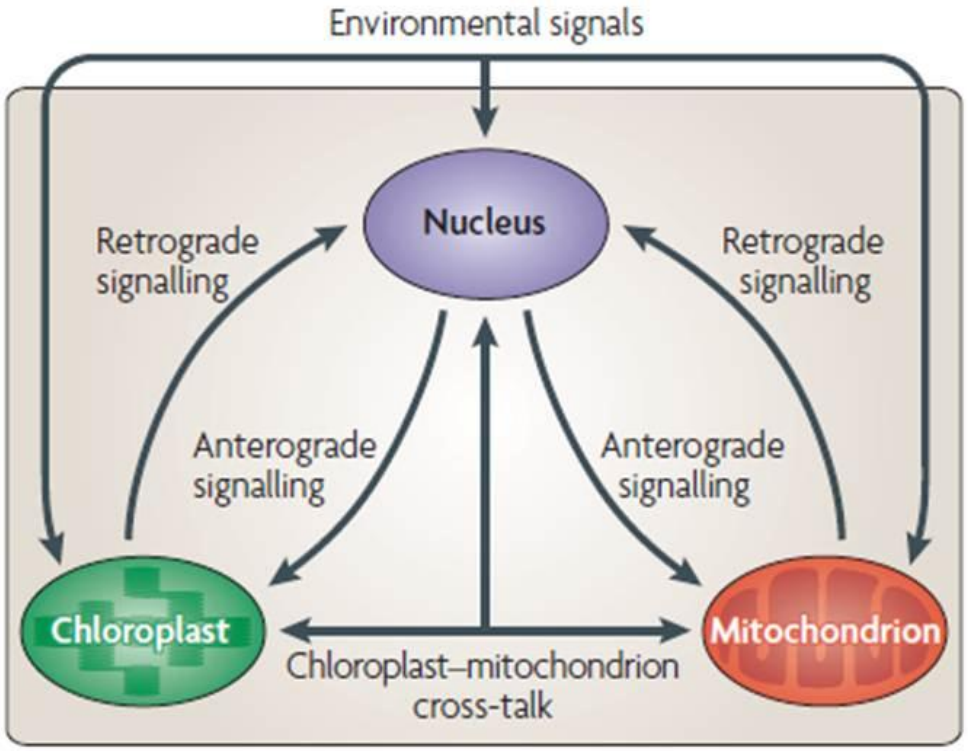

Figure 2: Illustrative model of anterograde and retrograde signalling between nucleus and organelles as well as cross-talk between organelles. Changes in the environment (e.g. light, temperature, O_2 availability) can be detected in different compartments depending on the nature of the stimuli. However, the connecting signalling pathways ensure that necessary actions are carried out in both organelles and the nucleus. After Woodson and Chory (2008).

As seen in Figure 2, in addition to anterograde and retrograde communication, there is also cross-talk going on between plastids and mitochondria as a result of their many interconnecting metabolic pathways (e.g. photorespiration (Noguchi and Yoshida, 2008)).

1.3.1 Anterograde signalling

Anterograde control of the nucleus over plastid gene expression is generally maintained by the requirement of nuclear-encoded proteins for transcription, translation and post-translational events in plastids (reviewed in Woodson and Chory (2008)). In addition to the NEP, sigma-factors, and ROGEs mentioned in chapter 1.2, a great number of ribosomal proteins and translation initiation factors are also encoded on the nuclear genome.

In addition to nuclear control over plastid gene expression, the metabolic activity of plastids is regulated by the expression of nuclear-encoded subunits which, as mentioned above, are part of most plastid-localized protein complexes (e.g. RuBisCO, ATP synthase and photosystems I and II). Cytosolic proteins destined for the plastid stroma or the thylakoid membrane must enter through the Tic-Toc (translocon of inner chloroplast membrane-translocon of outer chloroplast membrane) import machinery in order to pass the double membrane barrier surrounding these organelles (Strittmatter et al., 2010). Selective transportation into plastids is achieved by the import machinery recognizing N-terminal plastid transit peptides which are cleaved off after import (Bruce, 2000; Soll and Schleiff, 2004). The multiple subunits making up the Tic- and Toc- complexes are encoded on the nuclear genome, making the import system of plastids in itself subject to anterograde control (Bräutigam et al., 2007).

1.3.2 Retrograde signalling

Although the metabolic activity of plastids is mainly controlled by the nucleus via anterograde signalling, the plastids themselves are not mere recipients but produce a multitude of signals that affect nuclear gene expression (reviewed in Pfannschmidt (2010) and in Leister (2012)). Given the semi-autonomous nature of the plastids, their ability to give feedback to the nucleus is crucial to ensure that they receive the proteins needed to adapt their functions to the respective conditions. In addition to genome coordination, retrograde signalling can also induce appropriate responses in other cellular activities. E.g. enhanced plastidial production of singlet oxygen ($^1O_2$) induces growth inhibition and seedling lethality of *Arabidopsis thaliana*. This effect has been shown to be dependent on the expression of the nuclear-encoded *EXECUTER1* gene (Wagner et al., 2004), necessitating the involvement

of a retrograde signalling pathway. This exemplifies the vital role of plastids as receptors for external stimuli with the ability to affect the whole cell, or even the entire plant.

Retrograde signals going from plastid to nucleus can originate from several different processes occurring inside the plastids. Reactive oxygen species (ROS) such as $^1O_2$ and H_2O_2 are natural by-products of photosynthesis, but can accumulate in response to abiotic or biotic stress. In such cases, in order to avoid lethal oxidative damage, nuclear production of antioxidant enzymes and photosynthetic subunits is regulated. This nuclear response can be generated by ROS that act as retrograde signals (reviewed in Woodson and Chory (2008)). In addition to ROS-mediated stress responses, macroarray analyses have shown that light-induced fluctuations in the redox state of the photosynthetic electron transport chain affects the expression of nuclear-encoded photosynthesis-related genes (Fey et al., 2005), enabling a continuous modulation of the photosynthetic machinery in accordance with changing light conditions.

Treatment with the herbicide norflurazon leads to plastid dysfunction by inducing strong photo-oxidation. In addition, this treatment has been shown to induce repression of the nuclear gene *LHCB,* encoding chlorophyll a/b binding protein of PSII (Oelmuller and Mohr, 1986). In a screen for proteins involved in this signalling pathway, *genomes uncoupled* (*gun*) mutants were identified that failed to show down-regulation in expression of the *LHCB* gene despite their impaired plastids (Susek et al., 1993). While the GUN1 protein might be involved in plastid gene expression, the *gun2-5* genes all encode components of the tetrapyrrole biosynthesis pathway, leading to the proposal of the chlorophyll precursor magnesium protoporphyrin IX as the plastid retrograde signal (reviewed in Woodson and Chory (2008) and Strand (2004)). However, despite extensive research it is still not completely understood how plastid-to-nucleus signalling is disturbed in the *gun*-mutants, and, although it is clear that changes to the state of the plastids induce responses in other cellular compartments, no true retrograde signalling molecule leaving the chloroplasts has so far been found (reviewed in Pfannschmidt (2010) and Leister (2012)).

1.3.3 Bidirectional signalling with dually targeted transcription factors

As mentioned above, coordinated regulation of gene expression between the nucleus and the two DNA-containing organelles is crucial for plant cells to function correctly. However, timely expression of the gene alone is not enough. The synthesized protein must also be transported to the right compartment in order for it to carry out its function. In addition to evolving specific target sequences for nucleus, mitochondria and plastids, there are also cases in which a protein is targeted to two of these compartments (Krause and Krupinska, 2009; Silva-Filho, 2003; Small et al., 1998). There are two different basic mechanisms for dual targeting (Krause and Krupinska, 2009): the presence of two separate targeting sequences on the same peptide (e.g. the plastid- and nucleus-targeted transcription factor TF1 (see Figure 3)) or ambiguous targeting, in which a single target sequence is recognized by more than one import system (e.g. amino acyl-tRNA synthetases targeted to both mitochondria and plastids (Berglund et al., 2009).

Some years ago, two publications reported that transcription factors of eukaryotic origin (originating from the nucleus of the endosymbiont host) possess targeting signals that would direct them to both plastids and the nucleus (Schwacke et al., 2007; Wagner and Pfannschmidt, 2006). While dual targeting as such was already an undisputed phenomenon at that time, not many proteins were known to be targeted to these two DNA-containing compartments (Silva-Filho, 2003). Dually targeted transcription factors are especially interesting candidates for the coordinated regulation of gene expression from the nuclear and plastid genomes. Examples from other model organisms show that such proteins can execute their function in several compartments simultaneously (e.g. the Rpm2 yeast protein (Stribinskis et al., 2005)). In plants, an additional possibility has been brought up: namely that one compartment can function as an inactive storage place where the protein awaits developmental or environmental signals that induce transport to its site of activity (Caplan et al., 2008; Krause and Krupinska, 2009; Terasawa and Sato, 2009). Although no plastid exporters have so far been characterized, the translocation of proteins from chloroplasts to nucleus has been reported (Isemer et al., 2012).

1.4 TF1, a dually targeted transcription factor of the AP2/EREBP family

One of the dually targeted proteins identified by Schwacke and co-workers (2007) was TF1 (alias ERF034, locus tag At2g44940). This nuclear-encoded protein contains both an N-terminal plastid transit peptide (pTP) and an internal nuclear localization signal (NLS) (see Figure 3B), and was also documented to be localized in both nucleus and chloroplasts in Arabidopsis protoplasts (Schwacke et al., 2007) as seen in Figure 3A.

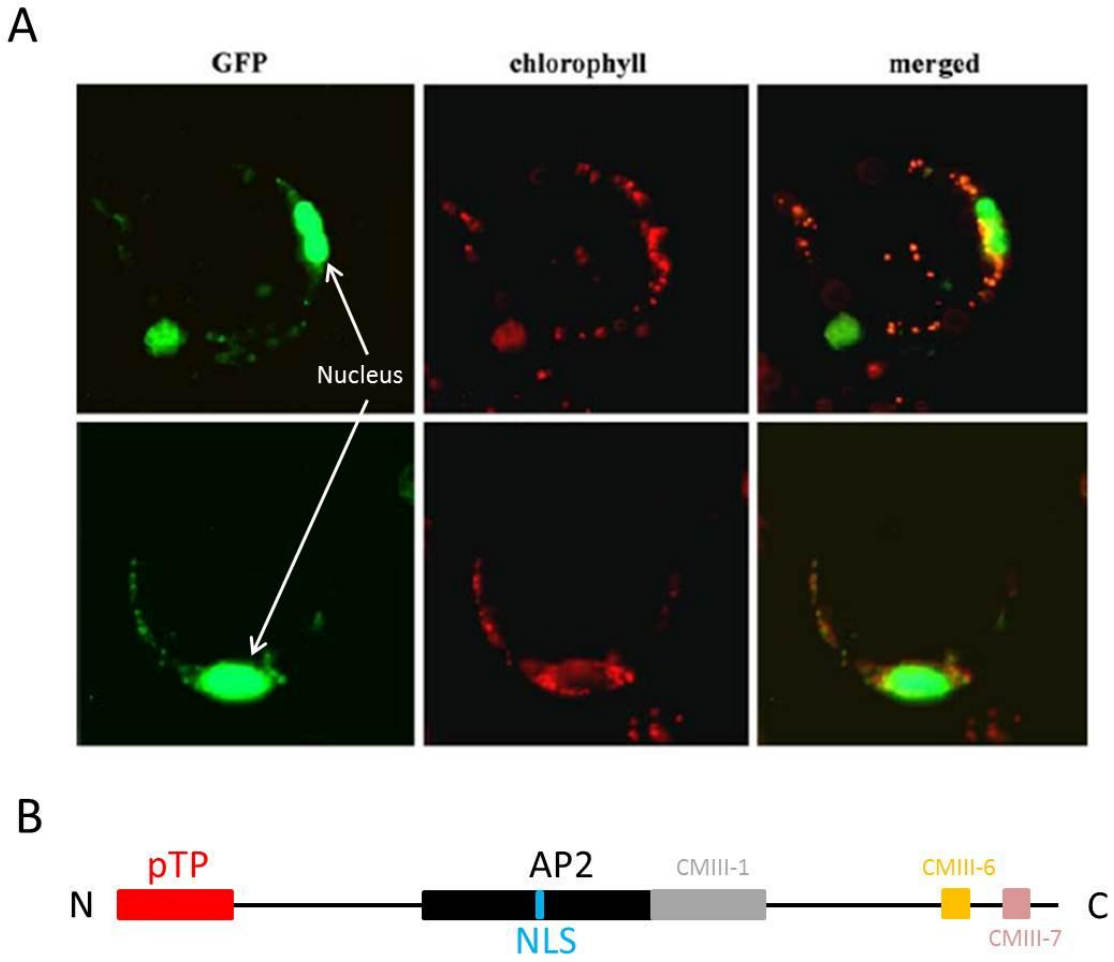

Figure 3: (A) Intracellular localization of TF1 fused to GFP (Green fluorescent protein) in Arabidopsis protoplasts. Chlorophyll autofluorescence is seen in red. The third picture column (from the left) shows a merged picture of the two previous pictures. Modified after Schwacke et al. (2007). (B) Structural domains of TF1: The N-terminal plastid transit peptide (pTP) (indicated in red) is presumably cleaved off upon plastid-import. The short nuclear localization signal (NLS) (indicated in blue) is located within the AP2 domain (Garcia-Bustos et al., 1991; Jofuku et al., 1994; Schwacke et al., 2007). The CMIII-1, 6 and 7 domains do not have any known functions, but are conserved in other DREBs (Nakano et al., 2006). The relative sizes of the boxes illustrating the different domains of TF1 are not accurately representing the real sizes of the protein domains.

The APETALA 2/ethylene response element binding protein (AP2/EREBP) family of transcription factors constitutes 147 individual gene loci in *Arabidopsis thaliana* (Nakano et al., 2006). This corresponds to about 9% of the more than 1600 transcription factors found in *A. thaliana* (Dietz et al., 2010). The AP2/EREBPs are characterized by the presence of at least one AP2 DNA-binding domain (Okamuro et al., 1997). This motif consisting of about 60 amino acids was first identified in the homeotic gene APETALA 2 (Jofuku et al., 1994), which is involved in floral development. Mutations in the *AP2* gene lead to dramatic changes in flower structure. Shortly afterwards, the same DNA-binding domain was found in proteins that interacted with a sequence-motif essential to ethylene-responsive promoters (Ohme-Takagi and Shinshi, 1995). Together, these two initial discoveries gave name to the AP2/EREBP family of transcription factors.

Due to the fact that the AP2/EREBP family of transcription factors is characterized by their DNA-binding domain, different members of this protein family naturally have a variety of different biological functions. They have been shown to be involved in development, abiotic stress response and hormonal signalling (reviewed in Dietz et al. (2010)). Transcription factors of this family were long thought to be present only in plants (Riechmann and Meyerowitz, 1998). However, recent evidence shows that they are also found in cyanobacteria and ciliates (Magnani et al., 2004). Being a large protein family with varying degrees of similarity between the members, AP2/EREBPs are further divided into four subfamilies: AP2, DREB, ERF and RAV subfamilies (Dietz et al., 2010). The dually targeted transcription factor TF1 is classified as part of the dehydration-responsive element binding protein (DREB) subfamily of AP2/EREBP transcription factor family.

1.4.1 DREBs and their DNA-binding specificity

Members of the DREB subfamily of AP2/EREBPs are related to DREB1A and DREB2A, which have been shown to bind specifically to the dehydration-responsive element (DRE) TACCGACAT (Liu et al., 1998; Sakuma et al., 2002). Transcription factors of this subfamily were thought to only play roles in osmotic- and cold-stress signal transduction pathways by recognizing the CCGAC core sequence found in the DRE and the C-repeat (CRT) (Shinozaki and Yamaguchi-Shinozaki, 2000). However, TINY (locus tag At5g25810), another transcription factor of the DREB subfamily, has been shown to interact with both DRE and another *cis*-regulatory element, the GCC box (also called ethylene-responsive element (ERE)) AGCCGCC, thereby connecting abiotic and biotic stress responses (Sun et al., 2008) and revealing the possibility for DREBs to bind more than one DNA-motif.

In a large screen for protein-protein and protein-DNA interactions between stele-enriched transcription factors, TF1 was shown to bind the promoter region of a nuclear-encoded Dof-type transcription factor (locus tag At5g60200) (Brady et al., 2011). Although the binding of TF1 did not have any effects on the expression of the target gene, the fact that one of the closest homologues of TF1, ERF035 (locus tag At3g60490), also interacted with the same DNA sequence, indicates that the interaction is specific. However, since transcription factors recognize short stretches of DNA (<10bp) and the analysed promoter region was 3082bp in length, this report does not reveal much about TF1's specific binding-preferences.

1.4.2 Expression of *TF1*

High throughput data from microarray analyses indicate that the expression of *TF1* is induced by cold temperatures and light (Kilian et al., 2007; Michael et al., 2008; Smith et al., 2004), respectively. However, the expression of *TF1* does not seem to be affected by drought (Kilian et al., 2007).

Figure 4 illustrates some of the abiotic conditions under which the TF1 mRNA was found to be elevated. In particular, light and cold treatments have a positive influence on the abundance of *TF1* transcripts.

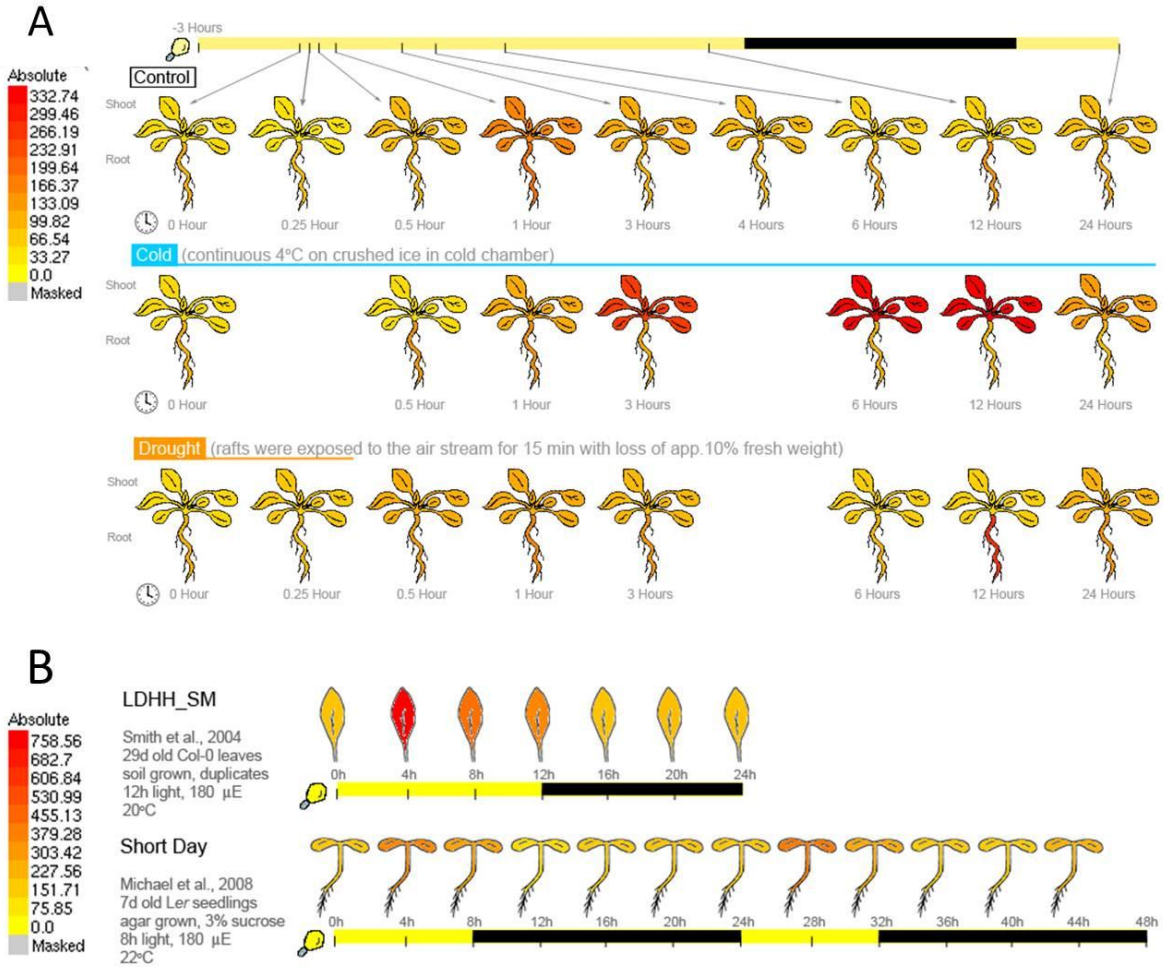

Figure 4: (A) Cold-, drought- and (B) light-induced effects on *TF1*-expression. Stronger red indicates larger amounts of *TF1* transcripts as indicated by the scales accompanying A and B. (A) Expression of *TF1* is increased by continuous cold treatment, but not affected by 15 min of dehydration (Kilian et al., 2007). (B) *TF1*-expression reaches a peak after four hours of light and thereafter gradually decreases (Smith et al., 2004). The light-induced increase and subsequent decrease in *TF1*-expression fluctuates in a circadian manner in seedlings grown under short day conditions (Michael et al., 2008). Modified after illustrations in the Arabidopsis eFP Browser at bar.utoronto.ca (Winter et al., 2007).

1.5 Aims of this study

Understanding how genomes function in unison with one another is a central question in the post-genomic era. Evidence that a dually targeted transcription factor, Whirly1, is released from plastids and subsequently accumulates in the nucleus (Isemer et al., 2012) has raised the question if plastid sequestration is a more widely used pathway. In order to answer this question, it will be necessary to learn more about other potentially sequestered candidates. The nuclear-encoded, dually targeted transcription factor TF1 of *Arabidopsis thaliana* was predicted with high confidence to be dually targeted to chloroplasts and the nucleus, and its presence in both cell compartments was also confirmed experimentally (Schwacke et al., 2007). However, nothing is known about the function of this protein in any of these two DNA-containing compartments.

In this thesis, investigations on TF1 will be performed with the goal to show whether this protein has an effect on plastid gene expression, and to unravel which DNA sequence-motifs are recognized by TF1. The comparison of TF1-induced effects on plastid gene expression with the transcription factor's influence on expression of related genes on the nuclear genome will grant knowledge concerning TF1's putative role in maintaining a coordinated expression between these two subgenomes. The identification of TF1-interacting DNA sequences in the promoters of TF1-regulated genes will make subsequent analysis of the protein's functional activity possible.

From previous analyses in the group of K. Krause, a *TF1* knock-down mutant was available. A transgenic line overexpressing TF1, on the other hand, proved to be difficult to obtain (Krause and co-workers, personal communication). However, the fact that TF1 is strongly upregulated by light and has a peak at four hours after dawn (see Figure 4B), offers an opportunity to study the effects of different levels of this protein in the wild type background.

In order to test whether a given chloroplast protein has an influence on plastid transcription, chloroplast run-on transcription assays have in the past proved to be a useful technique (Melonek et al., 2010). This method allows observation of gene-specific transcription rates in isolated chloroplasts and measures transcriptional activity directly without interference from RNA stability and RNA turnover.

By monitoring the transcription rates of individual plastid-encoded genes in *TF1* knock-down mutant (ΔTF1) and wild type (WT) *Arabidopsis thaliana* immediately before and four hours after daybreak (see Figure 5), the effects of TF1 on gene-specific transcription rates can be investigated. As specific chloroplast microarrays are not available, self-made macroarrays covering a range of plastid genes for different metabolic functions will be generated. If TF1 has an influence on plastid-encoded genes, expression of selected nuclear genes encoding imported proteins belonging to the affected protein complex(es) will be analysed as well. Since nuclear run-ons are more difficult to perform, RT-qPCR analysis will be employed for this purpose.

There are several publications on the DNA-binding specificity of transcription factors in the AP2/EREBP family (Allen et al., 1998; Brady et al., 2011; Hao et al., 1998; Sakuma et al., 2002; Sun et al., 2008). In order to probe the DNA-binding ability of TF1, DNA-motifs known to be recognized by DREBs are to be tested using yeast one-hybrid assays. This method uses a reporter gene system set up in yeast in order to identify protein-DNA interactions. By letting the interactions take place within yeast cells, the necessity for optimization of binding conditions (as required in *in vitro* assays) is avoided.

Identified DNA-motifs for which TF1 possesses an affinity will be compared with the gene expression data from run-on transcription assays and RT-qPCR. It would be a strong candidate for a direct target gene, if a sequence-motif which interacts with TF1 can be found in the promoter region of a gene whose expression is also affected by this transcription factor.

Ultimately, information collected in this study will not only help to shed light on the biological function of this dually targeted transcription factor, but also on the manner in which TF1-induced effects are accomplished. The observed abilities of this protein can then further be used to propose mechanisms for other dually targeted transcription factors in the coordination of gene expression between the nucleus and the semi-autonomous organelles.

2. Materials and Methods

2.1 Plant growth

Arabidopsis thaliana (ecotype Columbia-0) WT plants and a ΔTF1 mutant line (T-DNA insertion line in which At2g44940 has been disrupted (SALK_020979)) were grown for 8 weeks under short day conditions (8 h light/16 h dark) before either extracting RNA (see chapter 2.3.1) or isolating chloroplasts (see chapter 2.2.1) at specific time points in the 24 h day/night cycle (see Figure 5).

Figure 5: Schematic illustration of the 24 h light/dark regime used for growing WT and ΔTF1 *Arabidopsis thaliana*. Plants for downstream experiments were harvested at two different time points in the 24 cycle: right before light on (0 h) and four hours after light on (4 h). The two harvesting points are indicated with arrows.

2.2 Run-on transcription assay

In order to investigate the effect of TF1 on the transcription rate of certain plastid-encoded genes, run-on transcription with isolated chloroplasts, followed by hybridization of radioactively labelled transcripts to gene-specific probes was applied.

2.2.1 Isolation of chloroplasts

A slightly modified version of the protocol described in *Arabidopsis: A Laboratory Manual* (Weigel and Glazebrook, 2002) was used to extract and isolate intact chloroplasts from *Arabidopsis thaliana*. The method applies density gradient centrifugation of a cell extract on a discontinuous Percoll gradient in order to separate intact chloroplasts from broken ones, as well as from other organelles. All solutions were kept on ice and all procedures were carried out in the cold room (8°C). Centrifugations were done at 4°C.

Intact plastids were extracted from rosette leaves of 8 week-old WT and ΔTF1 plants at the very end of the dark period (0 h) and after four hours of light (4 h) (see Figure 5) for run-on

transcription assays. Since already short exposures to light might influence gene expression, the isolation of plastids at 0 h after daybreak was done in dim green light which has been shown to be unable to photoconvert protochlorophyllide to chlorophyll, and does thereby not promote photosynthesis (Klein and Mullet, 1986).

Rosette leaves from four plants (3-4 grams) were cut in pieces and carefully homogenized in 80ml Xpl homogenization buffer supplemented with BSA and sodium ascorbate using a small Waring blender. The homogenized suspension was filtered through two layers of Miracloth and one layer of cheesecloth (pre-soaked in homogenization buffer). Subsequently, the filtrate was centrifuged at 3500 rpm for 8 min (Beckmann Avanti J-20XP, JA14 rotor). After centrifugation, the supernatant was decanted and the pellet gently resuspended in 500µl homogenization buffer using a paint brush.

Percoll step gradients were prepared in 2ml tubes by layering 1ml 30% Percoll on top of 500µl 80% Percoll. The resuspended pellet was placed carefully on top of the Percoll step gradient using a plastic Pasteur pipette. The gradient was then centrifuged at 7500 rpm for 20 min without brakes (Eppendorf 5417R). Intact chloroplasts settled at the 30-80% boundary. These were carefully removed from the gradient using a Pasteur pipette. Intact plastids were washed with 3x volume of 50mM HEPES/330mM sorbitol (pH adjusted to 7,5 with KOH) and centrifuged at 3500 rpm for 5 min (Eppendorf 5417R). After repeating the wash step once the pellet was resuspended in 100µl of the same buffer.

The intactness of chloroplasts can be examined by phase contrast microscopy. Broken plastids appear dark and granulated while intact plastids have a shiny halo (Walker, 1965). The concentration of intact chloroplasts was determined microscopically using a Thoma counting chamber.

Xpl Homogenization Buffer*
60,2g/l sorbitol
50ml/l 1M HEPES (pH 7,5)
4ml/l 0,5M EDTA
1ml/l 1M $MgCl_2$

*After sterilization by autoclaving, BSA and sodium ascorbate were added to a final concentration of 2,5g/l and 1g/l, respectively.

PBF Percoll
30mg/ml PEG 4000
10mg/ml BSA
10mg/ml Ficoll
1ml/ml Percoll

80% Percoll	30% Percoll
0,8ml/ml PBF Percoll	0,3ml/ml PBF Percoll
4µl/ml 0,5M EDTA	4µl/ml 0,5M EDTA
1µl/ml 1M $MgCl_2$	1µl/ml 1M $MgCl_2$
1µl/ml 1M $MnCl_2$	1µl/ml 1M $MnCl_2$
50µl/ml 1M HEPES (pH 7,5)	50µl/ml 1M HEPES (pH 7,5)
165µl/ml 2M sorbitol	165µl/ml 2M sorbitol
	480µl/ml dH_2O

Isolation of chloroplasts was done in collaboration with Dr. Lan Yin (University of Tromsø).

2.2.2 *In vitro* transcription and dot blot hybridization

In order to study the rate of gene-specific transcription in isolated chloroplasts, run-on transcription assays were applied. The experimental procedure consists of *in vitro* transcription with freshly lysed plastids in the presence of radioactively labelled nucleotides. Following transcription, the labelled RNA is isolated and hybridized to gene-specific probes. The relative quantities of the radioactive signals from the respective probes will reflect the relative transcription rates for the examined genes.

In vitro transcription was carried out as has been earlier described in a number of publications (Klein and Mullet, 1990; Krupinska, 1992; Krupinska and Apel, 1989; Mullet and Klein, 1987) but with ^{33}P-UTP instead of ^{32}P-UTP as labelling agent. In order to incorporate ^{33}P-UTP exclusively into already initiated transcripts, heparin, a polysaccharide which has been shown to inhibit initiation of transcription but not elongation (Greenberg et al., 1984), was added to the run-on mix. Heparin has an additional beneficial effect by inhibiting RNA degradation (Klein and Mullet, 1990; Krause and Dieckmann, 2004).

Transcription was carried out in a total volume of 100µl consisting of 50µl 2X Run-on mix, 30µl dH_2O, 10µl ^{33}P-UTP and 10µl plastid suspension (2X 10^6 plastids/µl). The *in vitro* transcription reaction was started by pipetting up and down to disrupt the plastid membranes (Deng et al., 1987), and carried out for 6 min at 25˚C. The limited time period ensures that transcripts are not being degraded before hybridization to dot blots (Mullet and Klein, 1987). In order to stop the transcription, 20µl Stop buffer was added to the reaction mix. Before proceeding to hybridization, labelled transcripts were purified by gel filtration using illustra™ MicroSpin™ G-25 columns (GE Healthcare). The purification step is necessary in order to remove non-incorporated ^{33}P-UTP before hybridization.

Dot blots with serial dilutions of immobilized probes that target gene-specific mRNA (see Table 1) were prepared by first denaturing 320fmol/µl, 80fmol/µl and 20fmol/µl dilutions of each probe in 0,4M NaOH/10mM EDTA for 10 min at 99˚C. After cooling on ice, 200µl of each probe-dilution was spotted onto a pre-wetted nylon membrane (positively charged) using a dot blot apparatus connected to a vacuum source. When all oligos had been applied, wells were washed with 500µl 0,4M NaOH before disconnecting the apparatus. The membrane was rinsed in 2X SSC and air-dried before crosslinking oligos to the membrane using a Hoefer™ UVC 500 Ultraviolet Crosslinker. Prior to hybridization, crosslinked membranes were incubated in 12,5ml hybridization solution for 1 to 3 hours at 63˚C. Dot blot hybridization with purified, ^{33}P-UTP-labeled run-on transcripts was carried out in 12,5ml pre-heated hybridization solution for 16 to 18 hours at 63˚C using a rotating incubator (HYBAID Mini 10).

After hybridization, membranes were washed twice in 2X SSC/0,1% SDS and once in 1X SSC/0,1% SDS. All three wash steps were carried out for 10 min at 43˚C using a rotating incubator. Membranes were sealed in plastic foil immediately after washing and placed in storage phosphor screens (Imaging Screen-K (Bio-Rad)). After three weeks exposure, sites of phosphor oxidation on the screens, resulting from radioactive emission, were detected using the Personal Imager FX (Bio-Rad). Dot intensities were quantified using the Quantity One software (Bio-Rad).

Table 1: List of 60bp long gene-specific oligonucleotides used as probes in dot blot hybridization assays.

Gene	Gene description	Sequence (5′→ 3′)
pBS (1)	MCS in cloning vector pBS (negative control 1)	CGCAGCCTGAATGGCGAATGGAAATTGTAAGCGTTAATATTTTGTTAAAATTCGCGTTAA
pBS (2)	MCS in cloning vector pBS (negative control 2)	TTGAGAGTTTTCGCCCCGAAGAACGTTTTCCAATGATGAGCACTTTTAAAGTTCTGCTAT
psaA	PSI P700 apoprotein A1	TATGACTATCAAAATCGTGAGCATCAGCATGTAGGTTCCAGATCCAAGTGGTAGTATCAG
psaB	PSI P700 apoprotein A2	ATTCTGATAAAGACGTTCTTCAGTAATATCATCATGACTCTCGAAGTCATGTGCGGTAGC
psbA(1)	Photosystem II protein D1	GATCATCAAAACACCAAACCATCCAATGTAAAGACGGTTTTCAGTGCTAGTTATCCAGTT
psbA(2)	Photosystem II protein D1	GGGTAAAAATGCAATCCAATAGCTGCAGAAGTAGGAATAATGGCACCGGAAATAATATTG
psbB	Photosystem II P680 chlorophyll A apoprotein	TCCTAAACGAGTCATGAAAGGTATAACGAACATACCTTGTCTCCACATTGGATCAAGAAC
psbD	Photosystem II protein D2	CCCTAAAGCGAAATAGGCACAAGGAAAGAGCAATAGACCAGACCAACCTACAAAAACGAA
psbE	Cytochrome b559 alpha subunit	CGCAATGAATAGGGAAGGTATAGTAATGCTATGAATGACCCAGTATCGAATACTGGTAAT
psbN	Photosystem II reaction center N protein	AAGGCAGTATATAGAGCATACCCAGTAAAACTTACAAGTAACCCAGATATAAAGATGGCG
petD	Cytochrome b6/f complex subunit 4	GTTCTAAAACCGCTAAGCCTACGTTACAGGCAATGGTACCAAGAATAACTACTGGAAAAA
rbcL	RuBisCO large subunit	GAGTTACTCGGAATGCTGCCAAGATATCAGTATCCTTGGTTTCATATTCAGGAGTATAGT
atpB	ATP synthase CF1 beta subunit	AATTTCTTGACCAAGAGTATCTCGACCCTTAACCACCAGAGCATTGTAAATATTAGGCAT
rrn16	16S ribosomal RNA	ATTCGCGGCATGTCAAGCCCTGGTAAGGTTCTTCGCTTTGCATCGAATTAAACCACATGC
rrn23	23S ribosomal RNA	AATCGCTTTTGCTTTCTTTTCCTCTGGCTACTAAGATGTTTCAGTTCGCCAGGTTGTCTC
ndhA	NADH dehydrogenase subunit 1	ATCCCTGCAGATATTTCTCTTTCTAACCACACAATTACTAGTACACCTGTTATGATTCCC
ndhB	NADH dehydrogenase subunit 2	CAGAGGTTGAATCGATCATCAGAAGAAGAATTAGGCCAAAAATTAGGATACATTCTGGGA
ycf2	Essential gene, unknown function	ATGAAAGATCCCACTGAATTGAATTGGGTCCATGAATCTAAGAAATAGTGAGCATTCTTG
rpoA	RNA polymerase alpha subunit	TGGCCTTTCATAAGTGGAGACAGAATAAAGCGTCCATAATAAAGACGCTTACTGTCTCTT
rpoB	RNA polymerase beta subunit	AATCCCGCGGATACATATAATTCAGAAGAATATGTAAGTGATTCATAGACAGCATCTCGT
rpl2	50S ribosomal protein L2	GTAATTATTCCTCTGGCATTACGACCTTTACCACAATGATGCTGCCCACAGATCAAATTA
rps12	Ribosomal protein S12	CTTTACGTAAAGCAGAGTTTGGTTTTTTGGGGGTGATAGTATACACCCGAGTACATGTTC
clpP	ATP-dependent Clp protease proteolytic subunit	TAATCTTTCTCGATAAAGTCGGTTGTATATGTCAACCCAAGATGTATCTCCTTCTCCAGG
accD	Acetyl-CoA carboxylase beta subunit	CCCTAACAAAAAAGGTGTCATCCGATATGAAATTGCGAATGTCCTTGGAGCTAACTAAAA

2X Run-on mix
40U/µl RNasin
100mM HEPES(pH adjusted to 8 with KOH)
20mM $MgCl_2$
50mM K-acetate
20mM DTT
250mM ATP
250mM CTP
250mM GTP
1mg/ml heparin

Stop buffer
50mM Tris (pH adjusted to 8 with HCl)
25mM EDTA
5% Na-sarcosinate

Hybridization solution
5X SSPE
5X Denhardt's solution (2% BSA, 2% Ficoll, 2% PVP-360)
0,5% SDS
40µg/ml denatured Herring sperm DNA

20X SSPE
3,6M NaCl
20mM EDTA
200mM Na-phosphate (pH 7,7)

20X SSC
3M NaCl
300mM trisodium citrate (pH adjusted to 7 with HCl)

Run-on transcription and dot-blot hybridization were done in collaboration with Prof. Kirsten Krause (University of Tromsø).

2.3 RT-qPCR

In order to investigate the effect of TF1 on the expression of certain nuclear-encoded genes, reverse transcription on isolated RNA was used to generate cDNA for relative quantification by real-time PCR.

2.3.1 RNA isolation and cDNA synthesis

RNA was isolated from 8 week-old WT and ΔTF1 *A. thaliana* at 0 h and 4 h after daybreak (see Figure 5). In order to avoid light-induced changes in transcription, care was taken not to expose the 0 h-plants to light before RNA was extracted.

In this study, treatment with hot borate buffer (Hall et al., 1978) was applied to ensure complete extraction of total RNA from plant tissue.

Rosette leaves were quickly frozen in liquid nitrogen and stored at -80˚C for later RNA isolation. Total RNA was extracted by grinding 200-600mg frozen tissue using a bead beater. The powdered leaves were then mixed with 800µl borate buffer (pre-warmed to 65˚C) and 600µl phenol by vortexing. The mixture was incubated for 20 min at 30^{o}C and subsequently centrifuged for 10 min at 14000 rpm. Following centrifugation, the aqueous phase was transferred to a new tube and mixed with 600µl phenol:chlorophorm:isoamyl alcohol (25:24:1) by vortexing. After incubation at 30^{o}C for 10 min the tubes were centrifuged for 10 min at 14000 rpm. The aqueous phase was transferred to a new tube and mixed with 600µl chloroform:isoamyl alcohol (24:1) by vortexing. After incubation at 30^{o}C for 10 min the tubes were again centrifuged for 10 min at 14000 rpm. RNA in the aqueous phase was precipitated at 4˚C overnight by adding LiCl to a final concentration of 2M. The next day, the tube was centrifuged at maximum speed for 15 min. After washing the pellet twice with 70% ethanol, it was dried using a speed vacuum system (Savant SpeedVac), and subsequently resuspended in 30µl dH_2O.

Borate Buffer*
200mM Na-Borate
30mM EGTA
1% (w/v) SDS

*Before sterilization by autoclaving, pH was adjusted to 9 with NaOH.

Since gDNA isolated together with RNA will affect the later quantification by qPCR, the DNA-*free*™ Kit (Applied Biosystems) was used remove all DNA from the RNA isolates. The kit uses a recombinant DNase in an optimized reaction buffer to digest DNA followed by a cleanup step which removes the enzyme.

Reverse transcription reactions were carried out using the SuperScript II Reverse Transcriptase Kit (Invitrogen). An oligo-dT primer was used to synthesize cDNA from all mRNA with a poly(A) tail.

Isolation of RNA, removal of DNA, and cDNA synthesis was performed by Dr. Lan Yin (University of Tromsø).

2.3.2 qPCR

Initially in a PCR, the number of amplicons is doubled during each cycle. However, as the amount of PCR product increases some factors in the reaction mix (e.g. primers and dNTPs) will become limiting, causing the rate of amplification to drop. Since the product level at which the saturation occurs is independent of the amount of starting template, end-point analyses like agarose gel electrophoresis used in conventional PCR, is not quantitative (Kubista et al., 2006). To quantify the amount of dsDNA, the amount of amplified product is detected after each cycle during real-time PCR. This enables definition of the exponential phase, in which the number of amplicons is doubled every cycle. From the exponential phase, the amount of starting template can be reliably calculated. There are two major ways of monitoring the amplification of PCR products: non-specific DNA-binding dyes and specific dye-labeled probes. In this study, EvaGreen (Bio-Rad), a dye that fluoresces when bound to dsDNA was used. Since the dye binds non-specifically to all dsDNA, it is crucial to verify that only one specific amplicon is being made. This is achieved by doing a melt-curve analysis after the amplification cycles.

It was mentioned earlier that the amount of PCR product is doubled after each cycle in the exponential phase. However, this is only true if the PCR efficiency is 100%. In order to check the efficiency for a given primer pair, a standard curve based on serial dilutions of the template was made for each target amplicon.

In this study, qPCR was applied to analyse the expression level of the nuclear genes *TF1* (locus tag At2g44940), *RBSC1A* (locus tag AT1G67090) and *PSBO2* (locus tag AT3G50820) in WT and ΔTF1 *Arabidopsis thaliana* at 0 h and 4 h after daybreak (see Figure 5).

Table 2: List of primers used for quantitative real-time PCR.

Primer	Sequence (5'→ 3')
TF1 forward	GACACAAGCACGACGACGAC
TF1 reverse	GCTGCCACGTGGACGAGTAG
ACT8 forward	TCCCGGCGATAAGAGAGAGAAAGAG
ACT8 reverse	GCATCGGCCATGGTCTACGATCT
RBCS1A forward	ACCTTATCCGCAACAAGTGG
RBCS1A reverse	CGAATCCGATGATCCTAATG
PSBO2 forward	GGTTTTGCTCTAGCCACCTC
PSBO2 reverse	TCTTGCCTGTGTACTTACCA

Table 3: 20µl qPCR reaction.

Reagent	Volume
SsoFast™ EvaGreen Supermix	10µl
10^{-3} cDNA dilution*	5µl
2,5µM for and rev primer	4µl
dH_2O	1µl

*For negative controls, dH_2O was used instead of cDNA.

PCRs were executed in optical 96-well plates using the CFX96™ Real-Time PCR Detection System (Bio-Rad). Mastermixes were made with SsoFast™ EvaGreen Supermix, cDNA and dH_2O, leaving primers to be added separately to each well. All samples were run in technical duplicates.

Table 4: Real-time PCR program.

Step	Temperature	Duration
Initial denaturation	95˚C	30 sec
Denaturation*	95˚C	5 sec
Annealing/Extension*	61˚C	5 sec
Melt-Curve Analysis	65-95˚C	5 sec (0,5˚C increment)

*The steps denaturation and annealing/extension were repeated in 40 cycles.

In order to monitor the amount of amplicons, fluorescence readings were executed after each PCR cycle and each 0,5˚C increment in the melt-curve analysis. The efficiency corrected ΔΔCq-method (Pfaffl, 2001) was used to calculate the relative expression of a target gene in different samples (see Figure 6). This method normalizes the Cq-value of a sample to a reference gene in order to account for differences in amount of starting template between samples. For this normalization to be valid, the expression level of the reference gene must be constant in all samples. In this study, *ACT8* (Han and Kim, 2006) was used as reference gene. In addition to reference gene-normalization, the Pfaffl method corrects for differences in PCR efficiency between different amplicons. Data were analyzed using the CFX Manager™ 2.0 Software (Bio-Rad).

$$\text{Normalized fold expression} = \frac{(E_{\text{target}})^{\Delta Cq,\ \text{target}}}{(E_{\text{reference}})^{\Delta Cq,\ \text{reference}}}$$

Figure 6: The Pfaffl equation for efficiency corrected calculation of relative gene expression based on differences in Cq-values between sample and control. E_{target}= (% Efficiency of target amplicon * 0,01) + 1. $E_{reference}$= (% Efficiency of reference amplicon * 0,01) + 1. ΔCq, target = average $Cq_{control}$ – average Cq_{sample} (target). ΔCq, reference = average $Cq_{control}$ – average Cq_{sample} (reference). The average Cq indicates the mean Cq of technical duplicates.

2.4 Yeast one-hybrid assay

Yeast one-hybrid (Y1H) is a method for detecting protein-DNA interactions. The advantage of this technique compared to many biochemical methods (e.g. gel mobility shift assay) is that it does not require any optimization of *in vitro* conditions since the protein-DNA interaction takes place inside the nucleus of yeast cells where the protein should be in its native state. The system consists of a prey protein and a bait DNA sequence upstream of a reporter gene. Binding of the prey protein to the bait sequence will activate transcription of the reporter gene. The activation is ensured by fusing the prey protein to a strong *trans*-activation domain that recruits the RNA polymerase. This means that the assay is not restricted to transcription factors that promote gene expression, but can also be used to identify DNA-binding repressors of transcription.

The reporter gene used in this study is named *HIS3*. The expression of *HIS3* will allow histidine auxotrophic yeast strains to grow on medium lacking histidine. Continuous expression of the DNA-binding protein (DBP)-activation domain (GAL4AD) fusion is ensured by the constitutive yeast promoter *ADH1*. Binding of the DBP to the bait sequence results in transcription of *HIS3*, enabling histidine auxotrophic yeast cells to form colonies on histidine-deficient medium (see Figure 7).

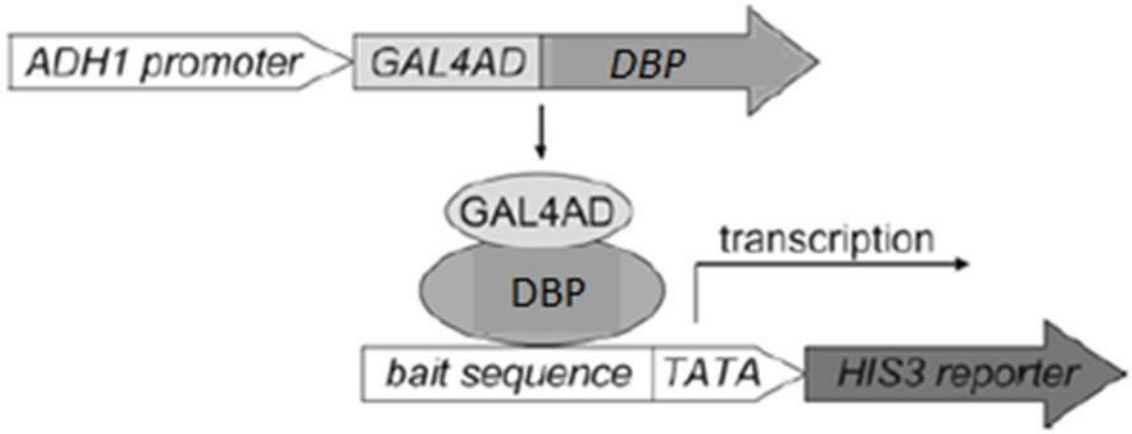

Figure 7: Schematic overview of the yeast one-hybrid system. Binding of the DBP to the bait sequence enables the GAL4AD domain to recruit the transcription machinery to the transcription start site of *HIS3*, thereby activating transcription of the reporter gene. The expression of the *HIS3* gene allows histidine auxotrophic yeast strains to grow on medium lacking this amino acid. Modified after Ouwerkerk and Meijer (2011).

In this study the yeast one-hybrid system was used to test for interactions between TF1 and specific DNA sequences. Another transcription factor of the APETALA 2/ethylene response element binding protein (AP2/EREBP) family, TINY (Sun et al., 2008), was used as a control to verify that the experimental setup was working. Most of the bait sequences used in the yeast one-hybrid assays consisted of short nucleotide sequences (7-9bp) in four tandem repeats (see Table 22). The use of repeated bait sequences enables the prey protein to bind to the DNA at the optimal distance for transcriptional activation (Lopato et al., 2006). All procedures were executed as described in Ouwerkerk and Meijer (2011) with only a few minor modifications.

2.4.1 Solutions and media used in yeast one-hybrid assays

10X TE
100mM Tris (pH adjusted to 7,5 with HCl)
10mM EDTA

10X Lithium acetate
1M Lithium acetate (pH adjusted to 7,5 with acetic acid)

50% PEG
50% (w/v) PEG-4000

YAPD*
10g/l yeast extract
20g/l peptone
20g/l glucose

*After autoclaving, 20mg/ml adenine (in 1M HCl) was added to a final concentration of 20mg/l. For making YAPD-G418 plates, 150mg/ml G418 was added to a final concentration of 150mg/l after autoclaving.

SD*
6,7g/l Yeast Nitrogen Base (- amino acids/+ ammonium sulphate) (Invitrogen)
20g/l glucose
600mg/l –Ade/-His/-Leu/-Trp DO Supplement (Clontech)
20mg/l adenine
20mg/l histidine
100mg/l leucine
20mg/l tryptophan

*For making SD/-His, SD/-Leu and SD/-His/-Leu, the respective amino acids were not added. 1M 3-amino-1,2,4-triazole (3-AT) was added after autoclaving to the desired final concentration.

All solutions/media were sterilized by autoclaving. In order to prevent caramelization of glucose, media containing this sugar was autoclaved for no longer than 15 min at 121˚C. For making agar-plates, 20g/l agar was added before autoclaving. Select Agar (Invitrogen) was used for the yeast drop-out media (SD/-His, SD/-Leu and SD/-His/-Leu) in order to avoid amino acid contamination.

2.4.2 Generation of reporter constructs

Double-stranded bait sequences with sticky overhangs corresponding to NotI and XbaI restriction sites were cloned into the pINT1-HIS3NB vector (kindly provided by Prof. Pieter B.F Ouwerkerk (University of Leiden, Netherlands)) using the NotI and XbaI sites of this vector (see Figure 36 for vector map). An exception to this way of making reporter constructs was made for the promoter region of At5g60200. Because of its size (3082bp), this bait sequence could not be generated by synthetic oligonucleotides, and a different strategy had to be chosen. A blunt-end restriction site (StuI) was constructed in the pINT1-HIS3NB vector by cloning the double-stranded NotI-StuI-NotI fragment into the NotI site of the construct. Blunt-end fragments of the 3kb promoter sequence were generated by PCR with gDNA of WT *Arabidopsis thaliana* as starting template. The PCR product was then cloned into the StuI site of the pINT1-HIS3NB+StuI vector (see Figure 37 for vector map). After verifying correct insertions by sequencing using the vector specific primers pINT1-HIS3NB forward and reverse, the reporter constructs were linearized by cutting with NcoI and AscI/SacI (see Figure 8). A linear fragment (without a large part of the vector backbone) is used for transformation to avoid single cross-over recombination into the yeast genome, which can be unstable (Ouwerkerk and Meijer, 2011).

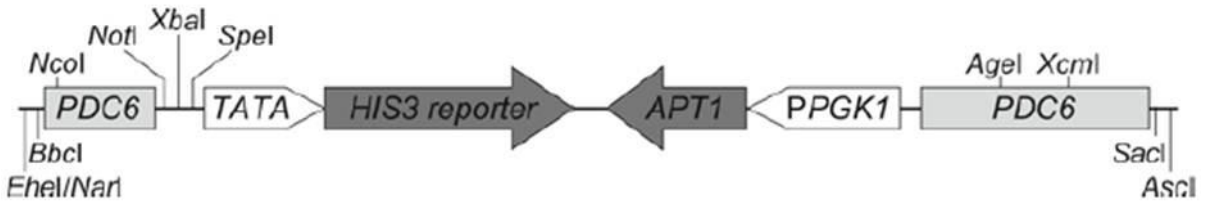

Figure 8: Schematic illustration of the *PDC6* fragment from the pINT1-HIS3NB vector which is integrated into the yeast genome by homologous recombination. Upstream of the *HIS3* reporter gene are the three restriction sites NotI, XbaI and SpeI which are used for insertion of bait sequences. Other restriction sites in the flanking *PDC6* regions are also indicated. These are applied to cut the integration fragment out of the pINT1-HIS3NB vector. Expression of the *APT1* selection gene is maintained by the yeast *PGK1* promoter. After Ouwerkerk and Meijer (2011).

Detailed descriptions of the steps leading to finished pINT1-HIS3NB reporter constructs ready for transformation into yeast can be found in chapter 2.5.

2.4.3 Preparation of lithium acetate-competent yeast cells

Yeast strain AH109 was transformed using a lithium acetate transformation procedure. All centrifugations were carried out at room temperature. 50ml YAPD was inoculated with AH109 and incubated with shaking overnight at 30˚C. On the next day the culture was diluted to OD_{600} = 0,25 and incubated with shaking at 30˚C until reaching a OD_{600} = 0,4 - 0,8 (2 h is sufficient). The yeast cells were then pelleted in a 50ml falcon tube by centrifugation for 1 min at 2500 x g (Heraeus Megafuge 1.0, swing-out rotor). The supernatant was decanted and the pellet resuspended in 50ml dH_2O. Following resuspension the cells were centrifuged again for 1 min at 2500 x g (Heraeus Megafuge 1.0, swing-out rotor). After decantation of the supernatant the pellet was resuspended in 1ml 1X TE/1X lithium acetate and transferred to a 1,5ml microcentrifuge tube. The yeast cells were then pelleted by centrifugation for 30 sec at maximum speed in a microcentrifuge and after removal of the supernatant resuspended in 250µl 1X TE/1X lithium acetate.

2.4.4 Transformation of pINT1-HIS3NB reporter constructs into yeast

Between 100ng and 500ng linearized pINT1-HIS3NB reporter construct were mixed with 30µg Blocking DNA (from Herring sperm) in a maximum volume of 10µl. 50µl of the prepared yeast suspension and 300µl 40% PEG/1X TE/1X lithium acetate (freshly made) were then added. Following mixing by vortexing, the transformation reaction was first incubated for 30min with shaking at 30˚C, and then for 15 min at 42˚C. The linearized vector is integrated into the yeast genome by double cross-over in the non-essential *PDC6* locus (see Figure 8).

After incubation, the transformed yeast cells were pelleted by centrifugation for 30 sec at maximum speed in a microcentrifuge and resuspended in 1ml YAPD. Subsequently, the yeast suspension was transferred to 15ml falcon tubes and incubated for 3h with shaking at 30˚C. This recuperation step is necessary for the transformed yeast cells to express *APT1* (see Figure 8), which confers resistance towards the selective agent G418.

Following recuperation the yeast suspension was transferred to a 1,5ml microcentrifuge tube, pelleted by centrifugation for 30 sec at maximum speed in a microcentrifuge and resuspended in 100µl 1X TE. This was then plated out on a YAPD-G418 agar plate and incubated at 30˚C.

After 3 days, growing colonies were transferred to new YAPD-G418 plates and incubated again at 30˚C. Transformed cells grew quickly overnight and were used for downstream experiments.

In order to verify that the bait sequence was in fact transferred to the yeast genome, colony PCR was executed on the different reporter strains using pINT1-HIS3NB forward and reverse primers as described in chapter 2.5.3.

2.4.5 Determining possible leaky expression of *HIS3*

Due to the possibility of activation of the *HIS3* reporter gene by endogenous yeast proteins, it is necessary to test the growth of the yeast reporter strains on histidine-deficient medium and reduce it, if required. This was done by streaking G418-resistant clones on SD/-His plates with a concentration series of 3-AT: 0, 5, 10, 25 and 50mM and incubating them for a week at 30˚C. 3-AT is a competitive inhibitor of the HIS3 enzyme and can therefore be used to reduce background growth as a result of leaky expression of the reporter gene.

2.4.6 Transformation of reporter strains with fusion expression constructs

Lithium acetate-competent reporter strains were prepared as described in chapter 2.4.3. For transformation, 1µg TINY-pGADT7 or TF1-pGADT7 was mixed with 30µg Blocking DNA in a maximum volume of 10µl. 50µl of the lithium acetate-competent yeast reporter strain and 300µl 40% PEG/1X TE/1X lithium acetate (freshly made) were then added. Following mixing by vortexing, the transformation reaction was first incubated for 30 min with shaking at 30˚C, and then for 15 min at 42˚C. The transformed yeast cells were pelleted by centrifugation for 30 sec at maximum speed in a microcentrifuge and resuspended in 1ml 1X TE. Of this, 100µl were plated on SD/-Leu plates and incubated for 3-4 days at 30˚C. Expression of the *Leu2* gene in the pGADT7 construct (see Figure 38 for vector map) allows leucine auxotrophic yeast to grow on media without leucine. To test for interaction between the protein-GAL4AD fusion and the bait sequence, colonies growing on SD/-Leu plates were transferred to SD/-His/-Leu plates with 0mM, 5mM and 10mM 3-AT and incubated at 30˚C.

2.4.7 Generation of yeast freeze cultures

For long-term storage of yeast strains, growing colonies were transferred to 1,5ml tubes containing 300µl YAPD. After resuspension by vortexing the tubes were added 300µl 50% glycerol and mixed again by vortexing. The glycerol stocks were stored at -80˚C indefinitely.

Strain recovery was done by scraping of some of the ice and plating it out on the appropriate medium followed by incubation at 30˚C.

2.5 Molecular cloning

Here follows a selection of methods that were used for the construction, replication and/or verification of recombinant DNA. These methods were applied in order to make pINT1-HIS3NB reporter constructs and pGADT7 expression constructs for the yeast one-hybrid assays.

2.5.1 Hybridization of oligonucleotides

Double stranded bait sequences were generated from oligonucleotides with partially complementary sequences (see Table 6) following a protocol recommended by SIGMA-ALDRICH. With this method, one or more repetitions of the putative binding motif can be generated, depending on the ratio of single stranded oligos used. The oligos were mixed in annealing buffer as shown in Table 5 and heated to 95˚C for 4 min. The heating ensures complete denaturation and removal of any secondary structures. The complementary DNA strands were then allowed to hybridize by slowly cooling down to room temperature. Double-stranded oligos were stored at 4˚C before usage.

Annealing buffer
10mM Tris (pH adjusted to 7,5-8 with HCl)
50mM NaCl
1mM EDTA

Table 5: Volumes of oligonucleotides and annealing buffer mixed together in order to construct bait sequences with overhanging NotI (for)- and XbaI (rev)-sticky ends.

Name	$V_{forward\ oligo\ (100\mu M)}$	$V_{reverse\ oligo\ (100\mu M)}$	$V_{psbA\text{-}NotI\ (100\mu M)}$	$V_{psbA\text{-}XbaI\ (100\mu M)}$	$V_{Annealing\ buffer}$
DRE	10µl	10µl			80µl
DREmut	10µl	10µl			80µl
GCC	10µl	10µl			80µl
GCCmut	10µl	10µl			80µl
invGCC	10µl	10µl			80µl
invGCCmut	10µl	10µl			80µl
psbA	8µl	8µl	2µl	2µl	80µl
psbAmut	8µl	8µl	2µl	2µl	80µl
psbAcore4(a)	10µl	10µl			80µl
psbAcore4(b)	10µl	10µl			80µl
*NotI-StuI-NotI	10µl				40µl

*The NotI-StuI-NotI oligo was not used as bait sequence, but in order to create a StuI site in the pINT1-HIS3NB vector.

Table 6: List of oligonucleotides used for generation of double-stranded bait sequences.

Oligonucleotide	Sequence (5′→ 3′)
DRE forward	GGCCGCTACCGACATTACCGACATTACCGACATTACCGACATA
DRE reverse	CTAGTATGTCGGTAATGTCGGTAATGTCGGTAATGTCGGTAGC
DREmut forward	GGCCGCTACTGACATTACTGACATTACTGACATTACTGACATA
DREmut reverse	CTAGTATGTCAGTAATGTCAGTAATGTCAGTAATGTCAGTAGC
GCC forward	GGCCGCAGCCGCCAGCCGCCAGCCGCCAGCCGCCA
GCC reverse	CTAGTGGCGGCTGGCGGCTGGCGGCTGGCGGCTGC
GCCmut forward	GGCCGCATCCTCCATCCTCCATCCTCCATCCTCCA
GCCmut reverse	CTAGTGGAGGATGGAGGATGGAGGATGGAGGATGC
Inv. GCC forward	GGCCGCGGCGGCTGGCGGCTGGCGGCTGGCGGCTA
Inv. GCC reverse	CTAGTAGCCGCCAGCCGCCAGCCGCCAGCCGCCGC
Inv. GCCmut forward	GGCCGCGGAGGATGGAGGATGGAGGATGGAGGATA
Inv. GCCmut reverse	CTAGTATCCTCCATCCTCCATCCTCCATCCTCCGC
psbAcore4(a) forward	GGCCGCCATCCGACCATCCGACCATCCGACCATCCGACA
psbAcore4(a) reverse	CTAGTGTCGGATGGTCGGATGGTCGGATGGTCGGATGGC
psbAcore4(b) forward	GGCCGCATCCGACTAATCCGACTAATCCGACTAATCCGACTAA
psbAcore4(b) reverse	CTAGTTAGTCGGATTAGTCGGATTAGTCGGATTAGTCGGATGC
psbA forward	TTATCTACTCCATCCGACTAGTTCCGGGTTCGAGTCCCGGGCAACCCA
psbA reverse	GAACTAGTCGGATGGAGTAGATAATGGGTTGCCCGGGACTCGAACCCG
psbAmut forward	TTATCTACTCCATTTTTTTAGTTCCGGGTTCGAGTCCCGGGCAACCCA
psbAmut reverse	GAACTAAAAAAATGGAGTAGATAATGGGTTGCCCGGGACTCGAACCCG
psbA-NotI	GGCCCGGGTTCGAGTCCCGGGCAACCCA
psbA-XbaI	CTAGTGGGTTGCCCGGGACTCGAACCCG
*NotI-StuI-NotI	GGCCGCAGGCCTGC

*The NotI-StuI-NotI oligo was not used as bait sequence, but in order to create a StuI site in the pINT1-HIS3NB vector.

2.5.2 Polymerase chain reaction

Polymerase chain reaction (PCR) is a frequently used method to amplify a specific DNA sequence from a starting template. The reaction consists of three different temperature steps (denaturation, annealing and extension) that are repeated in a number of cycles (usually 25-35) to generate the desired amount of amplicons. In the denaturation step, the hydrogen bonds that connect the two strands in the DNA double helix are broken by heat (94-98˚C) resulting in ssDNA. Next, the temperature is lowered (50-65˚C) to allow annealing of primers (synthetically designed oligonucleotides that are complementary to the 3'ends of each strand of the sequence to be amplified). The temperature is then raised to 72˚C so that a thermostable DNA polymerase can catalyse the attachment of complementary dNTPs, starting from the free 3'end of both primers and proceeding in 5'→ 3' direction. In this way, the amount of amplicon is being doubled every cycle (Kubista et al., 2006).

Table 7: List of primers used for amplification of DNA by PCR.

Primer	Sequence (5'→ 3')
pINT1-HIS3NB forward	TCACGGCGATAACGTAGTATTTAG
pINT1-HIS3NB reverse	GGCTTTCTGCTCTGTCATC
TOPO-TINY forward	CACCATGATAGCTTCAGAGAGTACC
TINY reverse	TTAATAATTATACAGTCCTTGAAGATCCC
M13 forward	GTAAAACGACGGCCAG
SP/pGADT7-rfB/9236-2293	GAAAGGTCGAATTGGGTACC
At5g60200 promoter forward S8 in (Lee et al., 2006)	CCGAATTAGCATTAGGTCGAA
At5g60200 promoter reverse S8 in (Lee et al., 2006)	AAGAGCTGAATCTGAGAAGTTGC
At5g60200 promoter reverse_b	GCACTAACAGTTCAGACACCTTTT

DyNAzyme^{TM} II DNA Polymerase (Finnzymes) was used for all PCRs except when amplification of blunt-end products was needed. For this purpose, Phusion High-Fidelity DNA Polymerase (Finnzymes) was applied.

Table 8: 20µl DyNAzyme™ II DNA Polymerase PCR reaction. Different amounts of starting template were used.

Reagent	Volume
10X DyNAzyme™ buffer	2µl
2,5mM dNTPs	2µl
10µM forward primer	1µl
10µM reverse primer	1µl
DyNAzyme™ II DNA Polymerase (1U/µl)	0,2µl
Template	x
dH_2O	→ 20µl

Table 9: 20µl Phusion High-Fidelity DNA Polymerase PCR reaction. Different amounts of starting template were used.

Reagent	Volume
5x Phusion High-Fidelity reaction buffer	4µl
2,5mM dNTPs	2µl
10µM forward primer	1µl
10µM reverse primer	1µl
Phusion High-Fidelity DNA Polymerase (2U/µl)	0,2µl
Template	x
dH_2O	→ 20µl

Table 10: PCR program for (A) DyNAzyme™ II DNA Polymerase and (B) Phusion High-Fidelity DNA Polymerase PCR reactions.

Step	Temperature (A)	Duration (A)	Temperature (B)	Duration (B)
Initial denaturation	94˚C	2 min	98˚C	30 sec
Denaturation*	94˚C	30 sec	98˚C	10 sec
Annealing*	**	30 sec	**	30 sec
Extension*	72˚C	***	72˚C	***
Final extension	72˚C	5 min	72˚C	5 min
Hold	10˚C	∞	10˚C	∞

*The steps denaturation, annealing and extension were repeated in 30 cycles.

**The annealing temperature was set to 2˚C below the T_m of the primer with the lowest T_m.

***The extension time was adjusted to fit the size of the amplicon. The polymerization-speed of DyNAzyme™ II DNA Polymerase and Phusion High-Fidelity DNA polymerase is 40 sec/1kb and 30 sec/1kb, respectively.

2.5.3 Colony PCR

For bacterial cells such as *E. coli*, the initial denaturation step of a PCR will disrupt the cell wall and make intracellular DNA accessible. Because of this, PCR with single colonies of transformed *E. coli* as starting template was frequently used to confirm the presence of a plasmid with the correct insert.

The cell walls of yeast are not as easily broken as prokaryotic cell walls. Therefore, in order to release DNA from yeast, cells were resuspended in 30µl 0,2% SDS by vortexing before incubating at 90˚C for 4 min. Following centrifugation at 14000 rpm for 30 sec, the supernatant was saved and used for PCR. To prevent inhibition of PCR amplification by SDS, only 0,5µl of the supernatant was used as starting template.

Except for the starting template, colony PCRs were performed with the same reaction mix and program as conventional PCRs (see chapter 2.5.2).

2.5.4 Agarose gel electrophoresis

Due to the negatively charged phosphate backbone of nucleic acids they can be separated by size on an agarose gel when an electric field is applied. Shorter nucleic acids will migrate faster towards the positive pole since they move more easily through the pores of the agarose matrix. In order to visualize DNA fragments, the gel is stained with ethidium bromide which fluoresces orange under UV-light when it is intercalated in dsDNA.

Agarose gel electrophoresis was used to document the size of PCR products and to verify DNA digestion with restriction endonucleases.

1X TAE Buffer
40mM Tris (adjusted to pH 8,5 with acetic acid) **1mM EDTA**

0,5-2% (w/v) Agarose gel
*Agarose
**1X TAE Buffer
1 drop of EtBr Solution "Electran" (VWR)

*Different concentrations of agarose were used depending on the expected sizes of the DNA pieces. E.g., for separation of small fragments (50bp – 2000bp) a 2% agarose gel was used, while separation of larger fragments (500bp-10 000bp) was done on a 1% agarose gel.

** The volume of 1X TAE buffer depended on the size of the gel being made.

Agarose was solubilized in 1X TAE buffer by boiling in a microwave oven and subsequently poured into a gel frame, supplemented with EtBR, and allowed to polymerize for 30 min before running electrophoresis.

Before loading, 10X Loading Buffer was added to the samples to give a 1X final concentration. This ensures that the samples sink to the bottom of the wells and allows monitoring of their progression through the gel. In order to estimate sizes, DNA molecular weight markers (GeneRuler™ 1kb DNA Ladder and/or GeneRuler™ 50bp DNA Ladder, both from Fermentas) were included in all gel runs. Agarose gels were run at 100V.

10X Loading Buffer
250mM Tris (pH adjusted to 7,5 with HCl)
40% Glycerol
0,2% Bromophenol Blue

2.5.5 Extracting DNA from agarose gels

PCR products were isolated from agarose gels using Zymoclean™ Gel DNA Recovery Kit (ZYMO RESEARCH). The method uses a buffer system that allows separation of DNA from the agarose followed by adsorption of the DNA to a column matrix. After washing, the pure DNA is eluted with dH_2O.

2.5.6 Precipitation of DNA from aqueous solution

Nucleic acids are negatively charged and therefore soluble in polar solvents like water. Positive ions (such as Na^+ of sodium acetate) can neutralize the negative charges on the phosphate backbone and thereby make the molecule much less hydrophilic. However, since water has a high dielectric constant and forms hydration shells around charged molecules, the ionic forces between Na^+ and PO_3^- are very small. By adding ethanol (which has a lower dielectric constant than water), the oppositely charged ions can interact more easily and form stable ionic bonds, causing DNA to drop out of solution due to its increased hydrophobicity.

A slightly modified version of the procedure described in Current Protocols in Immunology (Moore, 2001) was routinely used for making more concentrated solutions of DNA. 0,1X volume of 3M sodium acetate (pH 5,2) was added to the DNA solution. 2,5X volumes of ice cold EtOH were then added and mixed by inverting. After 15 min incubation on ice the mixture was centrifuged for 15 min at maximum speed in a microcentrifuge. The supernatant was then removed and the pellet washed in 1ml ice cold 70% EtOH, followed by centrifugation for 5 min at maximum speed in a microcentrifuge. The supernatant was removed and the pellet air dried. Precipitated DNA was resuspended in the appropriate volume of dH_2O.

2.5.7 DNA digestion with restriction enzymes

Restriction endonucleases catalyse the breaking of phosphodiester bonds within a chain of nucleotides. The enzyme recognizes short (usually 4-8bp) nucleotide sequences which are normally inverted palindromes, resulting in cleavage of both DNA strands. Depending on the recognition sequence, restriction enzymes can make restriction fragments with either blunt ends (cleavage in the centre of the palindrome) or cohesive ends.

In this study, the pINT1-HIS3NB vector construct was digested with the enzymes NotI and XbaI (see Table 11) for the purpose of directional insertion of all bait sequences, except the At5g60200 promoter. This bait sequence was cloned into the vector using a blunt-end restriction site (StuI) which had been constructed in the pINT1-HIS3NB vector by cloning the

double-stranded NotI-StuI-NotI fragment into the NotI site of the construct (see Table 11 and chapter 2.5.8).

Also, pINT1-HIS3NB vector constructs with inserted bait sequences were linearized by cutting with NcoI and AscI/SacI (see Table 11).

Table 11: List of restriction digestions and the respective conditions.

Substrate	Enzyme(s)	Buffer system*	Total volume	Incubation	Deactivation
650ng pINT1-HIS3NB	5U NotI (10U/µl) and 5U XbaI (10U/µl)	2X Buffer Tango™ (Fermentas)	20µl	37˚C, overnight	65˚C, 20 min
650ng pINT1-HIS3NB	5U NotI (10U/µl)	1X Buffer Orange (Fermentas)	20µl	37˚C, 1 h	65˚C, 20 min
500ng pINT1-HIS3NB+StuI	5U StuI (10U/µl)	1X Buffer Blue (Fermentas)	20µl	37˚C, 1 h	80˚C, 20 min
1-4µg pINT1-HIS3NB+bait seq.	5U NcoI (10U/µl) and 5U AscI (5U/µl) or SacI (10U/µl)	1X Buffer Tango™ (Fermentas)	10µl	37˚C, overnight	65˚C, 20 min

*Diluted from a 10X stock of the respective buffer.

2.5.8 Ligation of linear DNA fragments

DNA ligase catalyses the formation of a phosphodiester bond between 5’ phosphates and 3’ hydroxyl termini of nucleic acids. It can therefore be used to join DNA fragments with either cohesive or blunt ends, and is commonly applied to ligate a specific DNA sequence into a vector construct which has been digested with a restriction endonuclease. If there is a high probability for re-ligation of the digested vector (e.g. when cutting with a single enzyme), it is beneficial to dephosphorylate the vector since a phosphate group at the 5’ terminus is necessary for ligation to occur. Custom made oligos are normally dephosphorylated, meaning that annealed oligonucleotides and PCR products will not contain 5’ phosphates. This makes it necessary to phosphorylate these fragments before ligation into a dephosphorylated vector. As with any chemical reaction, the efficiency of a ligation reaction is dependent on the likelihood of substrates and enzyme coming together at the right time for the reaction to happen. Therefore, in order to increase the reaction efficiency for difficult ligations, reaction mixes are supplemented with polyethylene glycol (PEG) as described in

Table 14. PEG acts as a volume excluder, resulting in DNA and enzyme being concentrated into a smaller volume than originally set up.

In this study, double-stranded bait sequences were ligated into the NotI- and XbaI-digested pINT1-HIS3NB construct (see Table 14). A double digestion greatly decreases the chance for re-ligation, making it unnecessary to dephosphorylate the vector before ligation. Also, a double digestion is directional since there is only one possible orientation for ligation of inserts with complementary overhangs.

In the special case of the At5g60200 promoter-bait sequence, the double-stranded NotI-StuI-NotI fragment was first ligated into the NotI-digested pINT1-HIS3NB, and, after digesting with StuI (see chapter 2.5.7), the bait sequence was inserted into the vector by blunt-end ligation (see Table 14). For these two ligations it was beneficial to pre-phosphorylate (see Table 12) the insert and pre-dephosphorylate (see Table 13) the vector in order to increase the chance of correct insertion.

Table 12: 5'-phosphorylation of DNA.

Reagent	Volume
Linear dsDNA	*
10X Reaction Buffer A (forward reaction)	2µl
10mM ATP	2µl
T4 Polynucleotide Kinase (10U/µl)	1µl
dH_2O	→20µl

*Different quantities of DNA were phosphorylated. The recommended amount is 1-20pmol 5'-termini.

The phosphorylation reaction was incubated at 37˚C for 20 min. Subsequent deactivation of the kinase was done by incubation at 75˚C for 10 min.

Table 13: Dephosphorylation of DNA 5'-termini.

Reagent	Volume
Linear dsDNA	*
10X FastAP™ Buffer	2µl
FastAP™ Thermosensitive Alkaline Phosphatase (1U/µl)	1µl
dH_2O	→20µl

*Different quantities of DNA were dephosphorylated. The recommended amount is 1pmol termini.

The dephosphorylation reaction was incubated at 37˚C for 10 min. The phosphatase was inactivated by incubation at 75˚C for 5 min.

Table 14: List of ligation reactions and the respective conditions.

Ligation	Insert:Vector (molar ratio)	Ligase	Buffer system	Additions	Total volume	Incubation	Comments
Sticky-end, directional	3:1	1µl T4 DNA Ligase (1U/µl)	2µl 10X T4 DNA ligase Buffer		20µl	22˚C, 1 h	
Sticky-end, non-directional	3:1	2µl T4 DNA Ligase (1U/µl)	2µl 10X T4 DNA ligase Buffer	2µl 50% PEG 4000	20µl	22˚C, 1 h	Dephosphorylated vector, phosphorylated insert
Blunt-end	3:1	1µl T4 DNA Ligase (5U/µl)	2µl 10X T4 DNA ligase Buffer	2µl 50% PEG 4000	20µl	16˚C, overnight	Dephosphorylated vector, phosphorylated insert

After ligation, 5µl of the reaction was used for transformation of 50µl chemically competent TOP10 cells (see chapter 2.5.12). Transformed bacteria were plated out on LB-Amp(Carb) since the pINT1-HIS3NB construct codes for ampicillin resistance (see Figure 36). Growing colonies were checked for insertions by colony PCR (see chapter 2.5.3) using pINT1-HI3NB forward and pINT1-HI3NB reverse primers (see Table 7). The nucleotide sequence of the insert was then revealed by DNA sequencing (see chapter 2.5.14) of either the PCR product after its extraction from the gel (see chapter 2.5.5) or the isolated plasmid vector (see chapter 2.5.13).

2.5.9 Generation of Entry Clones by TOPO cloning

The *TINY*-TOPO blunt-end PCR product was cloned into the pENTR™/SD/D-TOPO vector (see Figure 39 for vector map) using pENTR™ Directional TOPO cloning kit (Invitrogen). The technology utilizes the ability of Topoisomerase I from *Vaccinia* virus to perform sequence specific (CCCTT) cleavage and subsequent restoration of the phosphodiester backbone of nucleotide strands in order to insert DNA fragments into plasmid vector without the use of ligase. The insertion is made directional by adding the four bases CACC to the forward PCR primer. This four nucleotide long sequence is complementary to the GTGG overhang in the entry vector generated by the cleavage activity of topoisomerase. The reaction mixture for the TOPO cloning reaction is given in Table 15.

Table 15: 3µl pENTR™ Directional TOPO cloning reaction.

Reagent	Volume
TINY-TOPO PCR product (9ng/µl)	2µl
Salt Solution	0,5µl
Linearized pENTR™/SD/D-TOPO (15-20ng/µl)	0,5µl

The TOPO cloning reaction was incubated for 30 min at room temperature. Subsequently, the entire reaction was used to transform 50µl chemically competent TOP10 cells as described in chapter 2.5.12. Transformed bacteria were plated on LB-Kan since the pENTR™/SD/D-TOPO vector codes for a kanamycin resistance gene (see Figure 39). Growing colonies were checked for insertions by colony PCR (see chapter 2.5.3) using M13 forward and TINY reverse primers (see Table 7). Plasmid DNA was isolated from positive clones (see chapter 2.5.13) and sequenced (see chapter 2.5.14) in both directions using M13 forward and reverse primers (see Table 17).

2.5.10 Generation of Expression Clones by LR Recombination

TINY was transferred from the pENTR™/SD/D-TOPO vector to the pGADT7 expression plasmid (see Figure 38 for vector map) by the Gateway LR Recombination Reaction. The Gateway Technology uses the site-specific recombination properties of bacteriophage

lambda to move DNA fragments between vector systems. The reaction for the LR recombination reaction contained the components and volumes indicated in Table 16.

Table 16: 2,5µl LR Recombination Reaction.

Reagent	Volume
TE buffer (10mM Tris, 1mM EDTA (pH 8))	1µl
Gateway LR Clonase™ II Enzyme Mix (Invitrogen)	0,5µl
pGADT7 (150ng/µl)	0,5µl
pENTR™/SD/D-TOPO-*TINY* (375ng/µl)	0,5µl

The LR reaction was incubated for 30 min at room temperature. After that, the entire reaction was used to transform 50µl chemically competent TOP10 cells (see chapter 2.5.12). Transformed bacteria were plated on LB-Amp(Carb) since the pGADT7 construct codes for a gene conferring ampicillin resistance (see Figure 38). Growing colonies were checked for insertions by colony PCR (see chapter 2.5.3) using SP/pGADT7-rfB/9236-2293 and TINY reverse primers (see Table 7). Plasmid DNA was isolated from positive clones (see chapter 2.5.13) and used for yeast one-hybrid assays (see chapter 2.4).

The pGADT7-TF1 construct was made by Dr. Bernd Ketelsen (University of Tromsø) using the same approach.

2.5.11 Preparation of chemically competent TOP10 *E. coli* cells

In molecular biology, a cell is said to be competent when it is able to take up foreign DNA. Being large and negatively charged, DNA molecules are not able to passively diffuse across the hydrophobic core of the cell membrane. Because of this, methods for making cells competent are of great importance. There are in general two different techniques for generating competent cells: electroporation and chemical transformation. The first applies an electrical current across the cell to generate momentary pores in the cell membrane through which the DNA can pass. Cells can be made chemically competent by resuspension in a $CaCl_2$ solution at low temperatures (0˚C). The Ca^{2+} ions will mask the negative charge of the nucleic acid and create pores in the cell membrane which the DNA can pass through.

Here, a variant of the Hanahan protocol (Hanahan et al., 1991) was used to make chemically competent TOP10 *E. coli* cells. Freeze cultures of TOP10 were prepared by growing cells on solid SOB medium over night at 23˚C (room temperature). The next day, single colonies were picked and transferred to 2ml liquid SOB for overnight growth at 23˚C. Glycerol was added to a concentration of 15% and 1ml aliquots were stored at -80 ˚C indefinitely. 250ml SOB was inoculated with 1ml TOP10 freeze culture and incubated at 20˚C overnight. This should yield an OD_{600} of about 0,5. The culture was centrifuged at 3000 x g at 4˚C for 10 min. The supernatant was decanted and the pellet resuspended in 80ml ice cold CCMB80 buffer and incubated on ice for 20 min. After incubation the culture was centrifuged again at 3000 x g at 4˚C for 10 min. The supernatant was decanted and the pellet resuspended in 10ml ice cold CCMB80 buffer. The OD_{600} was measured using a mixture of 600µl SOB and 150µl resuspension. Based on the OD_{600}, ice cold CCMB80 buffer was added to the culture to yield a final OD_{600} of 1-1,5. 50µl aliquots were prepared in pre-chilled tubes, frozen immediately in liquid nitrogen and stored at -80˚C until use.

SOB*
5g/l yeast extract
20g/l tryptone
10mM NaCl
2,5mM KCl
20mM $MgSO_4$

*For making agar-plates, 20g/l agar was added before sterilization by autoclaving.

CCMB80 buffer*
10mM KOAc (pH 7)
80mM $CaCl_2$
20mM $MnCl_2$
10mM $MgCl_2$
10% glycerol

*Before sterilization by sterile filtration, pH was adjusted to 6,4 with HCl.

2.5.12 Transformation of chemically competent TOP10 *E. coli* cells

A version of the commonly used heat-shock method (van Die et al., 1983) was applied to facilitate the uptake of foreign DNA. 50µl chemically competent TOP10 cells were thawed on ice. Immediately after thawing, the appropriate amount of plasmid DNA was added to the cell suspension and gently mixed by tapping the tube. After 10-30 min incubation on ice the cells were heat shocked at 42˚C for 45 sec and thereafter incubated on ice again for 2 min. 250µl LB were then added to the cells followed by incubation at 37˚C with shaking for 1 h. 100-200µl of the cell suspension was plated out on LB plates with the suitable antibiotic for selection.

LB*
10g/l tryptone **5g/l yeast extract** **10g/l NaCl**

*For making agar-plates, 20g/l agar were added before autoclaving. Antibiotic stock solutions (50µg/µl) were added after autoclaving to a final concentration of 100µg/ml for LB-Amp(Carb) and 50µg/ml for LB-Kan.

2.5.13 Isolating plasmid DNA from *E. coli*

The GenElute Plasmid Miniprep Kit (Sigma-Aldrich) was used to isolate plasmids from liquid cultures of recombinant *E. coli*. 5ml overnight culture (LB supplemented with appropriate antibiotic and inoculated with a single colony before incubating at 37˚C with shaking) was centrifuged for 1 min at maximum speed in a microcentrifuge to harvest the cells. The bacteria were then subjected to a modified alkaline SDS lysis (Birnboim and Doly, 1979) followed by adsorption of re-natured plasmid DNA onto silica-columns in the presence of high salt concentration (Vogelstein and Gillespie, 1979). After a wash step, the plasmids were eluted from the column using the supplied elution solution or dH_2O. DNA concentration and purity was checked using a NanoDrop ND-1000 Spectrophotometer (NanoDrop Technologies).

2.5.14 DNA sequencing

Sanger sequencing, also known as dideoxy sequencing was used to determine the order of nucleotides in a stretch of DNA. The method applies a PCR reaction which contains the template to be sequenced, a single primer complementary to the 3'end of the strand to be sequenced, DNA polymerase and a mixture of dNTPs and fluorescently labelled ddNTPs. Since ddNTPs lack the 3'-OH group, an insertion of this type of nucleotide will terminate the extension. The result is a collection of many terminated strands of different sizes, all with a fluorescently labelled ddNTP at the 3'end corresponding to the position of that nucleotide in the original template. The PCR products are then size separated with single-base-pair resolution by capillary electrophoresis and excited to reveal the emission spectrum of the terminal ddNTP. Since the four different ddNTPs have different emission spectra the identity of each terminal ddNTP can be determined and, based on the sizes of the fragments, put together to a continuous DNA sequence (Shendure et al., 2008).

In this study, the BigDye Terminator v3.1 Cycle Sequencing Kit (Applied Biosystems) was used to sequence plasmid vectors and PCR products. The list of sequencing primers, the BigDye Terminator v3.1 PCR reaction and the PCR program for BigDye Terminator v3.1 Cycle Sequencing can be found in Table 17, Table 18 and Table 19, respectively.

Table 17: List of primers used for sequencing.

Primer	**Sequence (5'→ 3')**
pINT1-HIS3NB forward	TCACGGCGATAACGTAGTATTTAG
pINT1-HIS3NB reverse	GGCTTTCTGCTCTGTCATC
M13 forward	GTAAAACGACGGCCAG
M13 reverse	CAGGAAACAGCTATGAC

Table 18: 10µl BigDye Terminator v3.1 PCR reaction.

Reagent	**Volume**
BigDye Terminator v1.1/3.1 Sequencing Buffer (5X)	2µl
3,2µM primer	0,5µl
Template	*
BigDye v3.1 Ready Reaction Mix	0,5µl
dH_2O	→10µl

*150-300ng plasmid vector or 5-20ng gel extracted PCR product (500-1000bp) was used as template.

Table 19: PCR program for BigDye Terminator v3.1 Cycle Sequencing.

Step	Temperature	Duration
Initial denaturation	96˚C	1 min
Denaturation*	96˚C	10 sec
Annealing*	50˚C	5 sec
Extension*	60˚C	4 min
Hold	10˚C	∞

*The steps denaturation, annealing and extension were repeated in 25 cycles.

After running the BigDye Terminator v3.1 Cycle Sequencing PCR, the total volume of a PCR reaction was adjusted to 20µl by adding 10µl dH_2O, before delivering them to the sequencing facility. Purification of PCR products, capillary electrophoresis and emission detection was carried out by the DNA Sequencing Core Facility (Universitetssykehuset Nord-Norge).

2.6 Extraction of proteins from yeast

Total protein was extracted from yeast cells using a "fast and easy" protocol enabling proteins to be extracted directly from colonies growing on agar-plates (Kushnirov, 2000).

A patch of approximately 2X 10mm growing yeast cells was scraped of agar-plates and resuspended in 100µl dH_2O by vortexing. 100µl 0,2M NaOH were then added, and the mixture was incubated at room temperature for 5 min. Following incubation, the cells were pelleted by centrifugation for 1 min at 14000 rpm, the supernatant was removed and the pellet resuspended in 50µl SDS sample buffer. After boiling for 3 min at 99˚C, the cells were pelleted again by centrifugation for 1 min at 14000 rpm. The protein-containing supernatant was transferred to a new tube and used for SDS-PAGE.

SDS sample buffer
60mM Tris (pH adjusted to 6,8 with HCl)
5% glycerol
2% SDS
100mM DTT
0,0025% bromophenol blue

2.7 SDS-PAGE

Sodium dodecyl sulphate polyacrylamide gel electrophoresis (SDS-PAGE) is a widely used technique for separating proteins according to their molecular mass. In their native state, proteins will have different conformations depending on the chemical properties of the side chains of their amino acids residues. Because of this, polypeptides of the same length will migrate differently through a pore matrix in an electric field, due to differences in shape and charge. By treating with the anionic detergent SDS and the disulfide bond-reducing DTT, proteins are denatured and receive a negative charge proportional to their length, enabling them to be separated by gel electrophoresis based solely on their size.

Table 20: Reagents and the respective volumes needed to make one 1 x 60 x 85 mm 12% polyacrylamide gel.

Reagent	12% Resolving gel	4,5% Stacking gel
dH_2O	1ml	1,4ml
1M Tris	1,9ml (pH 8,8)	650µl (pH 6,8)
30% acrylamide	2ml	380µl
10% SDS	50µl	25µl
10% APS	25µl	25µl
TEMED	3µl	4µl

The resolving gel was poured to 1 cm below where the wells of the inserted comb ended and covered with EtOH to avoid inhibition of acrylamide polymerization by oxygen. After polymerization the EtOH was removed completely and the stacking gel poured before placing the well comb on top.

The pH and low acrylamide concentration (large pore size) of the stacking gel cause all proteins to migrate at the same speed, forming a thin band. As a result, all proteins enter the resolving gel at the same time, leading to an accurate size separation.

Electrophoresis was carried out in 1X Laemmli buffer (Laemmli, 1970) for approximately 2 h at 15mA/gel.

10X Laemmli buffer
250mM Tris
1,92M Glycine
1% SDS

2.8 Coomassie Brilliant Blue R-250 staining

Coomassie Brilliant Blue R-250 is a dye that binds to almost all proteins. It can therefore be used to visualize proteins separated by SDS-PAGE (Meyer and Lamberts, 1965).

Following electrophoresis, polyacrylamide gels were incubated with gentle agitation in Coomassie staining solution for about 1 h. Subsequent destaining was done in destaining solution until bands were visible.

Coomassie staining solution
0,1% Coomassie R-250
40% MeOH
10% acetic acid

Destaining solution
10% acetic acid
20% MeOH

2.9 Western blotting

Western blotting is a commonly used technique to identify specific proteins after separation by gel electrophoresis. The term blotting refers to the transfer of proteins from the gel to a membrane. After the transfer, specific proteins can be detected using antibodies. Usually, two different antibodies are needed in order to create a protein-specific signal. The first (primary) antibody targets the protein of interest, while the secondary antibody targets the primary antibody and is coupled to an enzyme that allows its detection.

In this study, the Thermo Scientific SuperSignal West Pico Chemiluminescent Substrate (Thermo Scientific) was used to detect secondary antibodies conjugated with horseradish peroxidase (HRP). For detection of proteins expressed by the pGADT7 construct, anti-HA primary monoclonal antibody from mouse (diluted 1:1000 in TBS-T) and anti-Mouse IgG HRP-conjugated secondary antibody (diluted 1:2000 in TBS-T) were used.

For the specific detection of TF1, anti-TF1 primary antibody from rabbit (polyclonal; diluted 1:800 in TBS-T) and anti-Rabbit IgG HRP-conjugated secondary antibody (diluted 1:2000 in TBS-T) were used.

After electrophoresis, proteins were transferred to a PVDF membrane using the Trans-Blot SD Semi-Dry Electrophoretic Transfer Cell (Bio-Rad). The membrane was pre-wetted in MeOH prior to equilibration of both the gel and the membrane in Bjerrum and Schafer-Nielsen transfer buffer for 15 min. After assembling the transfer unit (see Figure 9), transfer was carried out at 10V for 30 min.

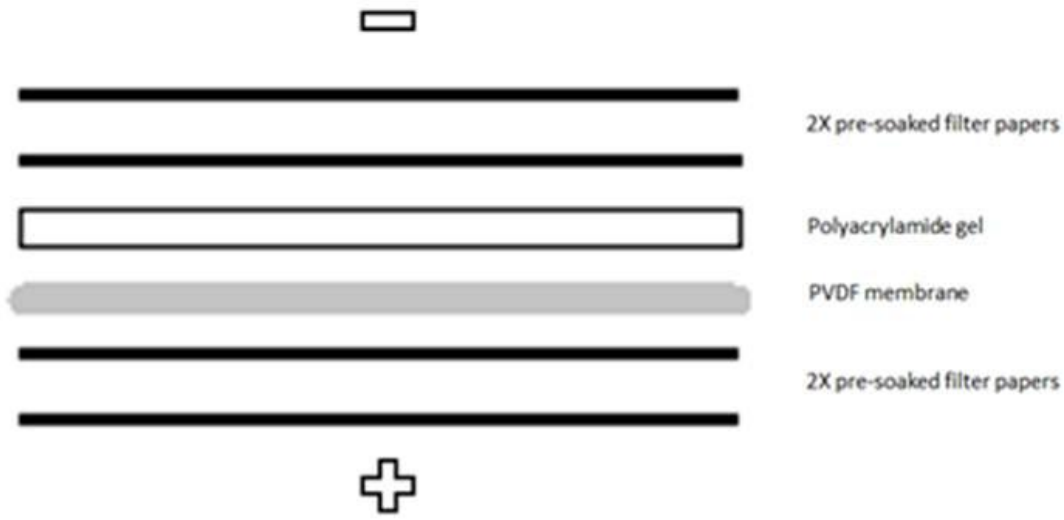

Figure 9: Schematic illustration of the transfer unit. Filter papers were pre-soaked in Bjerrum and Schafer-Nielsen transfer buffer.

Following transfer, the PVDF membrane was washed 2X 10 min in 1X TBS before incubating for 1 h in blocking buffer. After blocking, the membrane was washed 4X 5 min in 1X TBS-T before incubating overnight at 8˚C with the primary antibody. The following day, the membrane was washed 4X 5 min in 1X TBS-T before incubating for 1 h with the secondary antibody. The membrane was then washed again for 4X 5 min in 1X TBS-T.

All antibody-incubations and washing steps were done with gentle agitation.

In order to detect HRP-conjugated secondary antibodies, 500µl SuperSignal West Substrate Working Solution (1:1 of Luminol/Enhancer Solution and Stable Peroxide Solution, both from Thermo Scientific) were spread on top of the membrane by layering it between two plastic sheets. After 5 min incubation in the dark the membrane was wrapped in plastic foil and chemiluminescence was detected using the Fluor-S^{TM} MultiImager (Bio-Rad).

Bjerrum and Schafer-Nielsen transfer buffer
48mM Tris
39mM glycine
20% MeOH

10X TBS buffer
100mM Tris (adjusted to pH 7,5 with HCl)
1,5M NaCl

Blocking buffer
4% (w/v) milk powder
1X TBS buffer

10X TBS-T buffer
100mM Tris (adjusted to pH 7,5 with HCl)
1,5M NaCl
0,5% Tween 20

3. Results

In this thesis, the effect of the dually targeted AP2/EREBP transcription factor TF1 on the expression of plastid-encoded photosynthesis genes was investigated in order to study the protein's putative role in the regulation of these genes. In addition, to further address the possible involvement of TF1 in the coordination of plastid and nuclear gene expression, the expression of selected nuclear genes encoding photosynthesis-related proteins was also examined.

The transcription rates of plastid-encoded genes were studied using run-on transcription with isolated chloroplasts, followed by hybridization of radioactively labelled transcripts to gene-specific probes (see chapters 2.2 and 3.1 for methodical descriptions and results, respectively).

In order to observe the expression of nuclear-encoded genes, cDNA generated from the isolated steady state pool of mRNA was used for relative quantification by real-time PCR as described in chapter 2.3 (results are presented in chapter 3.2).

By comparing gene-specific expression rates between a *TF1* knock-down mutant (ΔTF1) and wild type (WT) *Arabidopsis thaliana* at different points in the 24 hours day/night cycle (see Figure 5) the effects of TF1 on plastid and nuclear gene expression could be examined using the above mentioned methods. As a counterpart to the knock-down mutant it would have been beneficial to do the same experiments with a transgenic plant line that overexpresses *TF1*. Efforts were made to obtain this genotype, but all remained futile (Krause and co-workers, personal communication). However, since the expression of the At2g44940 locus has been shown to increase from 0 hours light to 4 hours light under short day conditions (Michael et al., 2008), differential changes in gene expression between WT and mutant upon illumination will provide information about the effect of increased *TF1*-expression, as long as TF1 levels in the mutant remain suppressed and are undetectable in our assays.

3.1 TF1 influences transcription rates of plastid-encoded photosynthesis genes

In order to examine the effect of TF1 on the transcription rate of plastid-encoded genes, chloroplasts were isolated from WT and ΔTF1 at two different time points in the 24 h day/night cycle and used in run-on transcription assays as described in chapters 2.1 and 2.2, respectively. Quantification of changes in gene-specific transcript levels caused by four hours exposure to light was done by measuring mean intensities of each single dot using the Volume Circle Tool in the Quantity One software (Bio-Rad) (see Figure 11 and Figure 12). The relative changes in gene-specific transcript levels were calculated in relation to the total amounts of transcripts hybridized to the respective dot blot, as described previously (Krause et al., 1998).

Many of the genes examined here did not yield any detectable signals on the dot blots (see Figure 10). A reason for this might be that the radioactive isotope ^{33}P, used for detection of transcripts in this study, has a lower energy beta emission than the more commonly applied ^{32}P (^{33}P= 0,25meV and ^{32}P= 1,71meV). In addition, some of the genes in question have also been shown to be weakly expressed compared to *psbA* in previous studies (Krause et al., 1998; Krause et al., 2000).

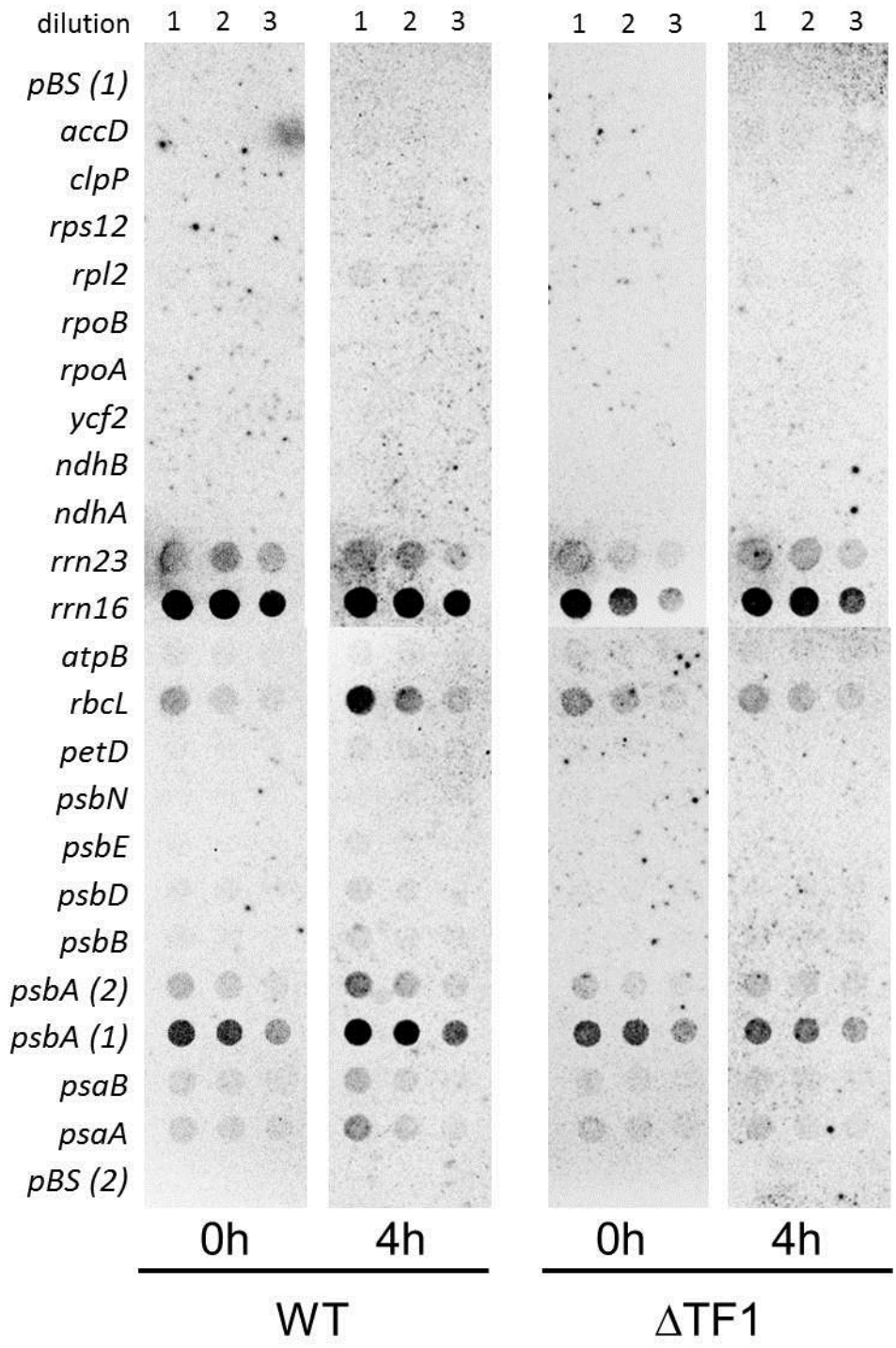

Figure 10: Dot blot hybridization of ^{33}P-UTP-labelled run-on transcripts from chloroplasts of WT and ΔTF1 *A .thaliana* isolated right before daybreak (0 h) and four hours after daybreak (4 h). Three different dilutions of the gene-specific probes were applied to the blots: 1 = 64pmol, 2 = 16pmol and 3 = 4pmol. Signals were detected using a Personal Imager FX (Bio-Rad) after three weeks exposure in an Imaging Screen-K cassette (Bio-Rad). The *pBS* oligonucleotides, being complementary to parts of the MCS in the pBS vector and not to plastid genes, function as controls for unspecific binding.

As is evident from Figure 11, the transcription rate of the photosynthesis-related genes *psaA*, *psaB*, *psbA* and *rbcL* did all increase in response to four hours of light in WT *Arabidopsis thaliana*. Interestingly, this light-induced upregulation in the transcription rate of the four genes encoding proteins involved in photosynthesis was not seen in the mutant (ΔTF1) in which the expression of *TF1* is abolished (see Figure 12). Consequently, the light-induced increase in the transcription rate of the plastid-encoded genes *rbcL, psbA, psaA* and *psaB* is seemingly dependent on the expression of *TF1*.

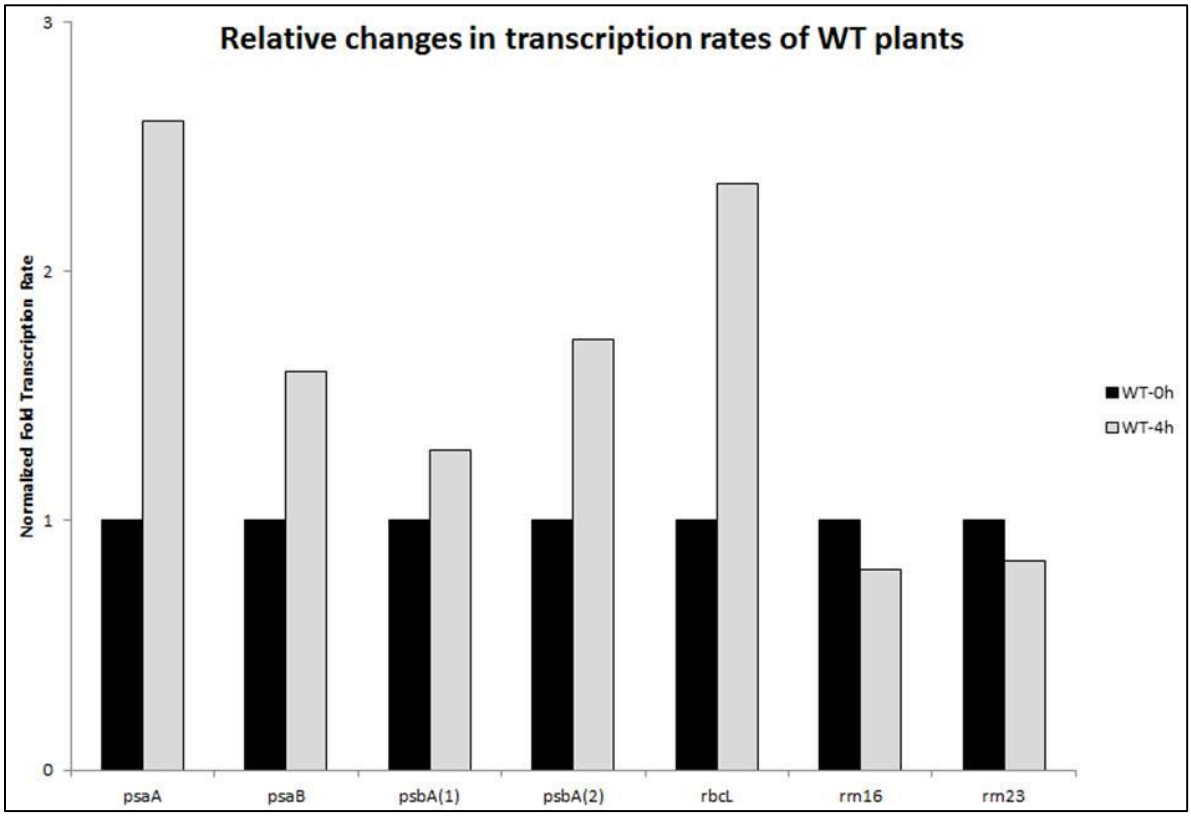

Figure 11: Quantification of dot blots hybridized with ^{33}P-UTP-labelled run-on transcripts from chloroplasts of WT *A. thaliana*. Chloroplasts were isolated right before light on (0 h) and four hours after daybreak (4 h). Dot blots were analyzed using the Volume Circle Tool in the Quantity One software (Bio-Rad). After subtracting background, mean dot intensities were normalized to the sum of all mean dot intensities in the respective blot. Normalized dot intensities for dilution 1 dots (see Figure 10) are here presented as fold changes over the corresponding WT-0h dot for the respective genes.

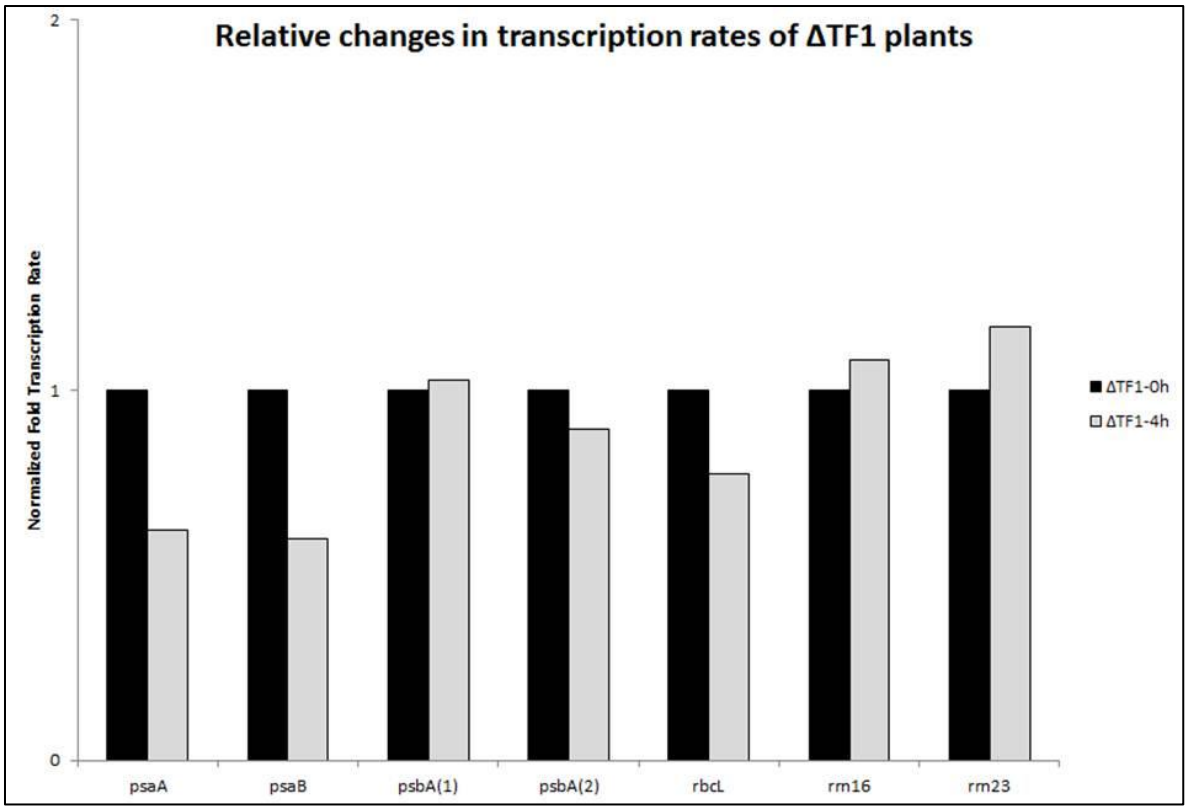

Figure 12: Quantification of dot blots hybridized with ^{33}P-UTP-labelled run-on transcripts from chloroplasts of ΔTF1 *A. thaliana*. Chloroplasts were isolated right before light on (0 h) and four hours after daybreak (4 h). Dot blots were analyzed using the Volume Circle Tool in the Quantity One software (Bio-Rad). After subtracting background, mean dot intensities were normalized to the sum of all mean dot intensities in the respective blot. Normalized dot intensities for dilution 1 dots (see Figure 10) are here presented as fold changes over the corresponding ΔTF1-0h dot for the respective genes.

The autoradiograms after hybridization with radioactively labelled chloroplast-transcripts from the different samples (see Figure 10) show that the gene encoding for 16S ribosomal RNA (*rrn16*) has the highest transcription rate in both genotypes (WT and ΔTF1) and at both harvesting times (0 h and 4 h). In Arabidopsis, the ribosomal genes *rrn16* and *rrn23* are located in the same operon and are transcribed together in one continuous transcript. However, Figure 10 shows that the intensity of the *rrn23* dots is greatly reduced compared to the intensity of the *rrn16* dots, indicating that there are fewer *rrn23* transcripts than *rrn16* transcripts. The reason for this could be that the *rrn16* probe hybridizes more strongly to the *rrn16* and *rrn23* containing transcript than the *rrn23* probe does. A similar incident is seen with the *psbA (1)* probe and the *psbA (2)* probe (see Figure 10). These probes are complementary to different regions of the same mRNA, but show large differences in the amounts of hybridized ^{33}P-UTP-labelled transcripts. However, the relative changes in the transcription rate of *psbA, rrn16* and *rrn23* from right before daybreak to four hours after

are similar for both *psbA*-probes and both ribosomal RNA-probes in the respective Arabidopsis genotypes (WT and ΔTF1), as seen in Figure 11 and Figure 12. This indicates that the observed inability of the *TF1* knock-down mutant to upregulate the transcriptional rate of plastid-encoded photosynthesis genes in response to light is reproducible, at least for the *psbA* gene.

3.2 Expression of nuclear-encoded photosynthesis genes is not dependent on TF1

RT-qPCR on RNA isolated from WT and ΔTF1 *A. thaliana* at two different time points in the 24 h day/night cycle was applied in order to study the effects of TF1 on the expression of the nuclear-encoded photosynthesis-related genes *PSBO2* and *RBCS1A* as described in chapters 2.1 and 2.3.

In order to calculate the PCR efficiency for a given primer pair and to see the range of starting template quantity over which the given efficiency can be used, standard curves were generated as described in chapter 2.3.2, and are illustrated in Figure 13. PCR efficiencies (E) were calculated from the slopes of the standard curves using the formula: $E = 10^{-1/slope}$, and subsequently converted to percentage: % Efficiency = (E-1)*100%. Data describing the respective standard curves are listed in Table 21.

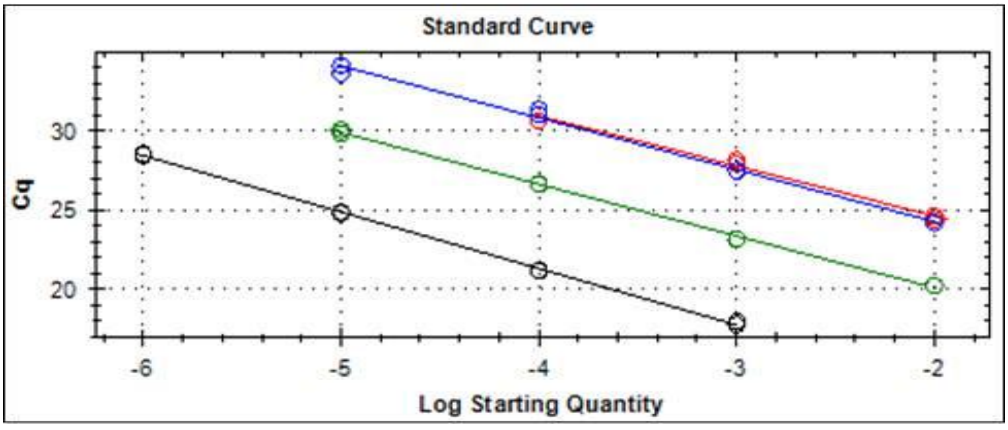

Figure 13: Standard curves for all four target genes were generated by amplifying 10-fold serial dilutions of starting template. Each dilution was assayed in duplicates. The respective Cqs are plotted against the log of the starting quantity of template for each dilution. Blue = *ACT8*, green = *PSBO2*, black = *RBCS1A* and red = *TF1*.

Table 21: PCR efficiencies calculated from the respective standard curves. The coefficient of determination (R^2) indicates how correctly the regression line describes the data, R^2=1 being the optimal.

Target	Slope	% PCR Efficiency	R^2
ACT8	-3,268	102,3%	0,995
PSBO2	-3,262	102,5%	0,999
RBCS1A	-3,553	91,2%	0,999
TF1	-3,154	107,5%	0,992

In Figure 14 it can be seen that the expression of *TF1* was greatly reduced in ΔTF1 compared to the WT. This result verifies that the At2g44940 locus is in fact disrupted in the mutant. The expression of all three investigated genes (*PSBO2, RBCS1A* and *TF1*) increased from the very end of the dark period to four hours after daybreak in WT Arabidopsis (see Figure 14). The light-induced increase in expression of the two photosynthesis-related genes *PSBO2* and *RBCS1A* was also seen in the ΔTF1 mutant, indicating that the light-controlled regulation of these genes is seemingly not affected by knock-down of the *TF1* gene.

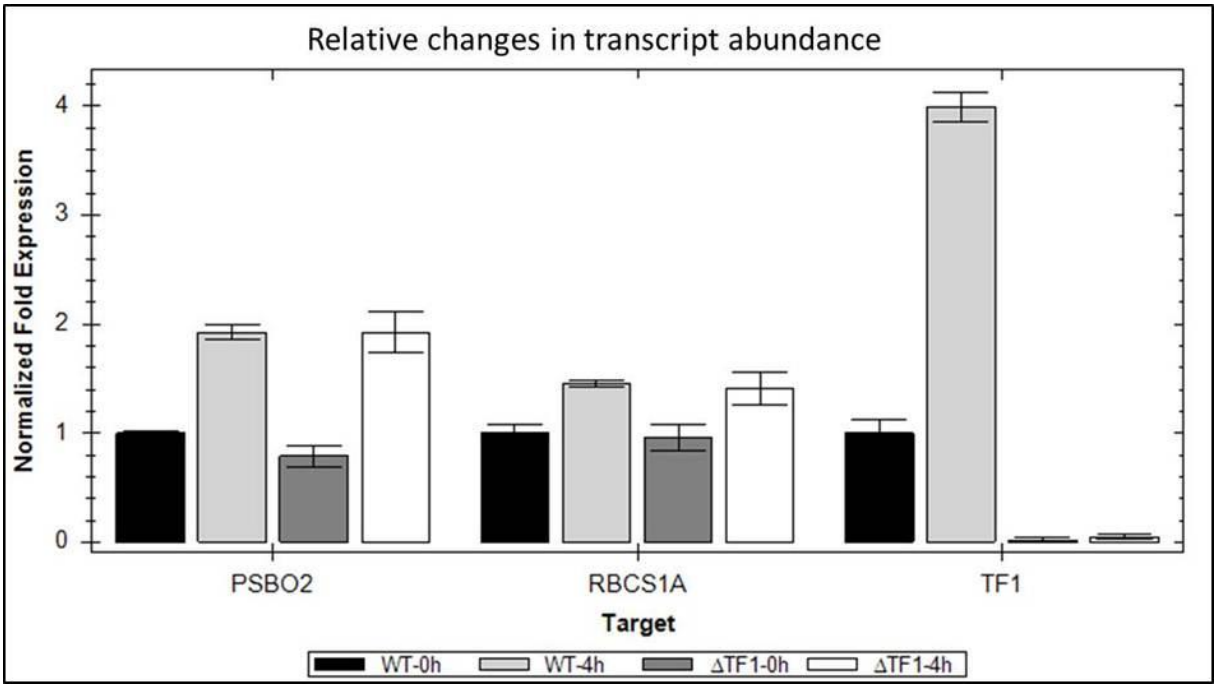

Figure 14: RT-qPCR expression analysis of two nuclear genes involved in photosynthesis (*PSBO2* and *RBCS1A*) in 8-week old *A. thaliana* WT and ΔTF1 plants. RNA was isolated at two different time points: at the very end of the dark period (0 h) and four hours after daybreak (4 h). Relative quantities (WT-0h was used as control) were normalized to *ACT8* and presented as relative expression levels to WT-0h (set to 1) for each target gene. Error bars represent the standard deviation for technical duplicates.

As can be seen in Table 21, the PCR efficiencies for *ACT8*, *PSBO2*, *RBCS1A* and *TF1* were 102,3%, 102,5%, 91,2% and 107,5%, respectively. The coefficient of determination (R^2) was very close to 1 for all targets, indicating that all dilutions fitted well with the regression line. Efficiencies below 100% indicate that the amount of amplicon is being less than doubled every cycle, suggesting suboptimal PCR conditions. On the other hand, PCR efficiencies over 100% may be caused by coamplification of a secondary product or the presence of PCR inhibitors in the reaction.

Since all calculated PCR efficiencies were close to 100%, and melt-curve analyses (see Appendix I) indicated that no secondary products were amplified, the quantifications of *PSBO2*-, *RBCS1A*- and *TF1*-transcripts relative to the abundance of *ACT8* transcripts, as performed by RT-qPCR in this study, can be said to be trustworthy.

3.3 Testing and optimization of the experimental design of Y1H assays

There are many ways in which a protein can influence the expression rates of specific genes. Transcription factors like TF1 possess a DNA-binding domain, enabling them to regulate gene expression through interaction with *cis*-regulatory elements in the promoter regions of genes. So far, there is no data on specific sequence-motifs recognized by this particular AP2/EREBP protein. Therefore, in order to address this possible mechanism by which TF1 might regulate gene expression, the DNA-binding specificity of TF1 was studied here using yeast one-hybrid assays with a selection of different bait sequences (see Table 22) as described in chapter 2.4. The results of the interactions between TF1 and specific DNA sequences are presented in chapters 3.4 and 3.6.

3.3.1 Verification of vector constructs by DNA sequencing

After cloning of bait sequences into the pINT1-HIS3NB construct (pINT1-HIS3NB+StuI for the At5g60200 promoter), correct insertion was verified by DNA sequencing (see chapter 2.5.14). Because of its size, the At5g60200 promoter-bait sequence was sequenced from both ends using pINT1-HIS3NB forward and reverse primers (see Table 17). All the other bait sequences were sequenced using the pINT1-HIS3NB forward primer (see Table 17).

Sequencing chromatograms (data not shown) revealed that in the psbAx3 and the psbAmutx3 bait sequence, a cytosine residue was missing in the second of the three tandem repeats (see Table 22). However, because of the laborious procedure of making these tandem repeated bait sequences, and the fact that the missing nucleotide might be a sequencing error, the bait sequences were used for yeast one-hybrid assays as they were. As seen in Table 22, no errors were found in any of the other bait sequences.

Table 22: List of bait sequences used in yeast one-hybrid assays. Tandem repeated regions are underlined. Nucleotides which should be present in the bait sequence, but were not detected by sequencing, are written in red letters.

Bait sequence	**Sequence (5′→ 3′)**
DRE	TACCGACATTACCGACATTACCGACATTACCGACAT
DREmut	TACTGACATTACTGACATTACTGACATTACTGACAT
GCC	AGCCGCCAGCCGCCAGCCGCCAGCCGCC
GCCmut	ATCCTCCATCCTCCATCCTCCATCCTCC
Inv. GCC	GGCGGCTGGCGGCTGGCGGCTGGCGGCT
Inv. GCCmut	GGAGGATGGAGGATGGAGGATGGAGGAT
psbA core4(a)	CATCCGACCATCCGACCATCCGACCATCCGAC
psbA core4(b)	ATCCGACTAATCCGACTAATCCGACTAATCCGACTA
psbAx1	GGTTCGAGTCCCGGGCAACCCATTATCTACTCCATCCGACTAGTTCCGGGTTCGAGTCCCGGGCAACCCA
psbAx3	GGTTCGAGTCCCGGGCAACCCATTATCTACTCCATCCGACTAGTTCCGGGTTCGAGTCCCGGGCAACCCA TTATCTACTCCATCCGACTAGTTCCGGGTTCGAGTCCCGGGCAACCCA TTATCTACTCCATCCGACTAGTTCCGGGTTCGAGTCCCGGGCAACCCA
psbAmutx1	GGTTCGAGTCCCGGGCAACCCATTATCTACTCCATTTTTTTAGTTCCGGGTTCGAGTCCCGGGCAACCCA
psbAmutx3	GGTTCGAGTCCCGGGCAACCCATTATCTACTCCATTTTTTTAGTTCCGGGTTCGAGTCCCGGGCAACCCA TTATCTACTCCATTTTTTTAGTTCCGGGTTCGAGTCCCGGGCAACCCA TTATCTACTCCATTTTTTTAGTTCCGGGTTCGAGTCCCGGGCAACCCA
At5g60200 promoter	*

*The At5g60200 promoter-bait sequence is 3082bp long and is therefore not written here. The full-length sequence can be found in the NCBI database (http://www.ncbi.nlm.nih.gov/gene/836142).

The TINY-pENTR™/SD/D-TOPO construct was sequenced using M13 forward and reverse primers (see Table 17), and found to contain no errors (data not shown).

3.3.2 Checking yeast reporter strains by colony PCR

In order to verify that bait sequences were in fact recombined into the yeast genome together with the *PDC6* homologous sequences of the pINT1-HIS3NB constructs, colony PCR was performed on reporter strains using vector specific primers (see Table 7). A picture of the PCR products after size separation by agarose gel electrophoresis is seen in Figure 15.

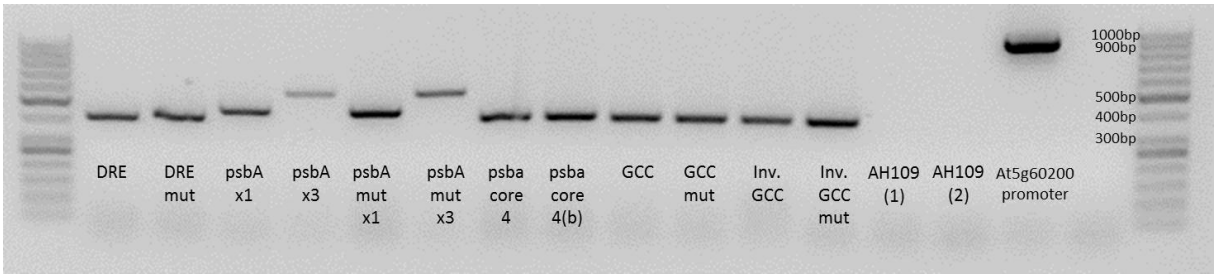

Figure 15: Colony PCR on yeast reporter strains. 10µl GeneRuler^{TM} 50bp DNA Ladder (Fermentas) was used as size marker. PCR products were separated on a 2% agarose gel. The occurrences of products of the expected sizes indicate that all strains were transformed successfully.

The pINT1-HIS3NB forward and reverse primers are located on either side of the MCS in the pINT1-HIS3NB plasmid, with 357bp between them (see Figure 36). The size of a bait sequence can therefore be deduced by subtracting 357bp from the size of a PCR product generated using this primer pair. For the 3082bp long At5g60200 promoter-bait sequence it was not possible to obtain a PCR product using the pINT1-HIS3NB forward and reverse primers. However, a product of the expected size was seen when using the pINT1-HIS3NB forward primer and an insert specific reverse primer, At5g60200 promoter reverse_b.

As seen in Figure 15, colony PCR on all reporter strains yielded amplicons with the expected sizes (bait sequences can be found in Table 22), indicating that the transformations were successful and that the correct bait sequence had been integrated into the yeast genome. The untransformed yeast strain AH109 was used as negative control and could be shown to contain no template for the primer combinations pINT1-HIS3NB forward and reverse or pINT1-HIS3NB forward and At5g60200 promoter reverse_b (see AH109(1) and AH109(2) in Figure 15, respectively).

3.3.3 Leaky expression of the *HIS3* reporter gene

Before yeast reporter strains could be transformed with the prey protein expression constructs, possible leaky expression of the *HIS3* gene had to be tested for. This was done by observing the growth of each individual reporter strain on SD/-His plates with different concentration of 3-AT (see chapter 2.4.5).

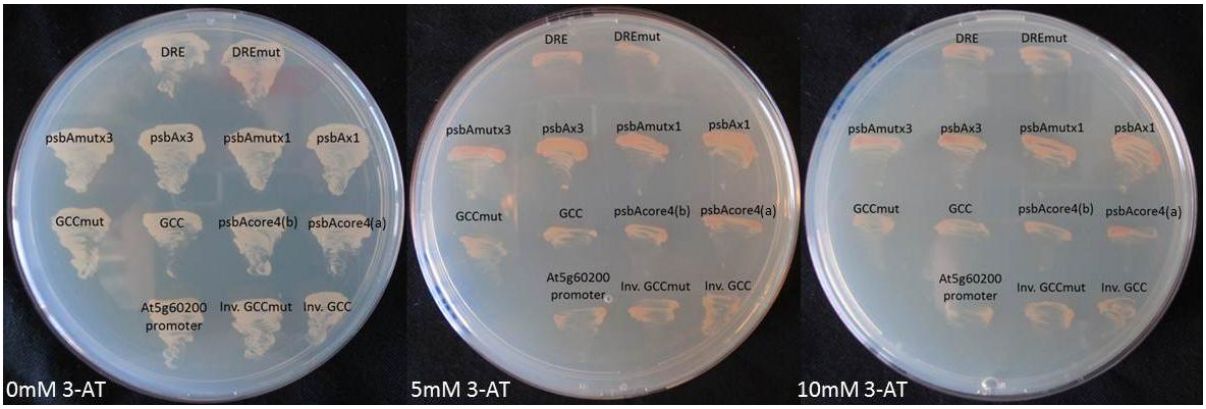

Figure 16: The concentration of 3-AT needed to reduce possible background growth of the *HIS3* reporter gene was determined by plating histidine auxotrophic yeast reporter strains on SD/-His with 0mM, 5mM and 10mM concentration of 3-AT. Plates were incubated at 30˚C for 3-4 days before documenting growth observations.

As can be seen in Figure 16, all reporter strains were able to grow on histidine-deficient yeast medium without any addition of the competitive inhibitor of HIS3, 3-AT. However, this background growth was greatly reduced when 3-AT at a final concentration of 5mM or 10mM was added to the medium. Consequently, interaction tests were carried out in the presence of 5mM or 10mM 3-AT. Both concentrations of 3-AT were used in subsequent assays in order to reveal possible differences in binding strength.

3.3.4 Verification of expressed prey protein in yeast reporter strains

Successful transformation of DBP-pGADT7 constructs to yeast reporter strains was verified by plating on SD/-Leu plates (see Figure 17) as described in chapter 2.4.6.

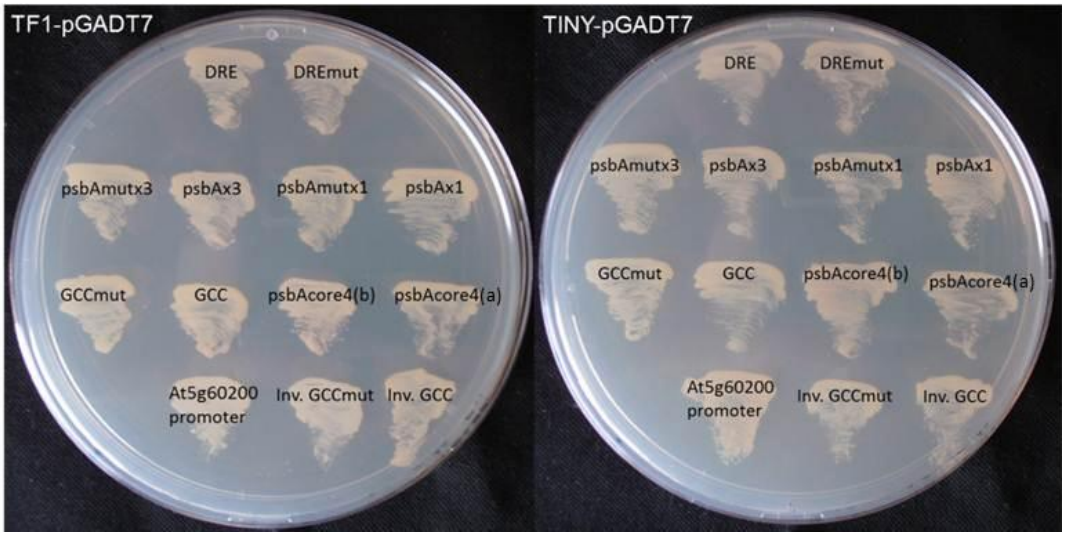

Figure 17: Leucine auxotrophic yeast reporter strains transformed with TF1-pGADT7 or TINY-pGADT7 were plated on SD/-Leu to verify that the constructs were successfully transformed with the *Leu*-encoding expression vectors. Plates were incubated at 30˚C for 3-4 days before documenting growth observations.

Since the expression of the *Leu* gene and the expression of the DBP-GAL4AD fusion protein are maintained by different promoters (see Figure 38 for vector map), the ability of the leucine auxotrophic yeast cells to grow on leucine-deficient plates is not a definite proof that the prey protein is being expressed. Also, the expressed protein might be degraded by the yeast cells for unknown reasons.

To prove that the specific prey protein was in fact present in the yeast cells after transformation with TF1- or TINY-pGADT7 constructs, total protein extracts from yeast were separated by SDS-PAGE and analyzed by western blotting as described in chapters 2.6, 2.7, 2.8 and 2.9.

This “prey protein expression-test” is usually not done, probably because it is more beneficial to test the interaction with a second independent method like chromatin immunoprecipitation or gel mobility shift assays (Brady et al., 2011; Sun et al., 2008).

However, due to the availability of a primary antibody that specifically targets TF1, it presented itself as an opportunity to further support the results of this study.

Detection of TF1 using the TF1-specific primary antibody did not reveal any detectable signals on the western blot (data not shown). However, some signals were detected with the anti-HA primary antibody (see Figure 18), which should bind to all HA-tagged protein-GAL4AD fusions expressed from the pGADT7 construct (see Figure 38 for vector map).

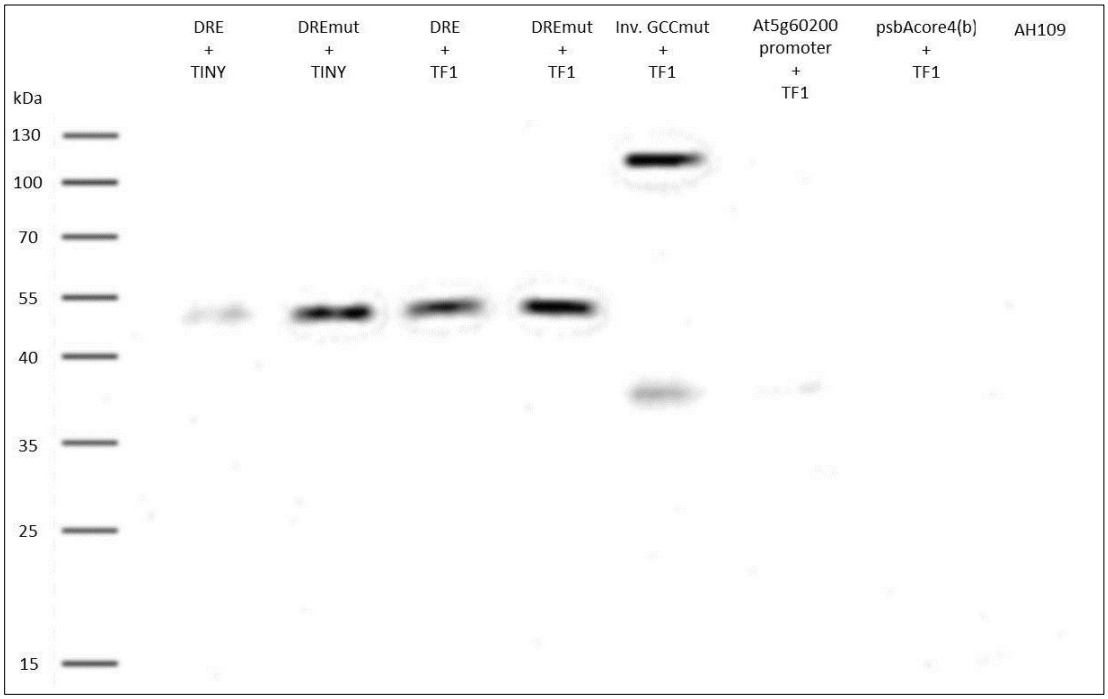

Figure 18: Detection of HA-tagged proteins by western blotting using anti-HA primary antibody and anti-mouse HRP-conjugated secondary antibody. Total protein extracts from yeast reporter strains transformed with either TF1-pGADT7 or TINY-pGADT7 were separated on a 12% SDS-PAGE. HRP-specific chemiluminescent signals were produced using the Thermo Scientific SuperSignal West Pico Chemiluminescent Substrate (Thermo Scientific) and detected by the Fluor-S™ MultiImager (Bio-Rad). 5µl PageRuler™ Prestained Protein Ladder (Fermentas) was used as size marker.

The protein sizes of TF1 and TINY are 32kDa and 24kDa, respectively. However, since the proteins used in the yeast one-hybrid assays are expressed in fusion with the NLS, the GAL4AD and the HA-tag, about 16kDa must be added to the weight of the single protein. Anyway, the sizes of the bands seen in the western blot (see Figure 18) do not correlate well with the expected sizes and are therefore believed to be caused by binding of the primary (or secondary) antibody to other proteins.

Figure 19 shows the total protein extracted from DBP-pGADT7-transformed reporter strains visualized by Coomassie staining. It must here be mentioned that the volume of extracted protein loaded for Inv. GCCmut+TF1, At5g60200 promoter+TF1 and psbAcore4(b)+TF1 had to be four times larger than the volume loaded for the other samples in order to achieve equal strengths of the protein bands. This differential loading might explain why the patterns of these three DBP-pGADT7-transformed reporter strains were strikingly different from the others (see Figure 19).

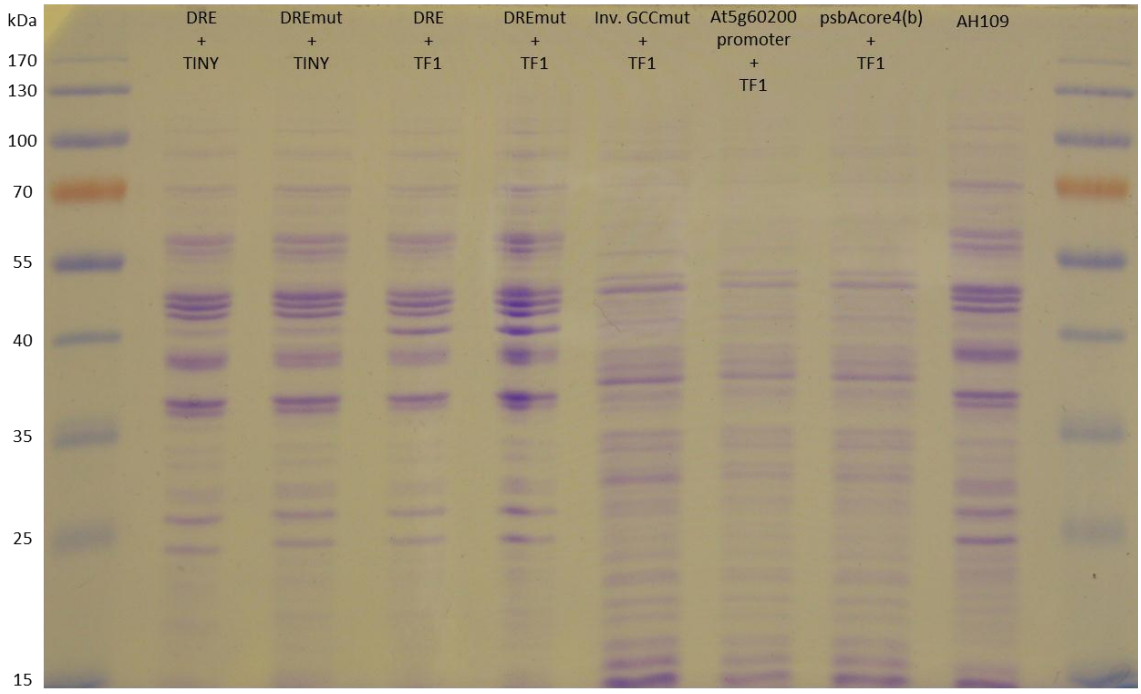

Figure 19: 12% SDS-PAGE of total protein extracts from yeast reporter strains transformed with either TF1-pGADT7 or TINY-pGADT7, in addition to the untransformed AH109 strain. 5µl PageRuler^{TM} Prestained Protein Ladder (Fermentas) was used as size marker. Proteins were visualized by Coomassie staining.

Despite the failure to detect the respective prey proteins by western blotting, protein-DNA interactions were still analyzed using yeast one-hybrid assays.

3.3.5 TINY binds specifically to the DRE and the GCC box

In order to verify that the experimental setup for the yeast one-hybrid assays was working properly, the previously published interactions between the transcription factor TINY and the DRE and the GCC box (Sun et al., 2008) were tested as described in chapter 2.4.

In Figure 20 it can be seen that the DRE reporter strain transformed with TINY-pGADT7 was able to grow on histidine- and leucine-deficient medium with both 5mM and 10mM concentration of 3-AT, indicating that the prey protein interacted with the bait sequence, resulting in an activation of transcription of the *HIS3* reporter gene. The specificity of this interaction is corroborated by the inability of TINY to interact with the mutated DRE motif (see DREmut in Figure 20). The one-nucleotide mutation (see DRE and DREmut in Table 22) was chosen based on the binding-requirements of DREB1A and DREB2A as reported by Sakuma et al. (2002).

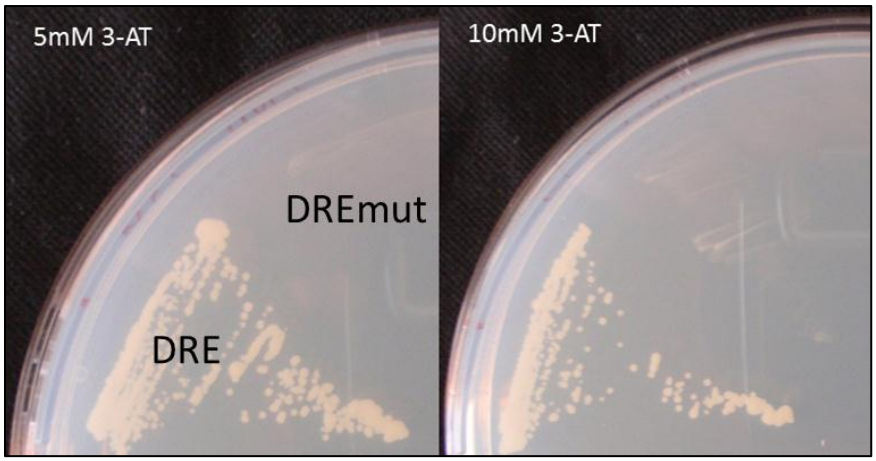

Figure 20: Testing the DRE- and DREmut-binding properties of TINY by yeast one-hybrid assay. Reporter strains transformed with TINY-pGADT7 were plated on SD/-His/-Leu plates with 5mM and 10mM concentration of 3-AT. Plates were incubated at 30˚C for 3-4 days before documenting growth observations.

The ability of the GCC reporter strain transformed with TINY-pGADT7 to grow on SD/-His/-Leu plates in the presence of 5mM and 10mM 3-AT showed that TINY interacted with the GCC box (see Figure 21). The interaction can be said to be specific since TINY did not appear to bind the mutated form of this bait sequence (see GCCmut in Figure 21).

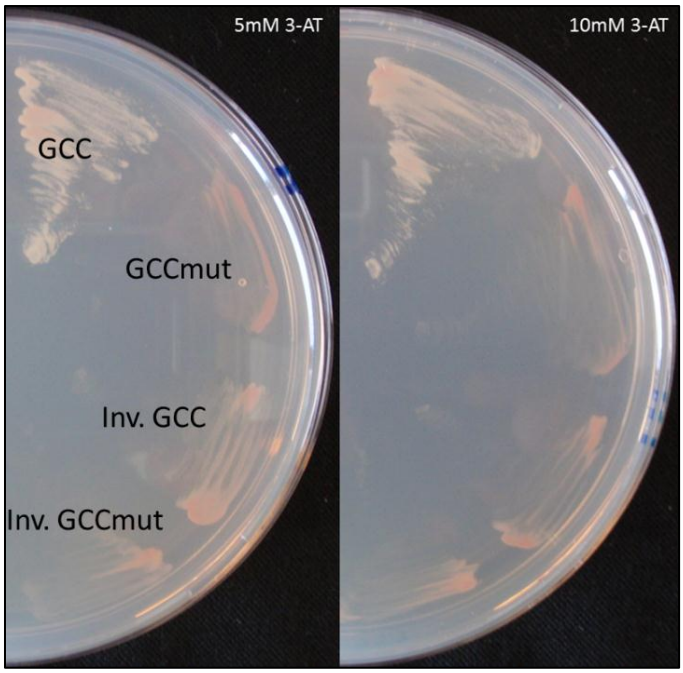

Figure 21: Yeast one-hybrid assay investigating the ability of TINY to bind the GCC, the GCCmut, the Inv. GCC and the Inv. GCCmut bait sequences. Reporter strains transformed with TINY-pGADT7 were plated on SD/-His/-Leu plates with 5mM and 10mM concentration of 3-AT. Plates were incubated at 30˚C for 3-4 days before documenting growth observations.

No growth on the medium selecting for prey protein-bait sequence interaction could be observed for the TINY-pGADT7-transformed reporter strains containing bait sequences with inverted GCC box motifs (see Inv. GCC and Inv. GCCmut in Figure 21), indicating that TINY did not bind any of these sequences. The inverted versions of the GCC box were included because a previous publication have shown that inverted forms of the GCC box can play essential roles in the regulation of gene expression (Eklund et al., 2011). The mutated forms of the GCC box motifs (GCCmut and Inv. GCCmut) were made based on previously published data for this *cis*-regulatory element (Hao et al., 1998).

The here observed specific binding of TINY to the DRE and the GCC box indicated that the experimental setup of the yeast one-hybrid assays was functional, and able to reproduce protein-DNA interactions which had been previously published.

3.4 Characterization of DNA sequences that interact with TF1

3.4.1 TF1 binds specifically to the DRE motif

As for TINY, the DRE- and DREmut-binding abilities of TF1 were tested using the yeast one-hybrid assay. DRE and DREmut reporter strains were transformed with TF1-pGADT7 and checked for growth on histidine- and leucine-deficient medium with both 5mM and 10mM concentration of 3-AT as described in chapter 2.4. In Figure 22 it can be seen that TF1 interacted with the DRE bait sequence, enabling the yeast cells to form colonies on plates selecting for expression of the *HIS3* reporter gene. The protein did not bind to the mutated form of the DRE motif (see DREmut in Figure 22).

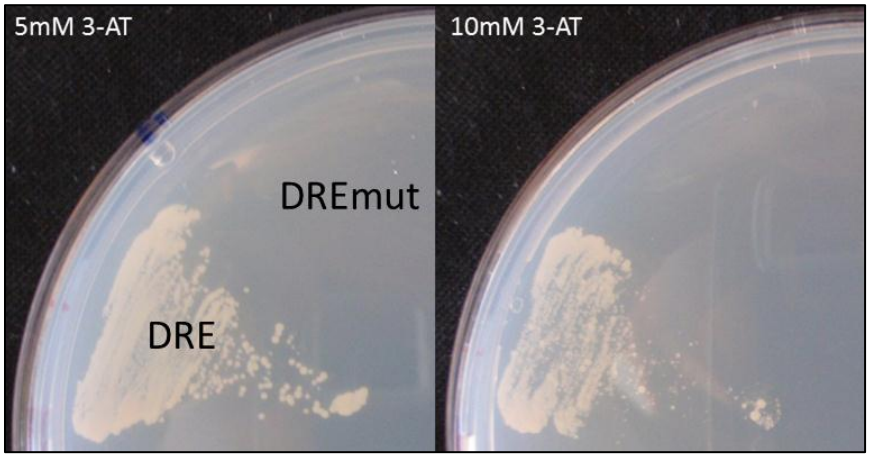

Figure 22: Binding-affinity of TF1 towards DRE and DREmut bait sequences as observed by yeast one-hybrid assay. Reporter strains transformed with TF1-pGADT7 were plated on SD/-His/-Leu plates with 5mM and 10mM concentration of 3-AT. Plates were incubated at 30˚C for 3-4 days before documenting growth observations.

This ability of TF1 to interact specifically with the DRE element has not been reported previously. However, considering the high similarity between the DNA-binding domains of these two AP2/EREBP transcription factors (see Figure 30), it is not surprising that TF1 displays the same binding-preference as TINY towards the DRE bait sequence.

3.4.2 TF1 binds to the inverted and mutated form of the GCC box

Whereas TINY exhibited specific binding of the non-mutated form of the GCC box (see Figure 21), yeast one-hybrid assays with TF1 and the reporter strains carrying GCC box-related bait sequences revealed that the TF1-pGADT7-transformed Inv. GCCmut reporter strain was able to grow on SD/-His/-Leu plates containing 5mM and 10mM 3-AT (see Figure 23). The fact that no growth was detected for any of the other GCC box related-reporter strains in which the TF1 prey protein was expressed (see Figure 23) indicated that TF1 might interact specifically with the inverted and mutated GCC box.

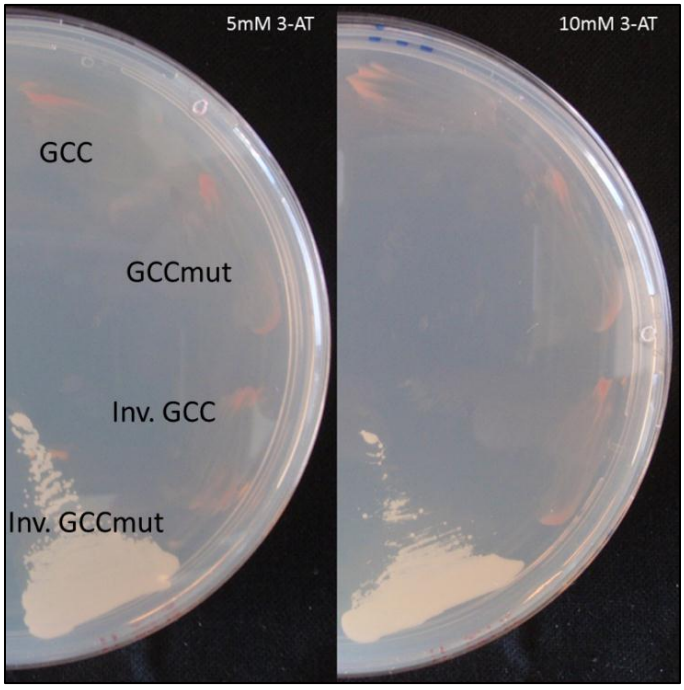

Figure 23: Detecting interactions between TF1 and GCC box related bait sequences using yeast one-hybrid assay. Reporter strains transformed with TF1-pGADT7 were plated on SD/-His/-Leu plates with 5mM and 10mM concentration of 3-AT. Plates were incubated at 30˚C for 3-4 days before documenting growth observations.

The binding of TF1 to the inverted and mutated form of the GCC box (GGAGGAT) is of particular interest since it presents a binding-preference of TF1 that was not seen for its close relative, TINY. In fact, searching PLACE (A Database of Plant Cis-acting Regulatory DNA Elements (Higo et al., 1999; Prestridge, 1991)) for this DNA-motif did not retrieve any hits, indicating that TF1 is so far the only protein reported to interact with this sequence.

3.4.3 TF1 binds to the promoter region of At5g60200

TF1 was previously reported to bind the 3kb long promoter region of the At5g60200 locus (Brady et al., 2011). This interaction was also tested here using yeast one-hybrid assay. The ability of the At5g60200 reporter strain transformed with TF1-pGADT7 to grow on 5mM and 10mM 3-AT containing SD/-His/-Leu plates, confirmed this interaction (see Figure 24A).

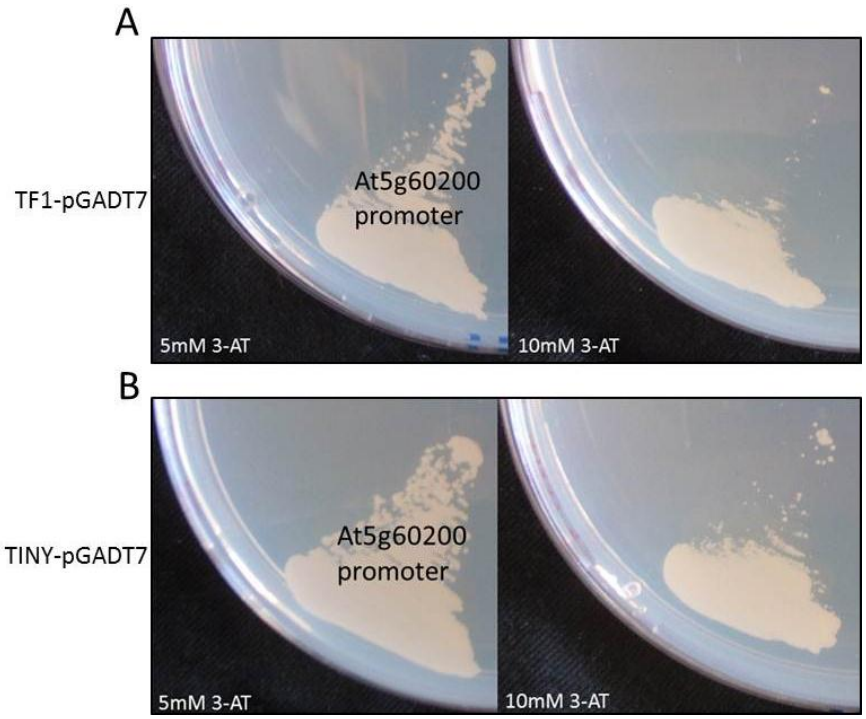

Figure 24: Yeast one-hybrid assays examining the ability of (A) TF1 and (B) TINY to interact with the promoter region of At5g60200. The reporter strain transformed with (A) TF1-pGADT7 and (B) TINY-pGADT7 was plated on SD/-His/-Leu plates with 5mM and 10mM concentration of 3-AT. Plates were incubated at 30˚C for 3-4 days before documenting growth observations.

In addition to containing a binding site for TF1, the ability of the At5g60200 reporter strain to grow on histidine- and leucine-deficient medium with 5mM and 10mM 3-AT when transformed with TINY-pGADY7 indicated that TINY also interacted with this bait sequence (see Figure 24B). Based on the DNA-binding preferences of TF1 and TINY observed in this study, searches for putative target sites in the 3082bp long sequence revealed an inverted and mutated GCC box motif (GGAGGA) and a DRE core motif (CCGAC) located 1273bp and 898bp upstream of the At5g60200 start codon, respectively (data not shown). However, further investigations to unravel which sequence(s) within this large bait sequence are recognized by the two DREBs have not yet been executed.

3.5 *In silico* search for putative target genes of TF1

Due to its possession of a DNA-binding domain, a possible way for TF1 to influence the expression of a gene would be through interaction with *cis*-regulatory elements in the gene's promoter region. As was mentioned earlier, members of the DREB subfamily of the AP2/EREBP transcription factor family have been reported to bind DRE and GCC box motifs (reviewed in Dietz et al. (2010)), the first of which has also been shown to interact with TF1 in this study (see Figure 22). Therefore, in order to look for putative TF1-binding sites in the promoters of the putative TF1 target genes identified earlier in this study (*psaA/B, psbA, rbcL* and *TF1*), the regions 1000 bp upstream of the start codon were searched for sequences similar to the DRE motif (TACCGACAT).

An interesting site was found upstream of the plastid-encoded photosynthesis-related gene *psbA*. Here, a DRE core motif (CCGAC) is found to be conserved across a wide range of land plant species as illustrated in Figure 25.

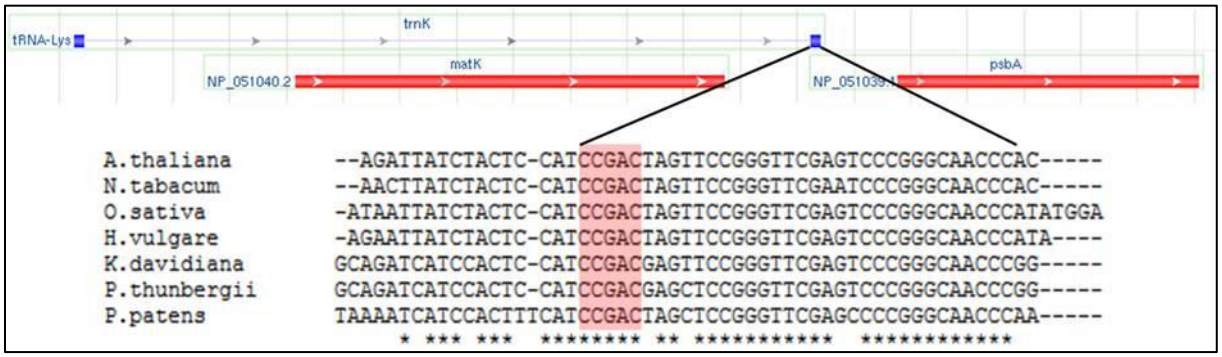

Figure 25: A conserved DRE core motif (indicated in red) can be found in the promoter region of the plastid-encoded gene *psbA*. The motif is located within an exon of the gene *trnK*. The *trnK*, *matK* and *psbA* gene illustration represents the locations on the chloroplast genome of *A. thaliana,* and was copied from the NCBI web page (http://www.ncbi.nlm.nih.gov/gene/844802). The alignment was made using the online general purpose multiple sequence alignment program ClustalW2, with default settings (Larkin et al., 2007).

The fact that the DRE core motif is located within an exon of the *trnK* gene explains why it is well conserved, without the necessity of it having another function. However, it does not exclude the possibility for this sequence to be a binding site for transcription factors.

Since the yeast one-hybrid assays indicated that TF1 interacts with the inverted and mutated form of the GCC box (see Figure 23), the same promoter regions as used above were also searched for sequences similar to this motif (GGAGGAT).

The plastid-encoded genes *psaA* and *psaB* are transcribed together in the *psaA/B* operon. A conserved nucleotide sequence, resembling the inverted and mutated GCC box was found in the promoter region of this operon (see Figure 26). A similar motif was also found to be conserved in the short non-translated region between the two genes (see Figure 26).

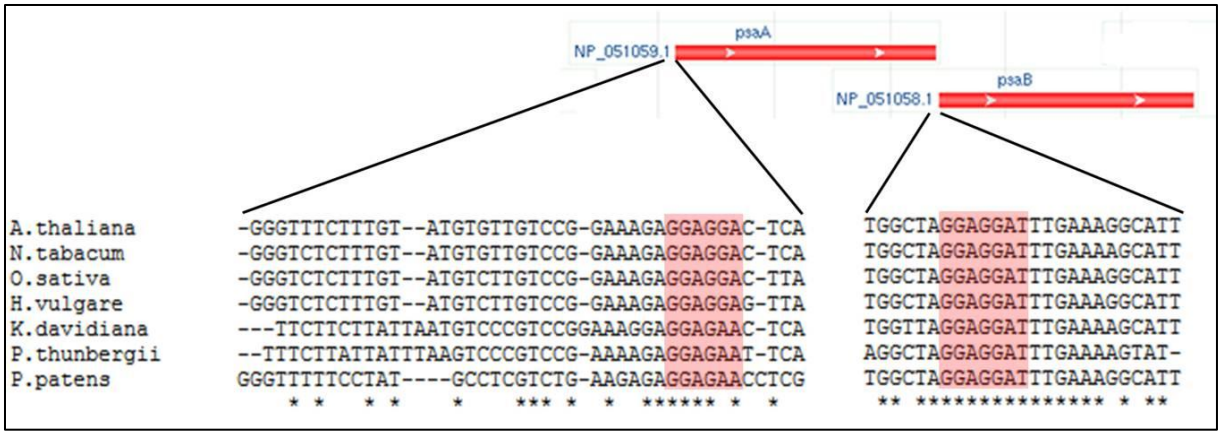

Figure 26: In the promoter region of the *psaA/B* and the short space between the stop codon of *psaA* and the start codon of *psaB,* a mutated and inverted form of the GCC box (indicated in red) is found to be conserved over a wide selection of land plants. The *psaA/B* gene illustration represents locations on the chloroplast genome of *A. thaliana,* and was copied from the NCBI web page (http://www.ncbi.nlm.nih.gov/gene/844768). The online general purpose multiple sequence alignment program ClustalW2 (with default settings) was used to make the alignment (Larkin et al., 2007).

When searching the NCBI protein database for polypeptides similar to TF1 using the protein BLAST program (Altschul et al., 1990), the hypothetical protein ARALYDRAFT_483623 shows the highest sequence similarity. An alignment of the promoter regions of these two genes revealed a common inverted and mutated GCC box motif in proximity to the ATG start codons (see Figure 27).

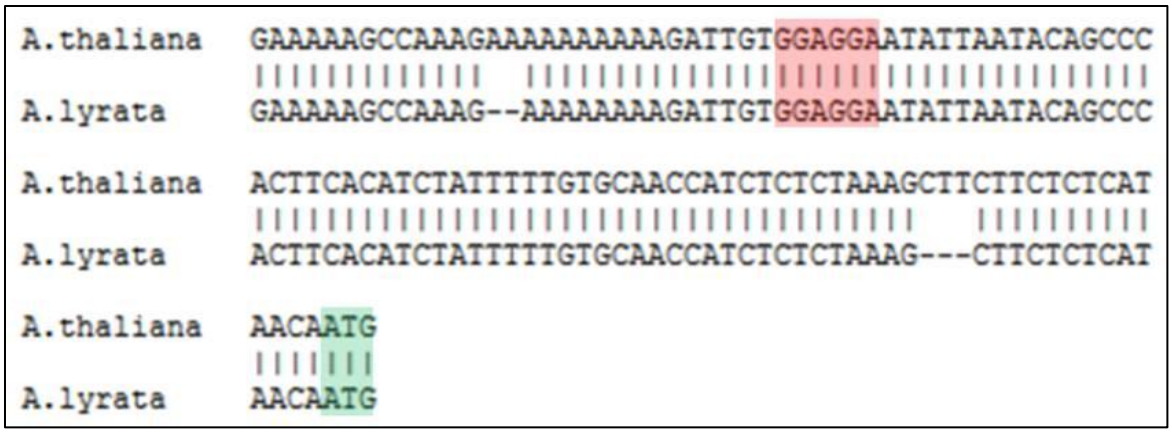

Figure 27: The promoter regions of At2g44940 (*TF1*) and its closest homologue in *Arabidopsis lyrata*, ARALYDRAFT_483623, both contain a mutated and inverted form of the GCC box (indicated in red) located in proximity to the start codons (indicated in green). The alignment was made using the online pairwise sequence local alignment tool EMBOSS Water, with default settings (Smith and Waterman, 1981).

The presence of this inverted and mutated GCC box-resembling sequence-motif in the promoter region of *TF1* revealed the possibility for TF1 to be involved in the regulation of its own expression through interaction with this DNA-motif.

Although the identification of short TF1-interacting DNA sequences within promoter regions of genes hypothetically suggests for the binding of TF1 to these promoters, the documentation of interactions between TF1 and larger parts of the native promoter regions would yield more correct data concerning which protein-DNA interactions might take place *in situ*.

3.6 TF1 binds to a conserved sequence in the *psbA* promoter region

In order to test if TF1 binds to the well conserved region of the *psbA* promoter, the entire 48bp long sequence was applied as bait sequence in yeast one-hybrid assays (see Table 22). To check if the DRE core motif (CCGAC) was the site of sequence-specific binding, a bait sequence in which these five nucleotides had been mutated was also tested for interaction with TF1 (see Table 22). As was mentioned in chapter 2.4, repeated bait sequences enable the prey protein to bind to the DNA at the optimal distance in order to activate transcription (Lopato et al., 2006). Therefore, three time tandem repeats of these sequences were also used as bait sequences (see Table 22).

The transformation of TF1-pGADT7 into reporter strains carrying full-length *psbA* bait sequences did not enable any of the strains to grow on SD/-His/-Leu plates with 5mM and 10mM 3-AT (see Figure 28A), indicating that TF1 was unable to bind any of these sequences under the conditions provided by the yeast one-hybrid assays. TINY was also tested for interaction with the full-length *psbA*-bait sequences using yeast one-hybrid assays, and as TF1, failed to interact with any of them (see Figure 28B).

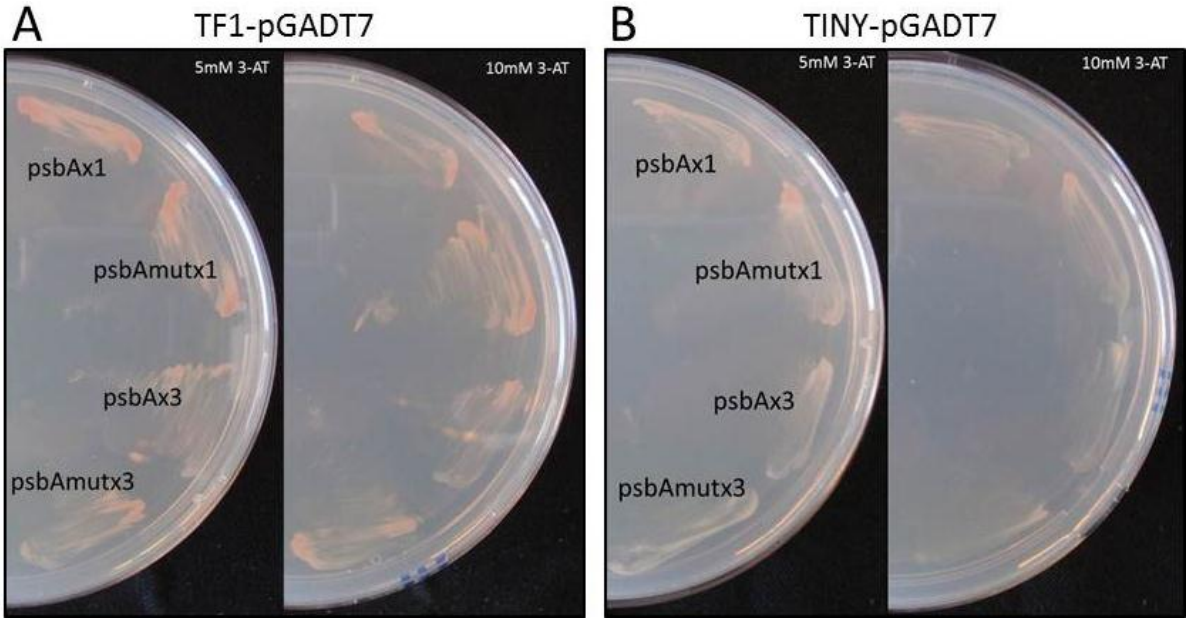

Figure 28: The ability of (A) TF1 and (B) TINY to bind a selection of *psbA* bait sequences were tested using yeast one-hybrid assays. Reporter strains transformed with (A) TF1-pGADT7 and (B) TINY-pGADT7 were plated on SD/-His/-Leu plates with 5mM and 10mM concentration of 3-AT. Plates were incubated at 30˚C for 3-4 days before documenting growth observations.

In addition to using the entire 48bp conserved *psbA* promoter region as bait sequence, two different variants of the region surrounding the DRE core motif (CCGAC) in the *psbA* promoter were tested: psbAcore4(a) and psbAcore4(b). These tandem repeated sequences are closer in size to the DRE and GCC box bait sequences used in the Y1H assays (see Table 22). As can be seen in Figure 29A, the psbAcore4(b) reporter strain expressing TF1 from pGADT7 grew on histidine- and leucine-deficient plates with 5mM and 10mM concentration of 3-AT. However, this indication of prey protein-bait sequence interaction was not seen for the psbAcore4(a) reporter strain transformed with TF1-pGADT7 (see Figure 29A).

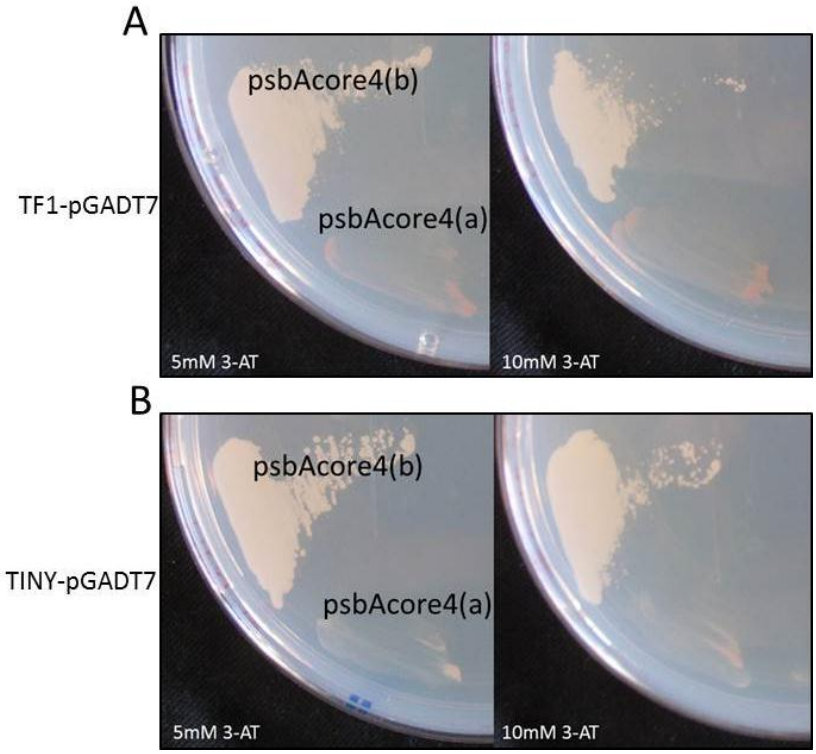

Figure 29: Yeast one-hybrid assays were applied to test for binding of (A) TF1 and (B) TINY to psbAcore4(a) and psbAcore4(b) bait sequences. Reporter strains transformed with (A) TF1-pGADT7 and (B) TINY-pGADT7 were plated on SD/-His/-Leu plates with 5mM and 10mM concentration of 3-AT. Plates were incubated at 30˚C for 3-4 days before documenting growth observations.

Transformation of TINY-pGADT7 into the psbAcore4(b) reporter strain enabled the yeast cells to grow on SD/-His/-Leu plates with 5mM and 10mM concentration of 3-AT (see Figure 29B), indicating that TINY also interacted with this bait sequence. Also in resemblance to TF1, the TINY prey protein did not appear to bind the psbAcore4(a)-bait sequence, as indicated by the inability of the TINY-pGADT7 transformed psbAcore4(a) reporter strain to grow on the plates selecting for protein-DNA interactions (see Figure 29B).

4. Discussion

All protein complexes executing major tasks in plastids consist of both nuclear- and plastid-encoded gene products. Therefore, a coordination of gene expression between these two compartments is necessary to avoid having too many or too few of the matching subunits. Transcription factors targeted to both nucleus and plastids are promising candidates for mediating the intercompartmental coordination of transcription, but so far little is known about this putative pathway.

In this study, the dually targeted transcription factor TF1 was investigated mainly with respect to its possible role in regulation of chloroplast gene expression. The inclusion of nuclear gene expression data, however, also allow for the drawing of some preliminary conclusions about the coordination of plastid and nuclear gene expression under the growth conditions applied in this study. In addition, the combination of observed TF1-mediated regulation of gene expression with data concerning the DNA-binding abilities of the transcription factor enables the proposal of mechanisms by which these regulations are carried out.

A tentative and simplified model for intracellular distribution and function of TF1, which will be the basis for future experiments, is presented at the end of the following discussion.

4.1 Knock-down of *TF1* influences plastid but not nuclear gene expression

The transcription factor TF1 is one of the many members of the AP2/EREBP family for which no function has been assigned (Dietz et al., 2010). The transcription of its mRNA is induced by light (Michael et al., 2008; Smith et al., 2004), which is also known to trigger the expression of photosynthesis-related genes. Several linkage analyses have shown that genes that are co-regulated often have related functions (Leister et al., 2011; Yao et al., 2011). From this viewpoint, a function of TF1 in the regulation of expression of photosynthesis-related genes would be feasible. This is supported by the fact that one of the intracellular locations of TF1 is the chloroplast compartment. To test whether TF1 can indeed regulate the expression of photosynthesis genes, light-induced changes in plastid and nuclear gene expression were investigated in two different genotypes of *Arabidopsis thaliana*.

Quite a large number of genes were investigated on the plastid genome (see Table 1). However, as can be seen in Figure 10, the expression level of the majority of genes was below the detection limit of the assay. Consequently, only those genes with detectable transcript levels will be mentioned in this discussion. These are the genes *psaA* and *psaB,* which are transcribed as one dicistronic operon and encode the apoproteins A1 and A2 (both core subunits of photosystem I), the *psbA* gene that encodes the chlorophyll-binding protein D1 of photosystem II, the *rbcL* gene encoding the large subunit of Ribulose-1,5-bisphosphate carboxylase oxygenase (RuBisCO) and the ribosomal RNA-encoding genes *rrn16* and *rrn23*. In addition to the nuclear-encoded photosynthesis genes *PSBO2* and *RBCS1A,* which encode an extrinsic subunit of photosystem II and the RuBisCO small subunit A1, respectively, the expression of the *TF1* gene itself was also analysed in this study with two goals: to confirm the knock-down in the mutant and the light-induced upregulation.

Figure 11 shows that the transcription rates of the plastid-encoded photosynthesis-related genes *psaA*, *psaB*, *psbA* and *rbcL* were all increased in response to four hours of light in wild type plants of *Arabidopsis thaliana*. This was also the case for the nuclear-encoded photosynthesis genes *PSBO2* and *RBCS1A,* as well as the *TF1* gene encoding the dually targeted transcription factor TF1 (see Figure 14). As can be expected from their function, the expression of photosynthesis-related genes (encoded both on the nuclear and plastid genome) is generally promoted by increased light-exposure and usually peak near the middle of the day (Taiz and Zeiger, 2006).

From the results presented in Figure 12 it can be seen that the loss of TF1 (ΔTF1) abolished the light-induced increase in transcription of the plastid-encoded photosynthesis genes *psaA*, *psaB*, *psbA* and *rbcL.* The fact that the ribosomal genes *rrn16* and *rrn23* was not likewise affected indicates that the consequence of a knock-down of *TF1* caused gene-specific rather than overall changes to plastid gene expression. The light-regulated transcription of the nuclear photosynthesis genes, *PSBO2* and *RBCS1A,* remained unaffected by knock-down of the *TF1* gene (see Figure 14).

In the introduction it was mentioned that the regulation of gene expression (both in the nucleus and in plastids) can take place on several different levels. In the case of chloroplast run-on transcription assays, the transcription rate, unaffected by RNA stability and turnover

is quantified. For assessing the positive or negative influence of a given transcription factor on its target genes, this is in fact the most direct method. While nuclear run-on transcription analysis is in principle also possible, one needs much higher amounts of radioactively labelled nucleotides than is the case for chloroplast run-on assays to ensure sufficient labelling of all nuclear transcripts. This would have been difficult to perform with the equipment available. Therefore, RT-qPCR was used to quantify the expression of selected nuclear genes at the level of their stably accumulating mRNAs in the cell. These stable RNAs, however, can be influenced by differential turnover rates, so that no direct information on the transcriptional activity of the gene is received. Theoretically, the influence of RNA degradation could contribute to mask any transcriptional changes caused by the absence of a transcription factor. Nevertheless, RT-qPCR is widely used as a method to investigate the influence of transcription factors (Brady et al., 2011; Eklund et al., 2011). In general, it is important to remember that a number of post-transcriptional regulatory processes like RNA processing, translation and post-translational modifications could (and probably would) also affect the overall expression of the respective gene. Consequently, in order to conclude that a knock-down mutation of TF1 causes a decrease in the number of metabolically active photosynthesis proteins, the respective protein levels would have to be monitored.

4.2 The DNA-binding specificity of TF1 shows similarities and differences to other AP2/EREBPs

The results presented in chapter 3.4 showed that TF1 interacted specifically with the DRE (TACCGACAT) and the inverted and mutated form of the GCC box (GGAGGAT) (see Figure 22 and Figure 23, respectively). The DRE motif is known to be bound by several AP2/EREBP transcription factors (reviewed in Dietz et al. (2010)), including TINY, which was used as a technical control in this study (see Figure 20). An online search for the inverted and mutated form of the GCC box (GGAGGAT) using PLACE (A Database of Plant Cis-acting Regulatory DNA Elements (Higo et al., 1999; Prestridge, 1991)) revealed no hits. This interaction is therefore very interesting since it displays a sequence-motif which so far is only known to be recognized by TF1.

TF1 was also found to interact with the 3082bp long promoter region of a Dof-type transcription factor (locus tag At5g60200) (see Figure 24A). This interaction had been documented before (Brady et al., 2011), and was included in this study as a positive control for TF1. The fact that TINY was also found to bind the promoter sequence (see Figure 24B) indicates that it might contain a common sequence-motif recognized by DREBs. On the other hand, it is also possible that TF1 and TINY recognize different motifs within the At5g60200 promoter region. Interestingly, searches for putative target sites in the 3082bp long sequence revealed an inverted and mutated GCC box motif (GGAGGA) and a DRE core motif (CCGAC). In order to further investigate which parts of the promoter region are recognized by TF1, yeast one-hybrid assays with truncated versions of the promoter region would be a suitable approach.

Even though the attempt to verify that the respective prey proteins were expressed in DBP-pGADT7-transformed reporter strains failed (see chapter 3.3.4), the fact that specific DNA-interactions are observed for both TINY and TF1 indicates that the prey proteins are indeed being expressed in the yeast reporter strains. A possible reason for the inability to detect the proteins is that they are expressed in very low amounts. This explanation would fit with the fact that no signals were detected with the TF1-specific antibody. Due to the presence of detergent in the buffer used for protein extraction (see chapter 2.6), it was not possible to measure the exact concentration of proteins by for instance Bradford assay (Bradford, 1976). This problem would be overcome by using a different technique for isolating proteins from yeast (e.g. enzymatic digestion of the cell wall followed by lysis or mechanical cell disruption using glass beads or liquid nitrogen (Dunn and Wobbe, 2001)). Nevertheless, it would probably be more effective to test the identified protein-DNA interactions using an independent method in order to confirm that they are reproducible.

Two conserved amino acid residues in the AP2 DNA-binding domain separate DREBs and ERFs (Liu et al., 1998). Valine-14 and glutamic acid-19 are conserved among DREBs, while the ERFs possess alanine and aspartic acid in these positions, respectively. Mutational studies have shown that the two conserved residues, while being important, are not the only amino acids involved in recognition of specific DNA sequences (Hao et al., 2002; Sakuma et al., 2002; Sun et al., 2008). For instance, Serine-15 of TINY was reported to be crucial for the interaction with the GCC box (Sun et al., 2008). As can be seen in Figure 30, all three of these

residues (V14, S15 and E19) are identical in TF1 and TINY. Thus, other TF1-residues must be involved in the binding of the inverted and mutated form of the GCC box.

As was mentioned in the introduction, the N-terminal plastid transit peptide of proteins destined to go to plastids is cleaved off upon import into the organelle. As a result, only a truncated form of TF1 (lacking the original N-terminal) is present to execute any functions within the boundaries of the plastid double membrane. In this study, the full-length form of TF1 has been used in the yeast one-hybrid assays. Although unlikely, it has not been excluded that the transit peptide interferes with the DNA-binding ability of the protein. Controls using the mature plastid-form of TF1 for yeast one-hybrid screens would be necessary to unambiguously answer this question.

4.3 TF1 might interact with DNA-motifs within the promoters of plastid-encoded genes

Although the identification of putative DNA-motifs bound by TF1 was an important step, this did not say anything about the biological function of the protein. In order to explain the effects of TF1 on plastid gene expression with the TF1-DNA interaction data, promoter regions of the genes *psaA/B, psbA* and *rbcL* were searched for sequence-motifs resembling those found to be bound by TF1. This search revealed a conserved region with a DRE core motif (CCGAC) in the promoter region of *psbA* (see Figure 25) and a conserved inverted and mutated GCC box motif (GGAGGA) in the promoter region of the *psaA/B* operon (see Figure 26).

The putative interaction between TF1 and *cis*-regulatory elements in the promoter region of *psbA* was further analysed by doing yeast one-hybrid assays with bait sequences representing the conserved region. Although no interaction was seen between TF1 and the entire 48bp region of the *psbA* promoter (see Figure 28A), TF1 did bind a four times repeated, 9bp long sequence of the promoter (ATCCGACTA) named psbAcore4(b) (see Figure 29A), that strongly resembles the DRE-sequence (TACCGACAT). This ability to interact independently of specific sequence identities outside of the CCGAC core is supported by mutational studies in which the identity of the nucleotides flanking the CCGAC core was not crucial for protein-DNA interaction (Sakuma et al., 2002).

Based on this knowledge of the CCGAC core being the site required for specific protein-DNA interaction, it is difficult to reason the incapability of TF1 to bind the psbAcore4(a) bait sequence (see Figure 29A). However, one possible explanation is that some flanking regions are needed between the tandem repeated core motifs in order to position the protein correctly for interaction with the nucleotides. This explanation would not apply to the failure of TF1 to bind to any of the full-length *psbA* sequences. In these cases, the length of the bait sequences (48bp) could restrict a DNA-binding protein from positioning at the appropriate distance for activation of transcription (Lopato et al., 2006). However, it may also reflect that TF1 does not target the promoter region of *psbA* on the plastid genome. All positive protein-DNA interactions identified by yeast one-hybrid assays in this study are enlisted in Table 23.

Table 23: List of bait sequences found to interact with any of the two prey proteins used in the yeast one-hybrid assays. Tandem repeated sequences are underlined. Binding of the respective protein to the respective sequence is indicated by +.

Bait sequence	Sequence (5'→ 3')	TF1	TINY
DRE	TACCGACATTACCGACATTACCGACATTACCGACAT	+	+
GCC	AGCCGCCAGCCGCCAGCCGCCAGCCGCC		+
Inv. GCCmut	GGAGGATGGAGGATGGAGGATGGAGGAT	+	
psbAcore4(b)	ATCCGACTAATCCGACTAATCCGACTAATCCGACTA	+	+
At5g60200 promoter	*	+	+

*The At5g60200 promoter-bait sequence is 3082bp long and is therefore not written here. The full-length sequence can be found in the NCBI database (http://www.ncbi.nlm.nih.gov/gene/836142).

The similarity between the binding-characteristics of TF1 and TINY (summarized in Table 23) questions how representative the protein-DNA interaction identified by yeast-based assays are for interactions occurring *in planta*. With 147 proteins containing the AP2 DNA-binding domain in *A. thaliana*, 57 of which are further classified as DREBs (Dietz et al., 2010) and putatively bind the DRE, one must assume that other factors conferring specificity to the interactions must exist. However, in the case of the plastid-encoded genes that were identified in this study, most AP2 proteins including TINY can be eliminated as binding candidates since they are not imported into the chloroplasts (12 AP2/EREBPs, 9 of which belong to the DREB subfamily, were *in silico* predicted to be dually targeted to plastids and

nucleus by Schwacke and co-workers in 2007). Nevertheless, one of the closest homologues of TF1, ERF035, does contain a plastid transit peptide and shares a major part of the AP2-residues that distinguish TF1 from TINY (see Figure 30).

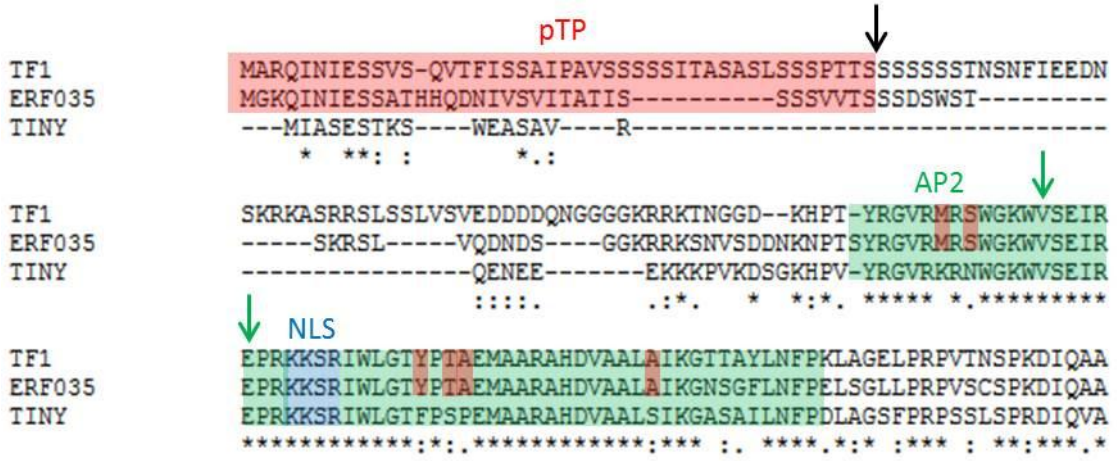

Figure 30: TF1 and ERF035 possess an N-terminal plastid transit peptide (pTP) (indicated in red) that is enriched with hydroxylated amino acids (Soll and Schleiff, 2004). The black arrow indicates the site were the pTP is cleaved upon plastid import (Schwacke et al., 2007). TINY does not have a pTP. All three proteins are targeted to the nucleus by the nuclear localization sequence (NLS) (indicated in blue) located within the AP2 domain. The green arrows indicate V14 and E19, which are conserved residues among DREBs (Liu et al., 1998). Residues of the AP2 domain which TF1 and ERF035 have in common but in TINY differ are indicated in brown. The alignment was made using the online general purpose multiple sequence alignment program ClustalW2, with default settings (Larkin et al., 2007). In this illustration, only the first <200 residues (starting from the N-terminal) of the alignment are shown.

Both TF1 and ERF035 have been reported to interact with the promoter region of At5g60200 (Brady et al., 2011). This indicates that the two proteins have corresponding binding-preferences. Hence, similar experiments as executed for TF1 in this study would be needed in order to reveal possible redundancies between these two proteins. Even so, redundancy between TF1 and ERF035 in the light-induced upregulation of the plastid-encoded photosynthesis genes *psaA*, *psaB*, *psbA* and *rbcL* is unlikely since the run-on transcription assays done in this study indicate that expression of *TF1* is required to achieve light-induced transcription of these genes.

No additional experiments have yet been executed to more closely study the possible interaction between TF1 and the conserved inverted and mutated GCC box motif in the promoter region of the *psaA/B* operon. However, in the future, it would be very interesting to do interaction studies with larger parts of this promoter, like was done for *psbA*. With respect to the conserved GGAGGAT sequence located between the end of the *psaA* gene and the start of the *psaB* gene in the dicistronic operon (see Figure 26), the fact that it lies downstream of the transcription start point makes it less likely to play a part in transcriptional regulation of the operon than the similar sequence located upstream of the *psaA* translational start codon. Nevertheless, since some DNA sequences (termed enhancers and silencers in Becker et al. (2006)) are known to affect gene-specific transcription rates independently of their location, it will require further experimental investigation to reveal whether or not this sequence-motif is a *cis*-regulatory element.

In the case of the *rbcL* gene, whose transcription was shown to be affected by TF1, no putative *cis*-regulatory elements could be found in the promoter region. There are two possible explanations for this: i) TF1 regulates the transcription of *rbcL* by binding a DNA-sequence that is different from the DRE and the mutated and inverted GCC box motif identified in this study. ii) TF1 regulates the transcription of *rbcL* indirectly by interaction with other proteins. The first possibility could be tested by doing yeast one-hybrid assays with TF1 and the entire (or different parts of) the *rbcL* promoter region. By doing yeast two-hybrid (or other protein-protein interaction assays) with TF1 and candidates for regulating the transcription rate of *rbcL* (e.g. sigma factors, RNA polymerase or other regulatory transcription factors) one could reveal ways for TF1 to affect *rbcL* transcription without direct interaction with the gene's promoter region.

4.4 Putative model for TF1 function

The previously published results on expression and localisation of TF1 (Michael et al., 2008; Schwacke et al., 2007), together with some unpublished results (Krause and Yin, personal communications, and the results obtained in this study, allow to propose a putative model suggesting functions and regulatory aspects connected to TF1 that shall be presented here, and that will serve as a basis for the design of future experiments.

In short, the model is based on the following observations:

- TF1 is dually targeted to chloroplasts and the nucleus (Schwacke et al., 2007).
- The expression of *TF1* is regulated by light ((Michael et al., 2008) and results obtained in this thesis).
- Changes in the expression of *TF1* were only found to affect the light-induced transcription of plastid-encoded genes, and seemingly did not have any effects on the light-regulated transcription of genes encoded on the nuclear genome (results obtained in this thesis). Consequently, the plastid signal that coordinates plastid and nuclear gene expression in mature plants as a response to the diurnal light-dark rhythm is dysfunctional in mutants in which the expression of *TF1* is abolished.
- In the yeast one-hybrid system, TF1 interacts with DNA sequence-motifs found in the promoter of three of the four plastid genes that are impaired in light-promoted transcription in ΔTF1 mutants (results obtained in this thesis).
- Intracellular localisation of TF1 in transiently transformed Arabidopsis protoplasts was occasionally found to depend on light exposure, the protein having a tendency to be more concentrated in the chloroplasts under high light exposure and vice versa in the nucleus under low light conditions (Krause, personal communication).
- It proved to be impossible to create transgenic lines with more than a two-fold increased *TF1*-expression, suggesting tightly regulated TF1 levels that may be controlled by feed-back inhibition (Yin et al., unpublished results).

The promoter region of TF1, as well as the promoter region of its closest homologue in *Arabidopsis lyrata*, ARALYDRAFT_483623, were found to contain a mutated and inverted GCC box motif (see Figure 27), which interacts with TF1 in yeast one-hybrid assays (see Figure 23). Hence, the encountered difficulties in generating a mutant line overexpressing TF1 could be explained by the activity of a negative feedback loop in which a high concentration of TF1 in the nucleus inhibits its own transcription by binding its own promoter region. It should here be said that a four-fold increase in the amounts of TF1-transcripts was observed from right before daybreak to four hours after daybreak in WT Arabidopsis (see Figure 14). This would at first glance contradict the statement that feed-back inhibition is the reason that no more than a two-fold increased *TF1*-expression could be generated in a mutant line. However, when taking into account the suggested light-dependent localization of TF1, the assumption can be made that the nuclear concentration of TF1 does not increase in response to light since the protein is to a large extent being imported into chloroplasts. It is known that a variety of internal and external signals can affect the cellular localization of proteins in plants (reviewed in Silva-Filho (2003)). For instance, the nuclear import of phytochromes has been shown to be regulated by light (Kircher et al., 2002).

Inside the plastids, binding of TF1 to the proposed *cis*-regulatory elements in the promoter regions of the photosynthesis genes *psbA* and *psaA/B* increases the transcription rate of the respective genes. The light-induced transcriptional promotion of *rbcL* is also dependent on TF1. However, since no TF1-binding sites could be found in the promoter region of this gene, it is here suggested that the transcription rate of *rbcL* is indirectly affected by TF1.

In the dark, nuclear import of TF1 is increased, leading to a downregulation of *TF1*-expression by feed-back inhibition and subsequently a decrease in the transcription rate of the plastid-encoded photosynthesis genes *psaA*, *psaB*, *psbA* and *rbcL* due to reduction in plastid-localized TF1. A manner for the plastids to further control the amounts of cytosolic (and indirectly nuclear) TF1 is if the protein could be exported out of the plastids to the cytosol. One could imagine that regulatory mechanisms inside the plastids are able to prevent TF1 from interacting with *cis*-regulatory elements in the promoter regions of *psaA*/*B* and *psbA,* and thereby fail to promote their transcription. This unbound form of TF1 would putatively be more receptive for transportation out of the plastid compartment than TF1 in

complex with DNA. Plastid export of TF1 would increase the cytosolic concentration of TF1 and thereby amplify the negative feedback signal generated by increased transport of TF1 into the nucleus (granted that the mature plastid-form of TF1 functions in the same way as the full-length protein). So far, no plastid exporters have been characterized. However, the recently reported translocation of the dually targeted transcription factor Whirly1 from chloroplasts to nucleus by Isemer et al. (2012) argues for the existence of protein transportation in this direction. As discussed in Krause and Krupinska (2009), several different mechanisms for protein transport from plastids to nucleus which does not require the presence of a membrane channel/transporter are possible (e.g. transport by close intercompartmental contact or vesicles).

The observation that abolishment of *TF1*-expression did not have any effects on the transcription rates of the nuclear-encoded photosynthesis genes *PSBO2* and *RBCS1A* indicates that TF1 does not play a part in the expressional regulation of nuclear-encoded photosynthesis-related genes, but is solely involved in the light-regulated transcription of plastid-encoded genes. However, disturbing the expression of plastid-encoded photosynthesis genes under various conditions, including light-dark treatment, is known to affect the nuclear expression of plastid-targeted photosynthesis genes by retrograde signalling (Leister, 2012; Pfannschmidt, 2010; Strand, 2004). Therefore, it is actually rather surprising that the transcription of the nuclear photosynthesis genes investigated here remained unaffected by *TF1* knock-down, while the light-induced upregulation of the plastid photosynthesis genes *psaA*, *psaB*, *psbA* and *rbcL* show total dependence on TF1. Especially, the transcription of *PSBO2* and *psbA*, and *RBCS1A* and *rbcL* should be tightly coordinated since they encode subunits of the same complexes, respectively. On these premises, the plastid signal informing the nucleus that the light-induced transcription of *psaA*, *psaB*, *psbA* and *rbcL* is impaired in the ΔTF1 mutant is seemingly also interrupted by the lack of TF1.

On the basis of the results discussed above, a proposition for a model describing the putative function of TF1 in the light-regulated transcription of nuclear- and plastid-encoded photosynthesis genes is presented in Figure 31. There is of course a multitude of proteins that take part in this regulation (Leister et al., 2011; Yao et al., 2011). However, in order to maintain simplicity, only the isolated putative role of TF1 in the light-controlled transcriptional regulation of the genes investigated in this study is illustrated.

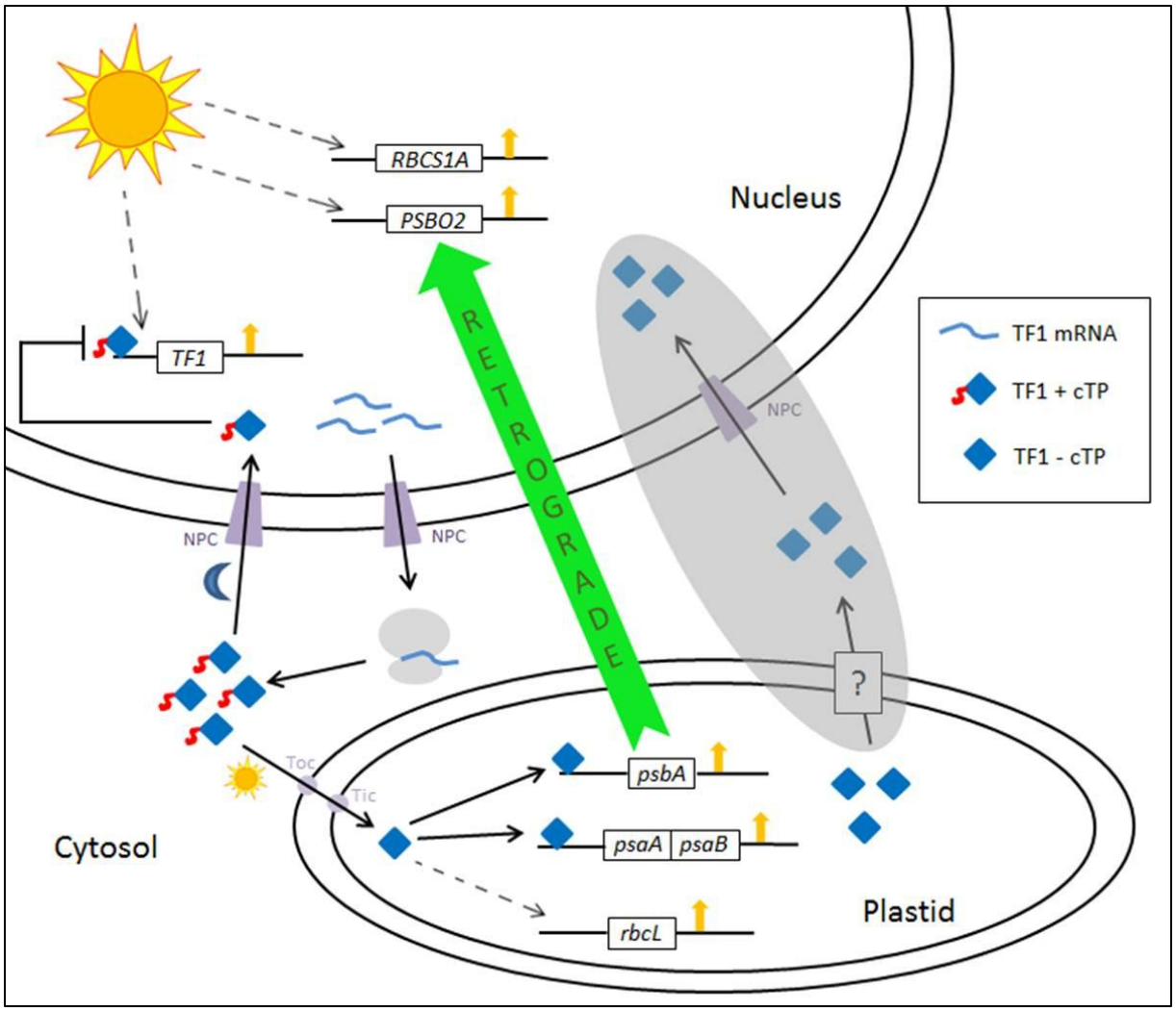

Figure 31: Simplified model for the putative function of TF1 in the light-regulated transcription of nuclear and plastid photosynthesis genes. The transcription of the nuclear-encoded genes *TF1*, *RBCS1A* and *PSBO2,* and the plastid-encoded genes *psbA, psaA/B* and *rbcL* are all upregulated by light (indicated by yellow arrows). Following nuclear export of TF1 mRNA through the nuclear pore complex (NPC), the transcripts are translated to polypeptides containing both an N-terminal plastid transit peptide (pTP) and an internal nuclear localization signal. Dually targeted TF1 proteins are imported both into the nucleus through the NPC and into the plastids through the Tic-Toc import complex. However, plastid import of TF1 is tentatively favored over nuclear import in the light, and vice versa in the dark (indicated by sun and moon). In light, the plastid-localized TF1 is suggested to promote transcription of *psbA* and *psaA/B* by binding putative *cis*-regulatory elements in their promoter regions. Transcription of the *rbcL* gene is also elevated by increased *TF1*-expression. However, this TF1-effect could be indirect since none of the so far identified DNA-interaction motifs were found in the *rbcL* promoter. In the dark, nuclear TF1 is suggested to repress its own transcription by binding a putative *cis*-regulatory element in its own promoter region, which in turn leads to a decrease in the transcription of the plastid-encoded photosynthesis genes by causing a reduction in the amount of plastid-localized TF1. Plastid export of TF1 could theoretically increase the nuclear concentration of TF1. However, since there are no data supporting plastidial TF1-export, the illustration of this event has been shaded grey. Retrograde signalling from plastid to nucleus is indicated by a large green arrow. On basis of the expressional data obtained in this study, the signal mediating coordinated transcription of plastid and nuclear-encoded photosynthesis genes is somehow abolished when TF1 is not expressed, indicating the involvement of TF1 in this retrograde signalling. Due to the innumerable ways TF1 might assist in the conduction of a plastid signal, no attempts have been made here to illustrate possible pathways. Rather, the reader is referred to one of several reviews and opinion papers published in recent years (Krause and Krupinska, 2009; Leister, 2012; Pfannschmidt, 2010; Strand, 2004).

It is important to emphasize that, other than the slightly slower growth of the mutant plants; no obvious difference could be seen between the WT *Arabidopsis thaliana* plants and the plants in which expression of *TF1* was knocked down (ΔTF1). When taking into account the vital functions of the genes which were dependent on the expression of the *TF1* gene for light-induced transcriptional promotion, it is surprising that such an inconspicuous phenotype was observed for ΔTF1. One possible explanation is that the light-induced upregulation of *psaA*, *psaB*, *psbA* and *rbcL* transcription rates is not crucial to keep the plants growing, and that the lower rates of transcription measured before daybreak are sufficient to maintain a sustainable photosynthesis rate. It is also possible that, even though a light-induced increase in the transcription rates of these genes is observed, the terminal expression rates (i.e. the number of functional proteins) of these genes are unaffected due to the activity of post-transcriptional regulatory mechanisms. This should of course be tested by measuring the respective protein levels.

4.5 Outlook

There are several additional experiments that should be executed in order to test the applicability of the above model for TF1 functionality (see Figure 31). Firstly, if the transcriptional differences observed between WT and ΔTF1 *A. thaliana* are indeed results of the presence vs. absence of the dually targeted transcription factor, and not the consequences of unknown artefacts caused by the transformation, the phenotype of ΔTF1 should be rescued by transforming ΔTF1 plants with constructs expressing TF1.

Import of proteins from cytosol to plastid stroma through the Tic-Toc import machinery is dependent on a plastid transit peptide located at the N-terminal of the protein (Jarvis and Soll, 2001). Hence, by removing this terminal target sequence, one would inhibit the targeting of the protein to chloroplasts. The transcriptional regulation of plastid-encoded genes by the binding of TF1 to *cis*-regulatory elements in their promoter regions as suggested here (see Figure 31) requires the physical presence of TF1 inside the chloroplasts. By transforming ΔTF1 plants with constructs expressing the mature TF1 (without the N-terminal transit peptide), the protein should still be able to carry out any functions in the cytosol or nucleus, but would not be imported into plastids. A successful rescue of the ΔTF1-

phenotype by this experiment would indicate that TF1 does not have to be localized inside the chloroplast to promote plastid transcription, thereby eliminating the possibility for TF1 causing these effects by direct interaction with plastid promoter regions. On the other hand, if the phenotype persists, this would corroborate that the plastid-localized TF1 directly influences the light-promoted transcription of plastid-encoded photosynthesis genes.

The model for TF1 functionality presented in this thesis (see Figure 31) is largely based on the light-dependent localization of TF1. Although this has been occasionally observed, it has not been scientifically documented (Krause, personal communication). By transforming Arabidopsis protoplasts with TF1-GFP fusion expression constructs and incubating them under various light conditions before microscopic observation, the light-induced effects on TF1-targeting can be further examined. In addition, to uncover possible TF1-export out of plastids, isolation of proteins from *A. thaliana* nuclei and plastids independently, followed by western blotting using the TF1-specific antibody would reveal if the mature TF1 is at all present in the nucleus.

Treatment with norflurazon leads to plastid impairment and has been applied to reveal mutants in which the nuclear genome and the plastid genome are uncoupled (Susek et al., 1993). As coordination between the expression of nuclear- and plastid-encoded photosynthesis genes appears to be disrupted when the *TF1* gene is knocked down, the ΔTF1 mutant is a possible *gun*-mutant. The obvious way to test this would be to treat ΔTF1 plants with norflurazon and subsequently measure the expression of the *gun*-mutant marker gene *LHCB.* If TF1 is necessary for this retrograde signalling pathway to function, the expression of *LHCB* should not be repressed by norflurazon.

However, since the putative pathway coordinating light-induced transcriptional promotion of the nuclear genes *RBCS1A* and *PSBO2* with the plastid genes *psaA*, *psaB*, *psbA* and *rbcL* might be separate from the traditional *gun*-pathway, it would also be interesting to see if treatment with norflurazon influences the light-regulated transcription rates of *RBCS1A* and *PSBO2* in the *TF1* knock-down mutant. If TF1 is needed for a retrograde signalling pathway coordinating the transcription of these genes with the state of the plastid, the nuclear genes should remain unaffected by the norflurazon-mediated plastid dysfunction.

Also, in order to properly verify that there is indeed coordination between the transcription of the nuclear-encoded *RBCS1A* and *PSBO2,* and the plastid-encoded *psaA*, *psaB*, *psbA* and *rbcL*, the light-induced effects on transcription of the nuclear genes would have to be measured in norflurazon-treated WT plants. In this case, if there is intercompartmental coordination, the transcription of *RBCS1A* and *PSBO2* should be downregulated.

With respect to the DNA-binding abilities of TF1, as identified in this study by yeast one-hybrid assays, verification of the documented protein-DNA interactions by other methods would be necessary in order to make any safe conclusions regarding which interactions are indeed taking place within the plant cell. Examples of other methods for detection of protein-DNA interactions are: gel-mobility shift assays, southwestern blotting and chromatin immunoprecipitation (ChIP) (reviewed in Dey et al. (2012)). The first two methods are biochemical techniques in which the conditions for the interaction has to be set up *in vitro*. Since different protein-DNA interactions might require different conditions, *in vitro* optimization can prove to be difficult. However, in the case of AP2/EREBP transcription factors, several protein-DNA interactions have been documented by gel mobility shift assays (Sakuma et al., 2002; Stockinger et al., 1997; Sun et al., 2008). Due to the high degree of conservation in the AP2 binding domain of AP2/EREBPs, it is proposed that members of this transcription factor family interact with DNA in a similar manner (Allen et al., 1998). Consequently, conditions used to study protein-DNA interactions for other AP2/EREBPs should be applicable to study the binding of TF1 to DNA.

The downside with gel mobility shift assays, southwestern blotting and also yeast one-hybrid assays is that in all three cases the interaction between protein and DNA is taking place in a different setting than it would in the plant. Although Y1H assays offer an intracellular environment for the interactions to take place in, the conditions of yeast nucleus and chloroplast nucleoids are not identical. Especially, protein modifications (e.g. phosphorylation, glycosylation, and methylation) or additional cofactors might influence the ability of TF1 to bind specific DNA-motifs. ChIP offers *in situ* detection of protein-DNA interaction by fragmentation of the entire plant genome followed by precipitation of protein-DNA complexes using an antibody specific for the protein of interest. After precipitation, PCR amplification methods are applied in order to reveal the identity of the DNA fragment(s) which the respective protein was bound to. The downside of this method is

that it is dependent on the amount of protein, and does not work for weakly expressed proteins. Given that all methods for studying protein-DNA interactions have their pros and cons, the safest conclusions to which interactions are happening *in planta* are made by using more than one technique.

As was mentioned in the introduction, expression of *TF1* is, in addition to being increased by light-exposure, also promoted by cold temperatures (Kilian et al., 2007). Therefore, in order to further expand the model suggested here for the function of TF1 in light-regulated expression of photosynthesis genes, it would be very interesting to see the effects of temperature on the expression of plastid- and nuclear-encoded genes in TF1 and ΔTF1.

References

Adam, Z., A. Rudella, and K.J. van Wijk. 2006. Recent advances in the study of Clp, FtsH and other proteases located in chloroplasts. *Curr Opin Plant Biol*. 9:234-240.

Allen, M.D., K. Yamasaki, M. Ohme-Takagi, M. **Tateno, and M. Suzuki. 1998**. A novel mode of DNA recognition by a beta-sheet revealed by the solution structure of the GCC-box binding domain in complex with DNA. *Embo J*. 17:5484-5496.

Altschul, S.F., W. Gish, W. Miller, E.W. Myers, and D.J. Lipman. 1990. Basic local alignment search tool. *J Mol Biol*. 215:403-410.

Arabidopsis Genome Initiative. 2000. Analysis of the genome sequence of the flowering plant Arabidopsis thaliana. *Nature*. 408:796-815.

Baumgartner, B.J., J.C. Rapp, and J.E. Mullet. 1989. Plastid transcription activity and DNA copy number increase early in barley chloroplast development. *Plant Physiol*. 89:1011-1018.

Berglund, A.K., C. Pujol, A.M. Duchene and E. Glaser. 2009. Defining the determinants for dual targeting of amino acyl-tRNA synthetases to mitochondria and chloroplasts. *J Mol Biol*. 393:803-814

Becker, W.M., L.J. Kleinsmith, and J. Hardin. 2006. The World of the Cell. Pearson Education, Inc., publishing as Benjamin Cummings, San Francisco, California.

Birnboim, H.C., and J. Doly. 1979. A rapid alkaline extraction procedure for screening recombinant plasmid DNA. *Nucleic Acids Res*. 7:1513-1523.

Bradford, M.M. 1976. A rapid and sensitive method for the quantitation of microgram quantities of protein utilizing the principle of protein-dye binding. *Analytical biochemistry*. 72:248-254.

Brady, S.M., L. Zhang, M. Megraw, N.J. Martinez, E. Jiang, C.S. Yi, W. Liu, A. Zeng, M. Taylor-Teeples, D. Kim, S. Ahnert, U. Ohler, D. Ware, A.J. Walhout, and P.N. Benfey. 2011. A stele-enriched gene regulatory network in the Arabidopsis root. *Mol Syst Biol*. 7:459.

Bruce, B.D. 2000. Chloroplast transit peptides: structure, function and evolution. *Trends in cell biology*. 10:440-447.

Bräutigam, K., L. Dietzel, and T. Pfannschmidt. 2007. Plastid-nucleus communication: anterograde and retrograde signalling in the development and function of plastids. *Cell and Molecular Biology of Plastids*. 19:400-455.

Caplan, J.L., P. Mamillapalli, T.M. Burch-Smith, K. Czymmek, and S.P. Dinesh-Kumar. 2008. Chloroplastic protein NRIP1 mediates innate immune receptor recognition of a viral effector. *Cell*. 132:449-462.

Deng, X.W., D.B. Stern, J.C. Tonkyn, and W. Gruissem. 1987. Plastid run-on transcription. Application to determine the transcriptional regulation of spinach plastid genes. *J Biol Chem*. 262:9641-9648.

Dey, B., S. Thukral, S. Krishnan, M. Chakrobarty, S. Gupta, C. Manghani, and V. Rani. 2012. DNA-protein interactions: methods for detection and analysis. *Molecular and cellular biochemistry*. 365:279-299.

Dietz, K.J., M.O. Vogel, and A. Viehhauser. 2010. AP2/EREBP transcription factors are part of gene regulatory networks and integrate metabolic, hormonal and environmental signals in stress acclimation and retrograde signalling. *Protoplasma*. 245:3-14.

Dunn, B., and C.R. Wobbe. 2001. Preparation of protein extracts from yeast. *Current protocols in molecular biology / edited by Frederick M. Ausubel ... [et al.]*. Chapter 13:Unit13 13.

Dyall, S.D., M.T. Brown, and P.J. Johnson. 2004. Ancient invasions: from endosymbionts to organelles. *Science*. 304:253-257.

Eklund, D.M., I. Cierlik, V. Staldal, A.R. Claes, D. Vestman, J. Chandler, and E. Sundberg. 2011. Expression of Arabidopsis SHORT INTERNODES/STYLISH family genes in auxin biosynthesis zones of aerial organs is dependent on a GCC box-like regulatory element. *Plant Physiol*. 157:2069-2080.

Fey, V., R. Wagner, K. Brautigam, M. Wirtz, R. Hell, A. Dietzmann, D. Leister, R. Oelmuller, and T. Pfannschmidt. 2005. Retrograde plastid redox signals in the expression of nuclear genes for chloroplast proteins of Arabidopsis thaliana. *J Biol Chem*. 280:5318-5328.

Garcia-Bustos, J., J. Heitman, and M.N. Hall. 1991. Nuclear protein localization. *Biochim Biophys Acta*. 1071:83-101.

Greenberg, B.M., J.O. Narita, C. Delucaflaherty, W. Gruissem, K.A. Rushlow, and R.B. Hallick. 1984. Evidence for 2 Rna-Polymerase Activities in Euglena-Gracilis Chloroplasts. *Journal of Biological Chemistry*. 259:4880-4887.

Hajdukiewicz, P.T., L.A. Allison, and P. Maliga. 1997. The two RNA polymerases encoded by the nuclear and the plastid compartments transcribe distinct groups of genes in tobacco plastids. *Embo J*. 16:4041-4048.

Hall, T.C., Y. Ma, B.U. Buchbinder, J.W. Pyne, S.M. Sun, and F.A. Bliss. 1978. Messenger RNA for G1 protein of French bean seeds: Cell-free translation and product characterization. *Proc Natl Acad Sci U S A*. 75:3196-3200.

Han, S., and D. Kim. 2006. AtRTPrimer: database for Arabidopsis genome-wide homogeneous and specific RT-PCR primer-pairs. *BMC bioinformatics*. 7:179.

Hanahan, D., J. Jessee, and F.R. Bloom. 1991. Plasmid transformation of Escherichia coli and other bacteria. *Methods in enzymology*. 204:63-113.

Hao, D., M. Ohme-Takagi, and A. Sarai. 1998. Unique mode of GCC box recognition by the DNA-binding domain of ethylene-responsive element-binding factor (ERF domain) in plant. *J Biol Chem*. 273:26857-26861.

Hao, D., K. Yamasaki, A. Sarai, and M. Ohme-Takagi. 2002. Determinants in the sequence specific binding of two plant transcription factors, CBF1 and NtERF2, to the DRE and GCC motifs. *Biochemistry*. 41:4202-4208.

Higo, K., Y. Ugawa, M. Iwamoto, and T. Korenaga. 1999. Plant cis-acting regulatory DNA elements (PLACE) database: 1999. *Nucleic Acids Res*. 27:297-300.

Isemer, R., M. Mulisch, A. Schafer, S. Kirchner, H.U. Koop, and K. Krupinska. 2012. Recombinant Whirly1 translocates from transplastomic chloroplasts to the nucleus. *FEBS Lett*. 586:85-88.

Jarvis, P., and J. Soll. 2001. Toc, Tic, and chloroplast protein import. *Biochim Biophys Acta*. 1541:64-79.

Jofuku, K.D., B.G. den Boer, M. Van Montagu, and J.K. Okamuro. 1994. Control of Arabidopsis flower and seed development by the homeotic gene APETALA2. *Plant Cell*. 6:1211-1225.

Kanamaru, K., and K. Tanaka. 2004. Roles of chloroplast RNA polymerase sigma factors in chloroplast development and stress response in higher plants. *Biosci Biotechnol Biochem*. 68:2215-2223.

Kilian, J., D. Whitehead, J. Horak, D. Wanke, S. Weinl, O. Batistic, C. D'Angelo, E. Bornberg-Bauer, J. Kudla, and K. Harter. 2007. The AtGenExpress global stress expression data set: protocols, evaluation and model data analysis of UV-B light, drought and cold stress responses. *Plant J*. 50:347-363.

Kircher, S., P. Gil, L. Kozma-Bognar, E. Fejes, V. Speth, T. Husselstein-Muller, D. Bauer, E. Adam, E. Schafer, and F. Nagy. 2002. Nucleocytoplasmic partitioning of the plant photoreceptors phytochrome A, B, C, D, and E is regulated differentially by light and exhibits a diurnal rhythm. *Plant Cell*. 14:1541-1555.

Klein, R.R., and J.E. Mullet. 1986. Regulation of chloroplast-encoded chlorophyll-binding protein translation during higher plant chloroplast biogenesis. *J Biol Chem*. 261:11138-11145.

Klein, R.R., and J.E. Mullet. 1990. Light-Induced Transcription of Chloroplast Genes - Psba Transcription Is Differentially Enhanced in Illuminated Barley. *Journal of Biological Chemistry*. 265:1895-1902.

Krause, K., and C.L. Dieckmann. 2004. Analysis of transcription asymmetries along the tRNAE-COB operon: evidence for transcription attenuation and rapid RNA degradation between coding sequences. *Nucleic Acids Res*. 32:6276-6283.

Krause, K., J. Falk, K. Humbeck, and K. Krupinska. 1998. Responses of the transcriptional apparatus of barley chloroplasts to a prolonged dark period and to subsequent reillumination. *Physiol Plant*. 104:143-152.

Krause, K., and K. Krupinska. 2009. Nuclear regulators with a second home in organelles. *Trends Plant Sci*. 14:194-199.

Krause, K., R.M. Maier, W. Kofer, K. Krupinska, and R.G. Herrmann. 2000. Disruption of plastid-encoded RNA polymerase genes in tobacco: expression of only a distinct set of genes is not based on selective transcription of the plastid chromosome. *Molecular and General Genetics*. 263:1022-1030.

Krupinska, K. 1992. Transcriptional Control of Plastid Gene-Expression during Development of Primary Foliage Leaves of Barley Grown under a Daily Light-Dark Regime. *Planta*. 186:294-303.

Krupinska, K., and K. Apel. 1989. Light-Induced Transformation of Etioplasts to Chloroplasts of Barley without Transcriptional Control of Plastid Gene-Expression. *Molecular & General Genetics*. 219:467-473.

Kubista, M., J.M. Andrade, M. Bengtsson, A. Forootan, J. Jonak, K. Lind, R. Sindelka, R. Sjoback, B. Sjogreen, L. Strombom, A. Stahlberg, and N. Zoric. 2006. The real-time polymerase chain reaction. *Molecular aspects of medicine*. 27:95-125.

Kushnirov, V.V. 2000. Rapid and reliable protein extraction from yeast. *Yeast*. 16:857-860.

Laemmli, U.K. 1970. Cleavage of structural proteins during the assembly of the head of bacteriophage T4. *Nature*. 227:680-685.

Larkin, M.A., G. Blackshields, N.P. Brown, R. Chenna, P.A. McGettigan, H. McWilliam, F. Valentin, I.M. Wallace, A. Wilm, R. Lopez, J.D. Thompson, T.J. Gibson, and D.G. Higgins. 2007. Clustal W and Clustal X version 2.0. *Bioinformatics*. 23:2947-2948.

Lee, J.Y., J. Colinas, J.Y. Wang, D. Mace, U. Ohler, and P.N. Benfey. 2006. Transcriptional and posttranscriptional regulation of transcription factor expression in Arabidopsis roots. *Proc Natl Acad Sci U S A*. 103:6055-6060.

Leister, D. 2012. Retrograde signaling in plants: from simple to complex scenarios. *Frontiers in plant science*. 3:135.

Leister, D., X. Wang, G. Haberer, K.F. Mayer, and T. Kleine. 2011. Intracompartmental and intercompartmental transcriptional networks coordinate the expression of genes for organellar functions. *Plant Physiol*. 157:386-404.

Liere, K., A. Weihe, and T. Borner. 2011. The transcription machineries of plant mitochondria and chloroplasts: Composition, function, and regulation. *Journal of plant physiology*. 168:1345-1360.

Liu, Q., M. Kasuga, Y. Sakuma, H. Abe, S. Miura, K. Yamaguchi-Shinozaki, and K. Shinozaki. 1998. Two transcription factors, DREB1 and DREB2, with an EREBP/AP2 DNA binding domain separate two cellular signal transduction pathways in drought- and low-temperature-responsive gene expression, respectively, in Arabidopsis. *Plant Cell*. 10:1391-1406.

Lopato, S., N. Bazanova, S. Morran, A.S. Milligan, N. Shirley, and P. Langridge. 2006. Isolation of plant transcription factors using a modified yeast one-hybrid system. *Plant Methods*. 2:3.

Magnani, E., K. Sjolander, and S. Hake. 2004. From endonucleases to transcription factors: evolution of the AP2 DNA binding domain in plants. *Plant Cell*. 16:2265-2277.

Melonek, J., A. Matros, M. Trosch, H.P. Mock, and K. Krupinska. 2012. The Core of Chloroplast Nucleoids Contains Architectural SWIB Domain Proteins. *Plant Cell*.

Melonek, J., M. Mulisch, C. Schmitz-Linneweber, E. Grabowski, G. Hensel, and K. Krupinska. 2010. Whirly1 in chloroplasts associates with intron containing RNAs and rarely co-localizes with nucleoids. *Planta*. 232:471-481.

Meyer, T.S., and B.L. Lamberts. 1965. Use of coomassie brilliant blue R250 for the electrophoresis of microgram quantities of parotid saliva proteins on acrylamide-gel strips. *Biochim Biophys Acta*. 107:144-145.

Michael, T.P., T.C. Mockler, G. Breton, C. McEntee, A. Byer, J.D. Trout, S.P. Hazen, R. Shen, H.D. Priest, C.M. Sullivan, S.A. Givan, M. Yanovsky, F. Hong, S.A. Kay, and J. Chory. 2008. Network discovery pipeline elucidates conserved time-of-day-specific cis-regulatory modules. *PLoS genetics*. 4:e14.

Moore, D. 2001. Purification and concentration of DNA from aqueous solutions. *Current protocols in immunology / edited by John E. Coligan ... [et al.]*. Chapter 10:Unit 10 11.

Mullet, J.E., and R.R. Klein. 1987. Transcription and RNA stability are important determinants of higher plant chloroplast RNA levels. *Embo J*. 6:1571-1579.

Nakano, T., K. Suzuki, T. Fujimura, and H. Shinshi. 2006. Genome-wide analysis of the ERF gene family in Arabidopsis and rice. *Plant Physiol*. 140:411-432.

Neuhaus, H.E., and M.J. Emes. 2000. Nonphotosynthetic Metabolism in Plastids. *Annual review of plant physiology and plant molecular biology*. 51:111-140.

Noguchi, K., and K. Yoshida. 2008. Interaction between photosynthesis and respiration in illuminated leaves. *Mitochondrion*. 8:87-99.

Oelmuller, R., and H. Mohr. 1986. Photooxidative Destruction of Chloroplasts and Its Consequences for Expression of Nuclear Genes. *Planta*. 167:106-113.

Ohme-Takagi, M., and H. Shinshi. 1995. Ethylene-inducible DNA binding proteins that interact with an ethylene-responsive element. *Plant Cell*. 7:173-182.

Okamuro, J.K., B. Caster, R. Villarroel, M. Van Montagu, and K.D. Jofuku. 1997. The AP2 domain of APETALA2 defines a large new family of DNA binding proteins in Arabidopsis. *Proc Natl Acad Sci U S A*. 94:7076-7081.

Ouwerkerk, P.B., and A.H. Meijer. 2011. Yeast one-hybrid screens for detection of transcription factor DNA interactions. *Methods Mol Biol*. 678:211-227.

Pfaffl, M.W. 2001. A new mathematical model for relative quantification in real-time RT-PCR. *Nucleic Acids Res*. 29:e45.

Pfannschmidt, T. 2010. Plastidial retrograde signalling--a true "plastid factor" or just metabolite signatures? *Trends Plant Sci*. 15:427-435.

Prestridge, D.S. 1991. SIGNAL SCAN: a computer program that scans DNA sequences for eukaryotic transcriptional elements. *Computer applications in the biosciences : CABIOS*. 7:203-206.

Richly, E., and D. Leister. 2004. An improved prediction of chloroplast proteins reveals diversities and commonalities in the chloroplast proteomes of Arabidopsis and rice. *Gene*. 329:11-16.

Riechmann, J.L., and E.M. Meyerowitz. 1998. The AP2/EREBP family of plant transcription factors. *Biol Chem*. 379:633-646.

Sakuma, Y., Q. Liu, J.G. Dubouzet, H. Abe, K. Shinozaki, and K. Yamaguchi-Shinozaki. 2002. DNA-binding specificity of the ERF/AP2 domain of Arabidopsis DREBs, transcription factors involved in dehydration- and cold-inducible gene expression. *Biochem Biophys Res Commun*. 290:998-1009.

Sato, S., Y. Nakamura, T. Kaneko, E. Asamizu, and S. Tabata. 1999. Complete structure of the chloroplast genome of Arabidopsis thaliana. *DNA research : an international journal for rapid publication of reports on genes and genomes*. 6:283-290.

Schwacke, R., K. Fischer, B. Ketelsen, K. Krupinska, and K. Krause. 2007. Comparative survey of plastid and mitochondrial targeting properties of transcription factors in Arabidopsis and rice. *Mol Genet Genomics*. 277:631-646.

Shendure, J.A., G.J. Porreca, and G.M. Church. 2008. Overview of DNA sequencing strategies. *Current protocols in molecular biology / edited by Frederick M. Ausubel ... [et al.]*. Chapter 7:Unit 7 1.

Shinozaki, K., and K. Yamaguchi-Shinozaki. 2000. Molecular responses to dehydration and low temperature: differences and cross-talk between two stress signaling pathways. *Curr Opin Plant Biol*. 3:217-223.

Silva-Filho, M.C. 2003. One ticket for multiple destinations: dual targeting of proteins to distinct subcellular locations. *Curr Opin Plant Biol*. 6:589-595.

Small, I., H. Wintz, K. Akashi, and H. Mireau. 1998. Two birds with one stone: genes that encode products targeted to two or more compartments. *Plant Mol Biol*. 38:265-277.

Smith, S.M., D.C. Fulton, T. Chia, D. Thorneycroft, A. Chapple, H. Dunstan, C. Hylton, S.C. Zeeman, and A.M. Smith. 2004. Diurnal changes in the transcriptome encoding enzymes of starch metabolism provide evidence for both transcriptional and posttranscriptional regulation of starch metabolism in Arabidopsis leaves. *Plant Physiol*. 136:2687-2699.

Smith, T.F., and M.S. Waterman. 1981. Identification of common molecular subsequences. *J Mol Biol*. 147:195-197.

Soll, J., and E. Schleiff. 2004. Protein import into chloroplasts. *Nat Rev Mol Cell Biol*. 5:198-208.

Stockinger, E.J., S.J. Gilmour, and M.F. Thomashow. 1997. Arabidopsis thaliana CBF1 encodes an AP2 domain-containing transcriptional activator that binds to the C-repeat/DRE, a cis-acting DNA regulatory element that stimulates transcription in response to low temperature and water deficit. *Proc Natl Acad Sci U S A*. 94:1035-1040.

Strand, A. 2004. Plastid-to-nucleus signalling. *Curr Opin Plant Biol*. 7:621-625.

Stribinskis, V., H.C. Heyman, S.R. Ellis, M.C. Steffen, and N.C. Martin. 2005. Rpm2p, a component of yeast mitochondrial RNase P, acts as a transcriptional activator in the nucleus. *Molecular and cellular biology*. 25:6546-6558.

Strittmatter, P., J. Soll, and B. Bolter. 2010. The chloroplast protein import machinery: a review. *Methods Mol Biol*. 619:307-321.

Sun, S., J.P. Yu, F. Chen, T.J. Zhao, X.H. Fang, Y.Q. Li, and S.F. Sui. 2008. TINY, a dehydration-responsive element (DRE)-binding protein-like transcription factor connecting the DRE- and ethylene-responsive element-mediated signaling pathways in Arabidopsis. *J Biol Chem*. 283:6261-6271.

Susek, R.E., F.M. Ausubel, and J. Chory. 1993. Signal transduction mutants of Arabidopsis uncouple nuclear CAB and RBCS gene expression from chloroplast development. *Cell*. 74:787-799.

Taiz, L., and E. Zeiger. 2006. Plant Physiology. Sinauer Associates, Inc., Sunderland, Massachusetts.

Terasawa, K., and N. Sato. 2009. Plastid localization of the PEND protein is mediated by a noncanonical transit peptide. *The FEBS journal*. 276:1709-1719.

Thomas, M.C., and C.M. Chiang. 2006. The general transcription machinery and general cofactors. *Critical reviews in biochemistry and molecular biology*. 41:105-178.

Unseld, M., J.R. Marienfeld, P. Brandt, and A. Brennicke. 1997. The mitochondrial genome of Arabidopsis thaliana contains 57 genes in 366,924 nucleotides. *Nat Genet*. 15:57-61.

van Die, I.M., H.E. Bergmans, and W.P. Hoekstra. 1983. Transformation in Escherichia coli: studies on the role of the heat shock in induction of competence. *Journal of general microbiology*. 129:663-670.

Vanyushin, B.F., and V.V. Ashapkin. 2011. DNA methylation in higher plants: past, present and future. *Biochim Biophys Acta*. 1809:360-368.

Vogelstein, B., and D. Gillespie. 1979. Preparative and analytical purification of DNA from agarose. *Proc Natl Acad Sci U S A*. 76:615-619.

Wagner, D., D. Przybyla, R. Op den Camp, C. Kim, F. Landgraf, K.P. Lee, M. Wursch, C. Laloi, M. Nater, E. Hideg, and K. Apel. 2004. The genetic basis of singlet oxygen-induced stress responses of Arabidopsis thaliana. *Science*. 306:1183-1185.

Wagner, R., and T. Pfannschmidt. 2006. Eukaryotic transcription factors in plastids--Bioinformatic assessment and implications for the evolution of gene expression machineries in plants. *Gene*. 381:62-70.

Walker, D.A. 1965. Correlation between Photosynthetic Activity and Membrane Integrity in Isolated Pea Chloroplasts. *Plant Physiol*. 40:1157-1161.

Weigel, D., and J. Glazebrook. 2002. Arabidopsis: A Laboratory Manual. Cold Spring Harbor Laboratory Press, New York.

Winter, D., B. Vinegar, H. Nahal, R. Ammar, G.V. Wilson, and N.J. Provart. 2007. An "Electronic Fluorescent Pictograph" browser for exploring and analyzing large-scale biological data sets. *PloS one*. 2:e718.

Woodson, J.D., and J. Chory. 2008. Coordination of gene expression between organellar and nuclear genomes. *Nature reviews. Genetics*. 9:383-395.

Yao, C.W., B.D. Hsu, and B.S. Chen. 2011. Constructing gene regulatory networks for long term photosynthetic light acclimation in Arabidopsis thaliana. *BMC bioinformatics*. 12:335.

Zoschke, R., M. Nakamura, K. Liere, M. Sugiura, T. Borner, and C. Schmitz-Linneweber. 2010. An organellar maturase associates with multiple group II introns. *Proc Natl Acad Sci U S A*. 107:3245-3250.

Appendix I

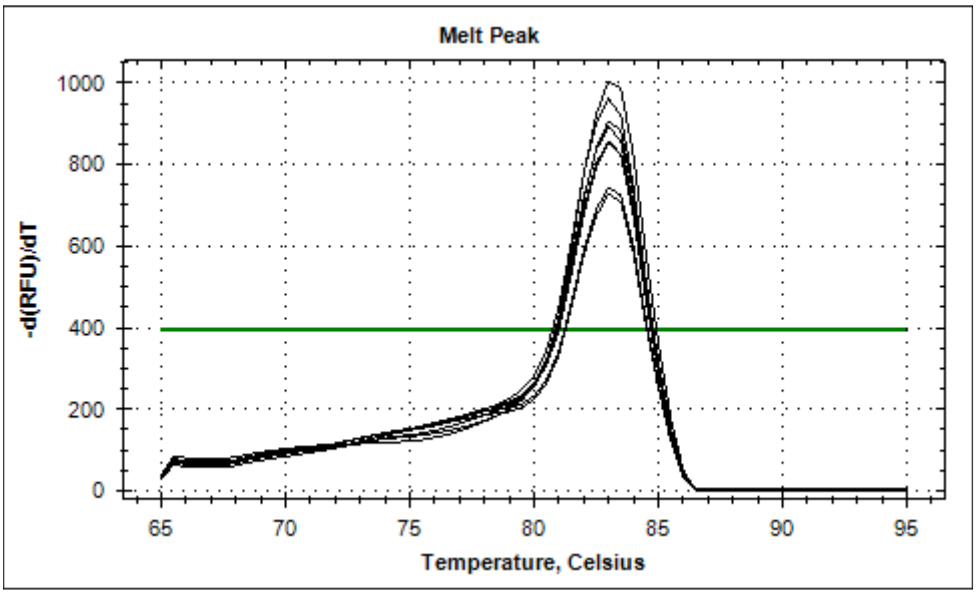

Figure 32: Melt-curve analysis for the *RBCS1A* amplicon showing the negative rate of change in RFU (Y-axis) as the temperature increases (X-axis). The peak indicates the melt temperature, which was determined to be 83˚C.

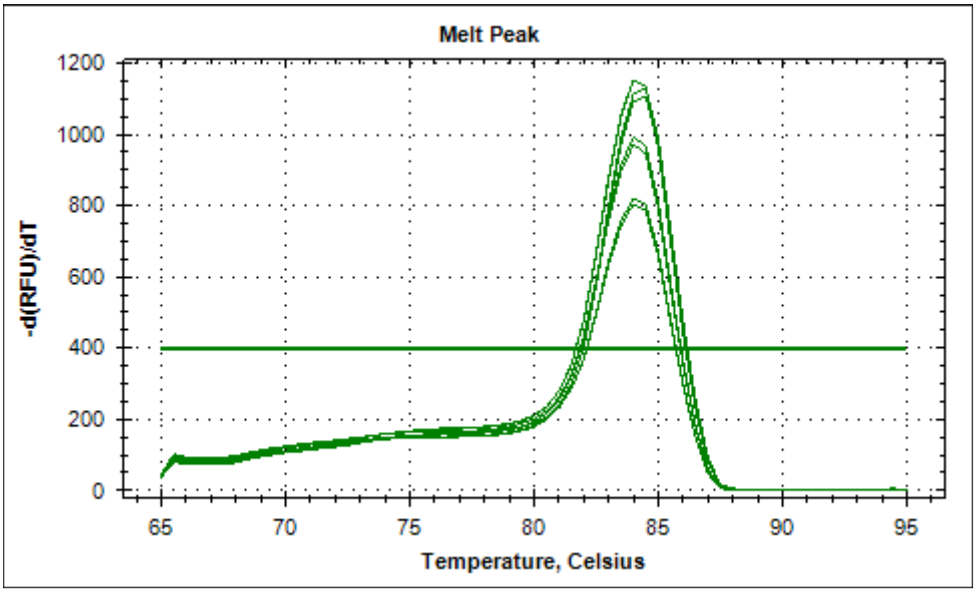

Figure 33: Melt-curve analysis for the *PSBO2* amplicon showing the negative rate of change in RFU (Y-axis) as the temperature increases (X-axis). The peak indicates the melt temperature, which was determined to be 84˚C.

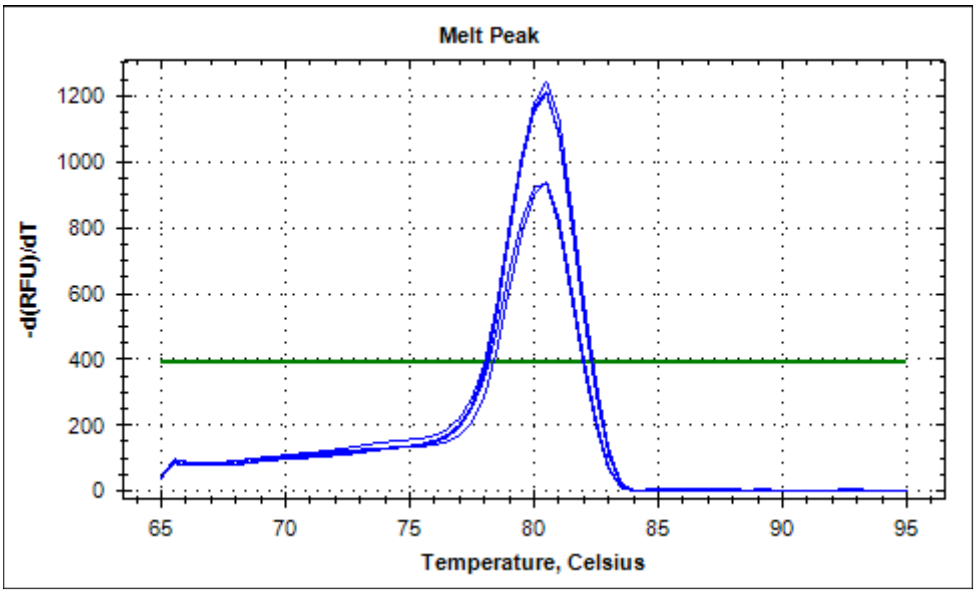

Figure 34: Melt-curve analysis for the *ACT8* amplicon showing the negative rate of change in RFU (Y-axis) as the temperature increases (X-axis). The peak indicates the melt temperature, which was determined to be 80,5˚C.

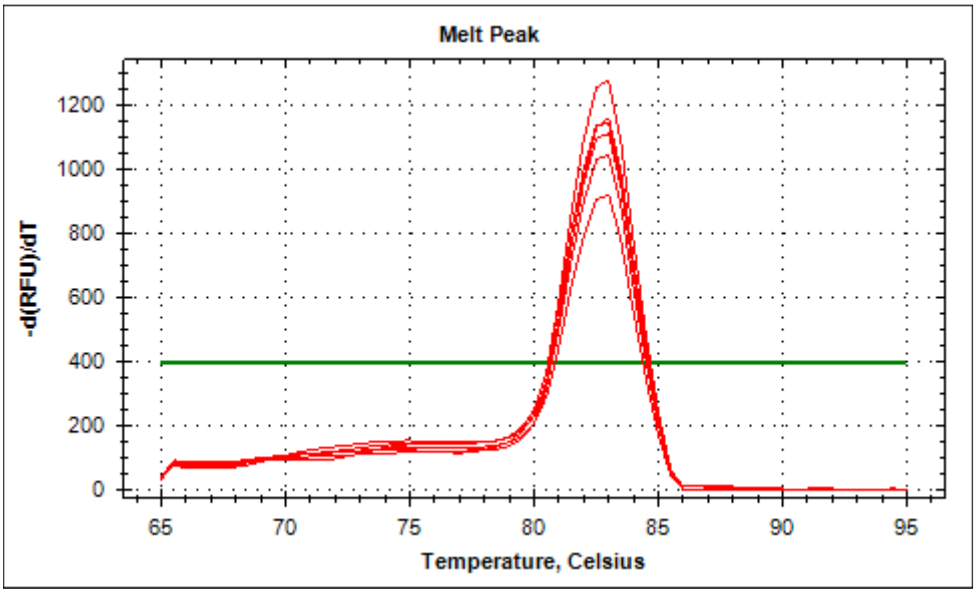

Figure 35: Melt-curve analysis for the *TF1* amplicon showing the negative rate of change in RFU (Y-axis) as the temperature increases (X-axis). The peak indicates the melt temperature, which was determined to be 83˚C.

Appendix II

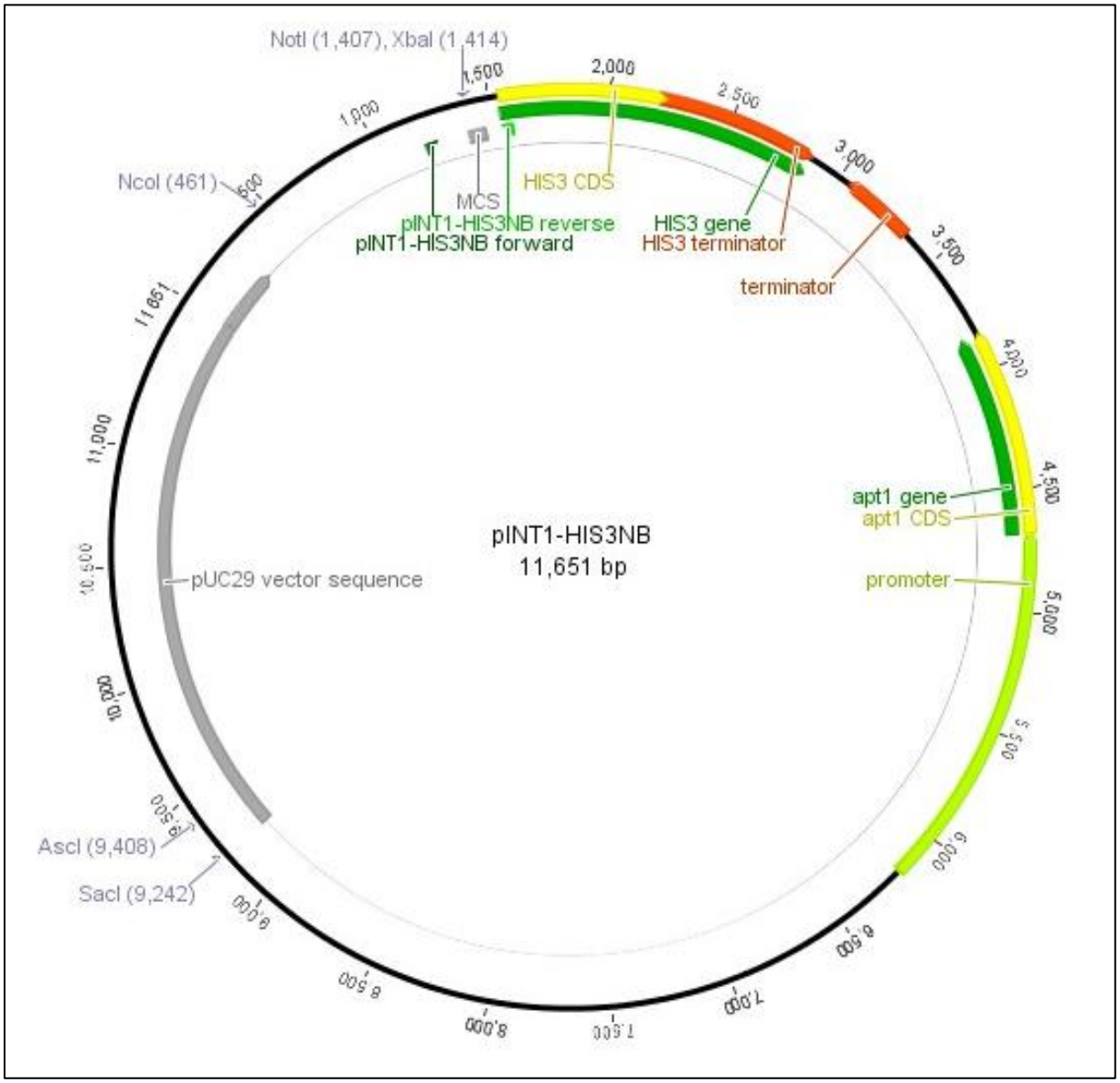

Figure 36: Vector map of pINT1-HIS3NB (GenBank accession number AY061966). The vector also codes for a gene conferring ampicillin resistance. This gene is located within the pUC29 vector sequence.

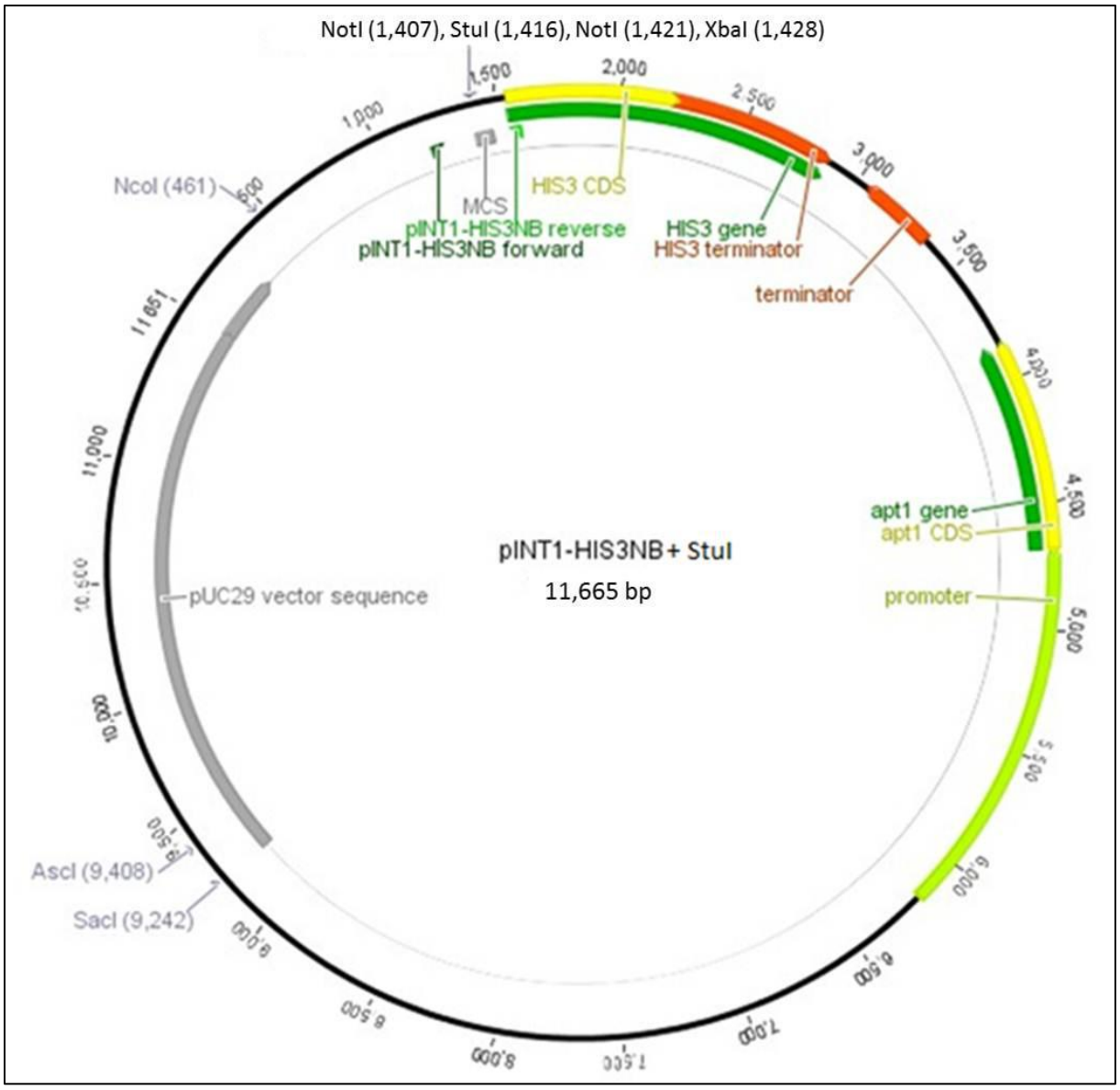

Figure 37: Vector map of pINT1-HIS3NB+StuI (modified MCS of pINT1-HIS3NB). The vector also codes for a gene bestowing ampicillin resistance. This gene is located within the pUC29 vector sequence.

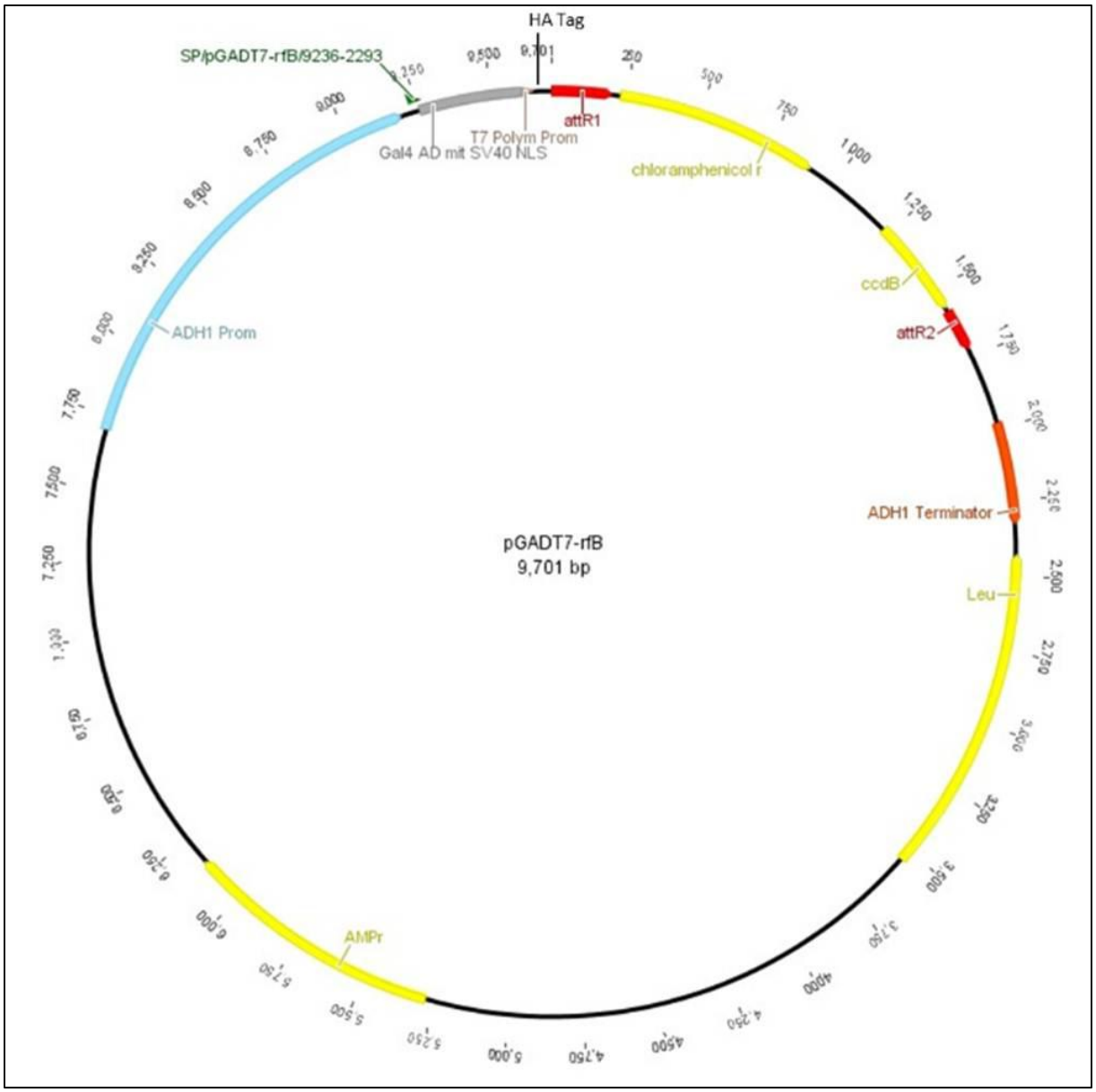

Figure 38: Vector map of pGADT7-rfB (modified version of pGADT7 (Clontech)). The SV40 nuclear localization signal (NLS) ensures that the GAL4AD fusion protein is transported to the yeast nucleus.

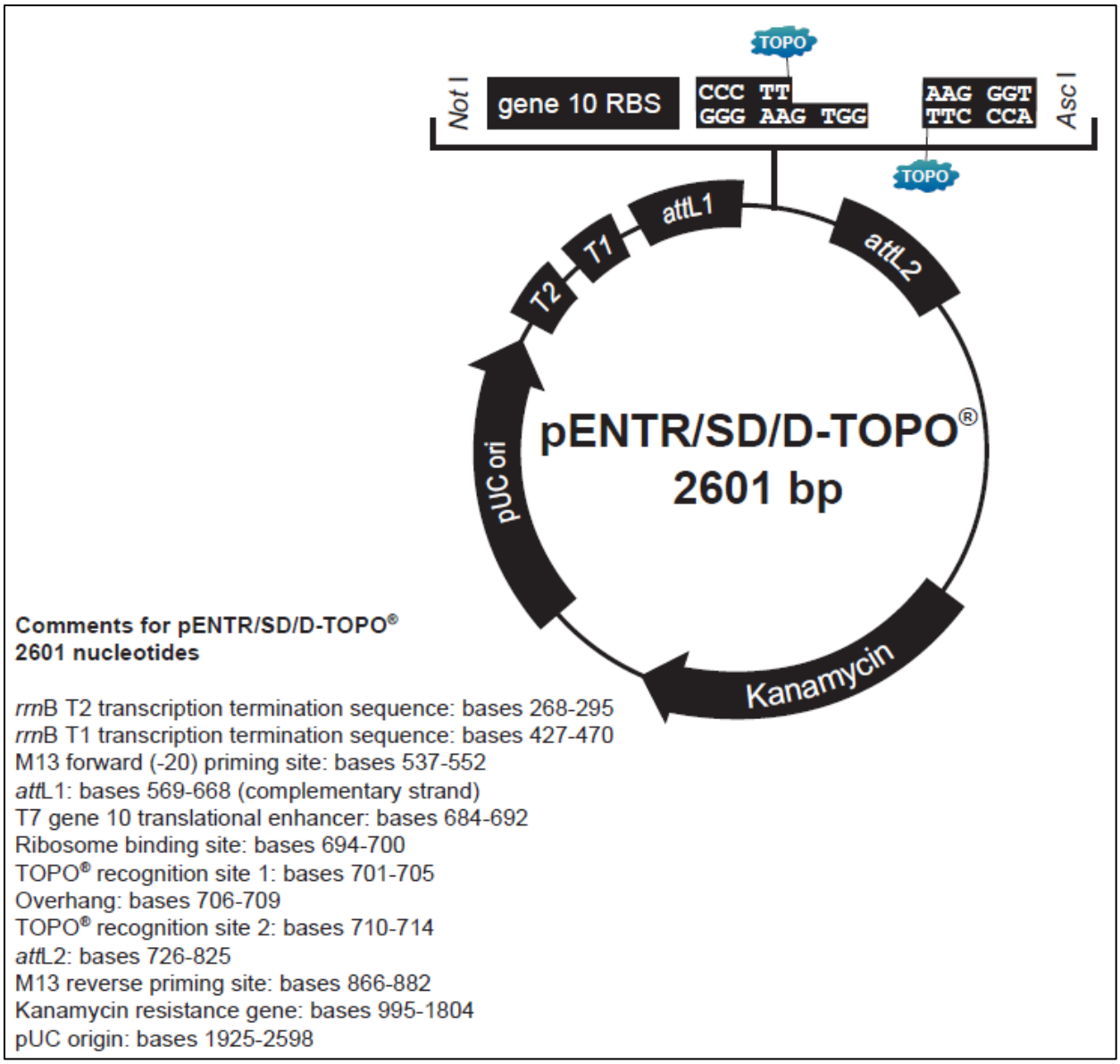

Comments for pENTR/SD/D-TOPO®
2601 nucleotides

*rrn*B T2 transcription termination sequence: bases 268-295
*rrn*B T1 transcription termination sequence: bases 427-470
M13 forward (-20) priming site: bases 537-552
*attL*1: bases 569-668 (complementary strand)
T7 gene 10 translational enhancer: bases 684-692
Ribosome binding site: bases 694-700
TOPO® recognition site 1: bases 701-705
Overhang: bases 706-709
TOPO® recognition site 2: bases 710-714
*attL*2: bases 726-825
M13 reverse priming site: bases 866-882
Kanamycin resistance gene: bases 995-1804
pUC origin: bases 1925-2598

Figure 39: Vector map of pENTR/SD/D-TOPO (Invitrogen).